

**Development of Disposable Sensors  
for Rapid Multianalyte Detection:  
Acetylcholinesterase and Microbial Biosensors**

**Entwicklung von Einmalsensoren zur  
schnellen Multianalytendetektion:  
Acetylcholinesterase- und mikrobielle Biosensoren**

**Bei der Fakultät Geo- und Biowissenschaften der Universität Stuttgart**

**eingereichte Dissertation**

**zur Erlangung des Grades eines  
Doktors der Naturwissenschaften  
(Dr. rer. nat.)**

**vorgelegt von**

**Till T. Bachmann  
aus Berlin**

**1999**

**1. Referent: Prof. Dr. Rolf D. Schmid  
2. Referent: Prof. Dr. Hans-Joachim Knackmuss  
eingereicht am 26.05.1999  
Tag der mündlichen Prüfung: 05.07.99**

Mein besonderer Dank gilt Herrn Prof. Dr. Rolf D. Schmid für die Bereitstellung des Themas, seine uneingeschränkte Unterstützung und die hervorragenden Arbeitsbedingungen am Institut für Technische Biochemie.

Bei Herrn Prof. Dr. Hans-Joachim Knackmuss möchte ich mich sehr herzlich für die Übernahme des Korreferates bedanken.

Herrn Prof. Dr. Isao Karube danke ich sehr für die Aufnahme an seinem Institut am Research Center for Advanced Science and Technology and der Universität Tokyo und seine ausgesprochene Gastfreundschaft. Weiterhin bedanke ich mich bei Dr. Satoshi Sasaki, Dr. Kazunori Ikebukuro und Dr. Kazuyoshi Yano für ihre hilfreiche Unterstützung beim Weg durch die japanische Wissenschaft.

Herrn Prof. Dr. Jean-Louis Marty danke ich für die Kooperation im Rahmen des PROCOPE-Projektes und seine Aufnahme am Centre de Phytopharmacie - UA CNRS, Universität Perpignan. In diesem Zusammenhang möchte ich Frau Dr. Béatrice Leca für Zusammenarbeit bei den Multisensormessungen mit den Acetylcholinesterasemutanten danken.

Für die Bereitstellung der *Drosophila melanogaster* Acetylcholinesterase und deren Mutanten möchte ich Herrn Prof. Dr. Didier Fournier und Dr. Francois Vilatte, Laboratoire d'entomologie appliquée, Université Paul Sabatier, Toulouse, danken.

Herrn Prof. Dr. Andreas Zell und Dipl. Chem. Fred Rapp, Universität Tübingen, danke ich für die Bereitstellung von NEMO und nützlicher Tips zum Umgang mit künstlichen neuronalen Netzen.

Bei Frau Dr. Nathalie Mionetto bedanke ich mich für anregende Diskussionen und die Überlassung der *Drosophila melanogaster* und der Rattenhirn Acetylcholinesterase.

Herrn Prof. Dr. Michael Schlömann danke ich für die Zusammenarbeit im ZSP Projekt und seine Diskussionsbereitschaft bei mikrobiologischen Fragen.

Mein Dank gilt weiterhin allen jetzigen und früheren Mitgliedern sowie den zahlreichen ausländischen Gästen der Arbeitsgruppe Analytische Biotechnologie / Biosensoren, welche mir auch während meiner Betreuungstätigkeit die Gelegenheit gegeben haben, mich meinen Experimenten zu widmen und dabei mit ihrem Interesse immer für viel Freude an der Wissenschaft gesorgt haben. Für ihre Mithilfe beim mikrobiellen Sensor danke ich Ute Nonhoff sowie besonders Dipl. Chem. Cho Seung-Jin für die zahlreichen Diskussionen und Hilfestellungen während meiner Zeit in Tokyo.

Für die finanzielle Unterstützung im Rahmen des Projektes A 3.6 U im Zentralen Schwerpunktprojekt (ZSP) Bioverfahrenstechnik der Universität Stuttgart bedanke ich mich beim Bundesministerium für Bildung und Forschung.

---

The objective of this work was to develop new biosensors for multianalyte detection. Target analytes were cholinesterase inhibiting insecticides and chlorinated aromatic hydrocarbons. The task was fulfilled by a combination of biological receptors bearing different selectivities for the desired analytes and data evaluation by feed-forward artificial neural networks (ANN). The basic sensor design consisted of a four-electrode thick film electrode which was fabricated by screen printing. As biological receptors for insecticide detection, variants of acetylcholinesterase (AChE) and for chlorinated aromatics *Ralstonia eutropha* JMP 134 cells were selected.

AChE-multisensors: Three types of sensitive amperometric biosensors for the rapid discrimination of paraoxon, carbofuran, and malaoxon in binary mixtures were developed. The analysis based on AChE inhibition and ANN data evaluation. Each wild type AChE-sensor employed four types of native and recombinant AChEs (electric eel, bovine erythrocytes, rat brain, *Drosophila melanogaster*). The sensors registered both analytes in a detection range of 0.2 - 20 µg/l. Thus, paraoxon and carbofuran in mixtures of 0 - 20 µg/l for each analyte could be analysed with prediction errors of 0.9 µg/l for paraoxon and 1.4 µg/l for carbofuran within less than 60 min. Improved AChE-sensors could be obtained with engineered variants of *Drosophila melanogaster* AChE. They consisted of wild-type *Drosophila* AChE and mutants Y408F, F368L, F368H, or F368W. Both multisensors were used for analysis of paraoxon and carbofuran mixtures in a concentration range of 0 - 5 µg/l within 40 min. The two analytes were best determined with prediction errors of 0.4 µg/l for paraoxon and 0.5 µg/l for carbofuran. In addition, multisensor II was also investigated for analyte discrimination in real water samples. Finally, the properties of the system was confirmed by simultaneous detection of binary organophosphate mixtures. Malaoxon and paraoxon in composite solutions of 0 - 5 µg/l were discriminated with prediction errors of 0.9 µg/l and 1.6 µg/l respectively.

Microbial multi-sensors: The starting point was the design of a novel miniature oxygen multi electrode. The disposable, Clark-type electrode was manufactured by a combination of screen printing, spin and drop coating and lamination techniques. Sensitivity, dynamic and stability characteristics proved essentially satisfactory. The sensor principle for simultaneous detection of halogenated aromatics based on the correlation of cell respiration and analyte concentration. Different selectivities of the receptor component were adjusted by selective induction of desired enzyme activities through cultivation of *R.eutropha* JMP 134 on 2,4-dichlorophenoxyacetic acid, 4-chloro-2-methylphenoxyacetic acid, 2-methylphenoxyacetic acid and phenol as carbon sources. The sensors were capable for a simultaneous detection of 2,4-dichlorophenol and phenol in mixtures of 0 - 40 µM with mean errors of 4.5 and 3.6 µM (0.62 and 0.34 mg/l), respectively. Mixtures of 2,4-dichlorophenol and 4-chlorophenol in the same concentration range were analysed with errors of 5.1 and 2.6 µM (0.33 and 0.7 mg/l), respectively.

The multisensors developed in this work are the first examples of disposable enzyme and microbial sensors in combination with data evaluation by artificial neural networks. They resemble advantageous tools for multi-analyte detection. Future considerations will focus on widening the analyte spectrum, further reduce of the assay time, and improve sensitivity and robustness of the sensors to evolve the preliminary prototypes to field systems for on-site environmental monitoring.

---

## A Zielsetzung

Der Gegenstand dieser Arbeit war die Entwicklung von neuen Biosensoren zum simultanen Nachweis und der Klassifizierung von Stoffgemischen in der Umweltanalytik. Diese neuartigen Systeme sollten zur Detektion Acetylcholinesterase hemmender Insektizide aus der Gruppe der Organophosphate und Carbamate sowie halogenorganischer Stoffe eingesetzt werden. Diese Substanzen spielen insbesondere in der Überwachung der Wasserqualität eine entscheidende Rolle. Das Sensorprinzip basierte auf der Idee, biologische Rezeptorkomponenten, die unterschiedliche Spezifität für die Zielanalyten aufweisen, zu kombinieren, und deren Signalmuster durch künstliche neuronale Netze (KNN) auszuwerten. Alle entwickelten Systeme verwendeten durch Siebdruck hergestellte Dickschicht-Multielektroden als Sensorbasis. Zur Mustererkennung von Insektiziden wurden Biosensoren eingesetzt, welche Acetylcholinesterase-Varianten variierender Selektivität enthielten. Die Detektion halogenorganischer Verbindungen in Mischungen erfolgte mittels Sensoren, die mit *Ralstonia eutropha* JMP 134 Zellen bestückt waren. Die verschiedenen Selektivitäten dieser Sensoren wurden durch Kultivierung der Mikroorganismen auf unterschiedlichen Wachstumssubstraten erreicht.

## B Acetylcholinesterase-Multisensoren

### B.1 Entwicklung des Elektrodenprototyps

Der Einsatz von Acetylcholinesterase (AChE) für die Bestimmung von insektiziden Organophosphaten und Carbamaten ist wiederholt in der Literatur beschrieben worden. Allerdings berichtete bisher keine Veröffentlichung von einem zur selektiven Bestimmung Cholinesterase hemmender Insektizide befähigten Einzelsensor. Aus diesem Grund beinhaltete der erste Schritt des Projektes die Entwicklung einer komplett durch Siebdruck herstellbaren Enzym-Multielektrode. Dabei kamen kommerzielle Siebdruckpasten und PVC-Folien mit einer Dicke von 0,5 mm für die Herstellung der Elektrodenbasis zum Einsatz. Als Referenzenzym für die Optimierung des Systems diente Acetylcholinesterase aus Zitteraal. Das Layout für den Biosensor bildete eine Mehrfachelektrode bestehend aus vier parallel betriebener Einzelsensoren. Neben einem massenproduktionsfähigen Herstellungskonzept stand als wesentlicher Gesichtspunkt eine schnelle und reproduzierbare Sensorantwort im Vordergrund. Von entscheidender Bedeutung für eine erfolgreiche Multianalytik war jedoch die Reproduzierbarkeit jedes der Sensoren innerhalb einer Produktionscharge.

Der eigentliche Insektizidnachweis erfolgte durch Messung der Enzymaktivität der AChE auf dem Sensor vor und nach Hemmung durch die untersuchte Probe. Die Konzentration von Thiocholin, bestimmt durch amperometrische Oxidation, diente

---

dabei als Maß für die hydrolytischen Aktivität der AChE. Dazu wurden Rhodiumgraphit oder TCNQ (7,7,8,8-Tetracyanoquinodimethan) in verschiedensten Pastenformulierungen als Mediatoren für einen erleichterten Elektronenübergang bei der Thiocholinoxidation an der Arbeitselektrode untersucht. Hierbei erwies sich eine Paste von TCNQ auf T13 Graphit in Suspension mit Hydroxyethylcellulose (HEC) als am geeignetsten. Unter den getesteten Immobilisierungsmethoden erbrachte der Siebdruck einer Paste bestehend aus AChE, Rinderserumalbumin und HEC und eine anschließende Quervernetzung in Glutaraldehydatmosphäre die besten Ergebnisse.

Mit dieser Methode hergestellte Sensoren zeigten eine Äquilibrierung innerhalb von 10 Minuten. Die Sensorantwort von 50 nA bei Anwesenheit von 1 mM Acetylthiocholin (ATCh) erfolgte sofort nach Zugabe des Substrates und erreichte in 60 Sekunden 90 % des Maximalwertes. Weitere Kenndaten des Sensors waren ein Sensorfehler von  $\pm 1,7\%$  bei ATCh-Messungen mit einem apparenten  $K_m$ -Wert von 0,08 mM. Bestimmungen des Organophosphats Paraoxon in der Konzentration 10  $\mu\text{g/l}$  ergab eine Meßgenauigkeit von  $\pm 11,5\%$  für einen Sensor und  $\pm 13,1\%$  für den Vergleich vier verschiedener Sensoren eines Multisensors. Aufbauend auf diesen Ergebnissen wurde mit der Herstellung der AChE-Multisensoren begonnen. Das dazu gehörige Herstellungsschema zeigt nachfolgende Abbildung B.1.

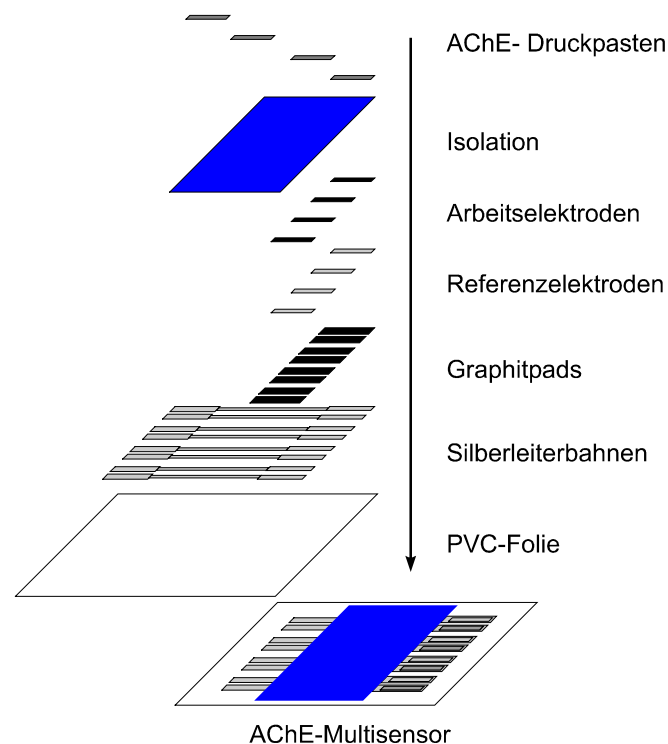


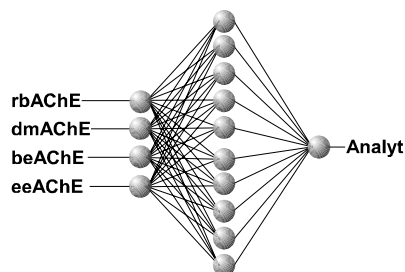
Abbildung B.1: Herstellung von AChE-Multisensoren durch Siebdruck

## B.II Multianalyt-Detektion mit AChE-Multisensoren

Für die Entwicklung des Multisensorsystems wurden Paraoxon und Carbofuran als je ein Vertreter aus der Gruppe der Organophosphate und der Carbamate gewählt. Zur Ausstattung des AChE-Multisensors gehörten vier Wildtyp Acetylcholinesterasen, die ein für beide Analyten individuelles Sensitivitätsmuster aufwiesen. Diese Eigenschaft zeigten zwei kommerziell erhältliche AChEs aus Zitteraal (*Electrophorus electricus*) (eeAChE) und Rindererythrocyten (beAChE), sowie zwei in Baculo-Virus System exprimierte rekombinante AChEs aus Rattenhirn (rbAChE) und *Drosophila melanogaster* (dmAChE). Die Einzelkomponenten des Multisensors zeigten in Inhibitionsversuchen mit 10 µg/l Paraoxon folgende Messgenauigkeiten: rbAChE  $\pm 2,3\%$ , dmAChE  $\pm 3,6\%$ , beAChE  $\pm 4,7\%$ , eeAChE  $\pm 23,4\%$ . Der lineare Messbereich für Paraoxon und Carbofuran erstreckte sich von 0 - 10 µg/l, außer für die hochsensitive Insektencholinesterase dmAChE. Hier wurde das Inhibitionsmaximum bereits bei 5 µg/l erreicht. Die Detektionsgrenze lag für beide Analyten bei 0,2 µg/l. Eine Bestimmung der Inhibitionskonstanten  $k_i$  ergab eine weitgehende Deckung mit Literaturwerten für freie Acetylcholinesterasen. Somit konnte ein ungünstiger Einfluss der Immobilisierung auf die Enzymkonformation und das Detektionsverhalten ausgeschlossen werden.

Die Multianalytbestimmung erfolgte in Analysen von 50 Mischungen von Paraoxon und Carbofuran in den Konzentrationen 0 - 20 µg/l mit dem AChE-Multisensor. Die dabei erhaltenen Datensätze wurden anschließend zum Aufbau von künstlichen neuronalen Netzen verwendet. Ausschlaggebend für ein optimales Diskriminierungsvermögen der neuronalen Netze war deren Topologie. Daher wurden die neuronalen Netze in ihrer Architektur für jeden Analyten getrennt angepasst. Bestandteil dieser Experimente war ein Vergleich von manuellem Netzwerkaufbau und automatisiertem Vorgehen mittels Pruningalgorithmen. Die resultierenden neuronalen Netze für die Prozessierung von Messungen binärer Mischungen mit dem AChE-Multisensor zeigt Abbildung B.2.

a.) Initiale Netzwerktopologie



b.) Optimierte Netzwerktopologie

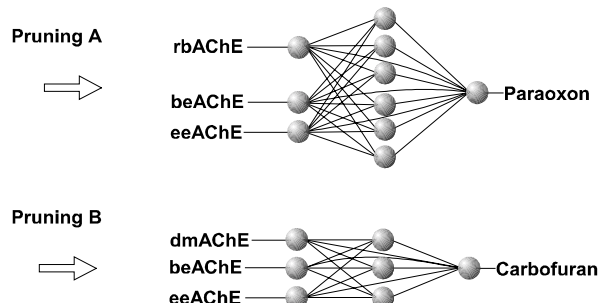


Abbildung B.2: Aufbau und Optimierung künstlicher neuronaler Netze zur Prozessierung von Multisensordaten für die simultane Bestimmung von Paraoxon und Carbofuran in binären Mischungen. Die Topologieoptimierung erfolgte für jeden Analyten getrennt (Pruning A, Pruning B)

Die Multianalysefähigkeit des Systems wurde in zwei Arten von Experimenten nachgewiesen. Im ersten Ansatz diente die Kreuzvalidierung der neuronalen Netze anhand der Messungen von Paraoxon und Carbofuranmischungen in Konzentrationen von 0 bis 20 µg/l in Standardpufferlösungen. Beide Analyten konnten hier mit einem Fehler von 0,9 µg/l für Paraoxon und 1,4 µg/l für Carbofuran bestimmt werden.

In weiterführenden Versuchen konnte dieses Ergebnis in Versuchsreihen mit Abwasserproben bestätigt werden. Da die Proben selbst keine Hemmung der Sensoren zeigten, wurden Aufstockversuche mit 5 µg/l Paraoxon oder Carbofuran sowie einer Mischung aus beiden Substanzen durchgeführt. Die Bestimmung mit dem AChE-Multisensor und Datenevaluierung durch die in Abbildung I.II gezeigten neuronale Netze ergab eine Identifizierung beider Analyten mit einer Genauigkeit von  $\pm 1,8$  µg/l. Dies war ein, besonders in Anbetracht des hohen Gehalts an organischen Verbindungen in der Probe ( $\text{BOD}_5 > 100$  mg/l), bemerkenswertes Ergebnis.

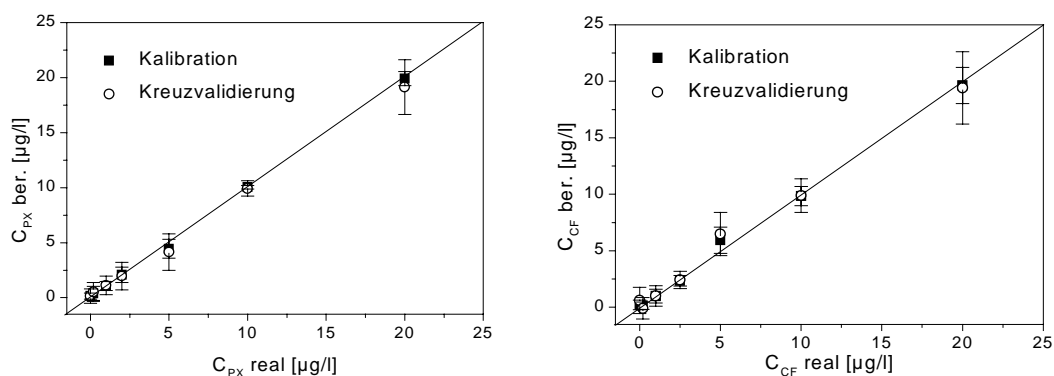


Abbildung B.3: Simultane Bestimmung von Paraoxon (PX) und Carbofuran (CF) in binären Gemischen. Auftragung der errechneten (ber.) gegen die tatsächliche (real) Inhibitorkonzentration.

### B.III Multianalyt-Detektion mit *Drosophila* AChE-Multisensoren

Nachdem bereits mit dem Wildtyp AChE-Multisensor eine Diskriminierung von Carbofuran und Paraoxon gezeigt werden konnte, sollte durch die Verwendung anderer, sensitiverer Acetylcholinesterasen, eine Verbesserung des Systems erreicht werden. Dazu wurden Varianten von *Drosophila melanogaster* AChE eingesetzt und die Immobilisierung weiter optimiert. Durch den Einsatz von PVA-SbQ, einem photovernetzbaaren Präpolymer für die Immobilisierung mittels Siebdruck, konnte die Äquilibrierungsphase der Sensoren auf 5 min gesenkt werden.

In den neuen AChE-Multisensoren bildeten *Drosophila melanogaster* AChE (dmAChE) und je drei Mutanten Y408F, F368L, F368H oder F368W die Rezeptorkomponenten. Ein wesentlicher Fortschritt konnte im Bereich der Sensorgrundströme gegenüber dem Wildtyp AChE-Multisensor erreicht werden. So zeigte Multisensor I im Mittel ein 58 nA Signal bei Zugabe von 1 mM ATCh

(Multisensor II 35 nA). Dabei betrug die Variation 6,7 % und 9,7 % gegenüber 25 % beim ersten AChE-Multisensor. Die Messgenauigkeiten der Einzelsensoren lagen für 5 µg/l Paraoxon bei  $\pm 8,6$ ; 1,2; 1,3 sowie 18,7% für dmAChE, Y408F, F368LF und 368W. Als Nachweisgrenzen von Multisensor I und II wurden bei 0,5 µg/l Paraoxon ( $1,8 \times 10^{-9}$  M) und Carbofuran ( $2,3 \times 10^{-9}$  M) bei einem mittleren Signal/Rauschverhältnis von 6,3 und 3,0 ermittelt. Wie bereits für den Wildtyp AChE-Sensor beschrieben, wurde auch hier eine wegehende Übereinstimmung der Inhibitionskonstanten für Paraoxon und Carbofuran mit Literaturdaten für Acetylcholinesterasen in Lösung gefunden.

Die linearen Meßbereiche der Multisensoren I und II erstreckten sich je von 0 - 5 µg/l für beide Analyten. Daher wurde in Versuchen zur simultanen Detektion binärer Substanzgemische dieser Konzentrationsbereich gewählt. Auch hier fand die Sensorcharakterisierung anhand von Messungen sowohl in Standardlösungen als auch in Realproben statt. Die Analyse von Paraoxon / Carbofuran-Gemischen mit Multisensor I führte zu neuronalen Netzen der Konfiguration 4:4:1 für Paraoxon und 4:3:1 für Carbofuran. Die Berechnungen der Analytkonzentrationen mittels dieser Netze erfolgten mit einer mittleren Genauigkeit für Paraoxon und Carbofuran von 0,6 µg/l und 0,5 µg/l in der Kreuzvalidierung.

Für die Enzymausstattung von Multisensor II wurde die AChE Mutante F368H im gegen die für Paraoxon erheblich insensitivere Variante F368W ausgetauscht. Der Einsatz dieser Mutante führte zu Netzwerkkonfigurationen von 2:2:1 für Paraoxon und 3:2:1 für Carbofuran und einer verbesserten Bestimmungsgenauigkeit von Paraoxon und Carbofuran mit 0,4 µg/l bzw. 0,5 µg/l in der Kreuzvalidierung. Eine Überprüfung von Multisensor II und neuronalem Netz wurde mittels Messung von binären Mischungen beider Analyten in der Konzentration 0,5 µg/l als unabhängige Testmenge vorgenommen. Das Ergebnis wies mit einem Bestimmungsfehler von 0,25 µg/l für Paraoxon und 0,17 µg/l für Carbofuran einen unerwartet guten Wert auf.

In der Analyse von Flusswasserproben mit Multisensor II zeigte sich eine Hemmung bereits durch die reine Probe. Aus diesem Ergebnis errechnete das neuronale Netz Konzentrationen von 0,4 µg/l Paraoxon und 0,2 µg/l Carbofuran. Bei den darauffolgenden Aufstockversuchen im Konzentrationsbereich 0 - 2,5 µg/l ermittelten Multisensor II und das zugehörige neuronale Netz beide Analyten mit einer Variation von 1,1 µg/l für Paraoxon und 0,7 µg/l für Carbofuran. Diese Ergebnisse zeigten einerseits die Anwendbarkeit des Sensors für die Messung von Realproben, machten aber auch den Entwicklungsbedarf, zum Beispiel hinsichtlich der Vermeidung von Matrixeffekten, deutlich.

Da wie gezeigt, eine Diskriminierung von einem Organophosphat und einem Carbamat mittels AChE-Multisensor und Datenevaluierung durch neuronale Netze problemlos möglich war, ließ sich das System auf die simultane Detektion von zwei Organophosphaten, Paraoxon und Malaoxon, erweitern. Daraufhin wurden aus Messung binärer Gemische beider Analyten im Konzentrationsbereich 0 - 5 µg/l neuronale Netze der Topologie 4:5:1 für Paraoxon und 4:4:1 für Malaoxon generiert und beide Analyten mit einer Genauigkeit von 1,6 µg/l (Paraoxon) und 0,9 µg/l (Carbofuran) erfolgreich identifiziert.

---



## C Mikrobielle Multisensoren

Projektziel war die selektive und simultane Erfassung von wichtigen Bestandteilen des Summenparameters der adsorbierbaren halogenorganischen Stoffe (AOX). Als Modellanalyten mit einer toxikologischen und ökologischen Relevanz wurden Chlorphenole gewählt. Für die Verwendung im Biosensor für diese Substanzen standen mehrere Chlorphenole oxidativ metabolisierende Mikroorganismenstämme zur Diskussion. *Ralstonia eutropha* JMP 134 war in dieser Gruppe aufgrund seiner katabolischen Fähigkeiten der geeignetste Stamm. Das Sensorprinzip bestand in der Korrelation von mikrobieller Sauerstoffzehrung mit der Konzentration des zugegebenen Analyten. Um diese Abnahme zu quantifizieren, wurden *R.eutropha* JMP 134 Zellen auf einer Sauerstoffelektrode immobilisiert. Um die dazu benötigte Meßanordnung zu erhalten, bestand ein wesentlicher Teil des Projektes in der Entwicklung einer planaren Sauerstoffmultielektrode vom Clark-Typ. Der fertige mikrobielle Multisensor bestand aus vier Einzelelektroden, auf denen jeweils verschieden induzierte Zellen von *R.eutropha* JMP 134 immobilisiert waren.

### C.1 Entwicklung einer planaren Sauerstoffelektrode

Die Herstellung der Elektrodenbasis erfolgte wie im Falle der AChE-Multisensoren durch Siebdruck. Als Arbeitselektrodenmaterial erwies sich Rhodium, vermischt mit Aktivkohle und Hydroxyethylcellulose, als vorteilhaft. Eine Beschichtung der aktiven Fläche der Sauerstoffelektroden und des Elektrolytraumes der Elektrode mit einer gaspermeablen Membran aus Silikongummi diente zur Isolation gegen das Messmedium und zur Vermeidung von Interferenzen. Als wesentlichen Schritt in der Elektrodenentwicklung stellte sich die Einführung einer Laminatmaske heraus. Diese verhinderte einen „Cross-talk“ zwischen den einzelnen Elektroden und erhöhte das Einzelsignal beim Biosensor. Die dynamischen Eigenschaften der Sauerstoffelektroden und deren Verhalten auf wechselnde Sauerstoffkonzentrationen zeigt Abbildung C.1.

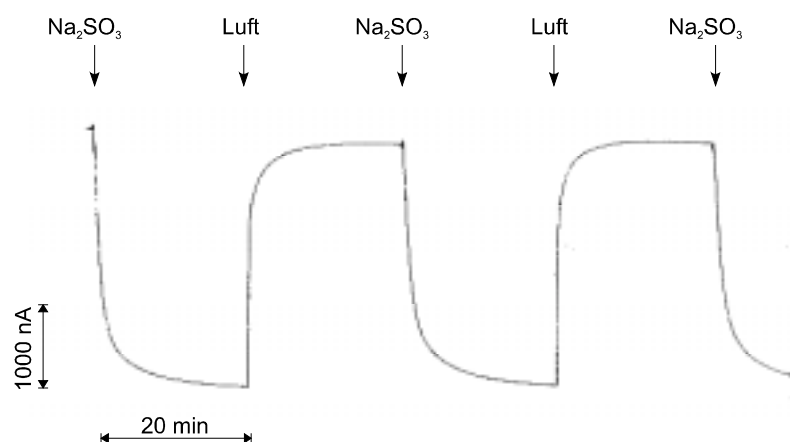


Abbildung C.1: Sauerstoffelektrodensignal bei Zugabe von sauerstoffgesättigtem (Luft) oder -freiem ( $\text{Na}_2\text{SO}_3$ ) Messmedium.

Die Sensoren für gelösten Sauerstoff zeigten ein für Elektroden dieses Typs übliches Äquilibrierungsverhalten mit einer Einstelldauer von 10 - 20 min. Eine Reaktion auf sich ändernde Sauerstoffkonzentrationen erfolgte sofort, und die Zeit bis zum Erreichen von 90 % des Gesamtsignals betrug im Mittel 130 s.

Die Immobilisierung der Mikroorganismen auf der Sauerstoffelektrode stellte einen wegen der starken Hydrophobizität problematischen Schritt dar. Wichtig für eine spätere Anwendung im Multisensor war eine hochgradig reproduzierbare Immobilisierung von ausgeprägter Stabilität. Die Schwierigkeiten mit der Haftung konnten durch den Einsatz von Silanisierung (4-Aminopropyl-triethoxysilan), in Verbindung mit Glutaraldehyd und Rinderserumalbumin gelöst werden. Durch diese Erhöhung der Hydrophilität der Silicongummimembran wurde eine starke und reproduzierbare Haftung von Alginatmembranen unter Beibehaltung der Elektrodenfunktion erreicht. Diese Immobilisierung wies im Gegensatz zu früheren Methoden eine ausreichende Haftung in Verbindung mit schneller Sensorantwort und hoher Arbeitsstabilität auf. Eine Lagerung der Sensoren konnte mit dieser Immobilisierung in feuchter Atmosphäre bei 4 °C erfolgen.

Den kompletten Herstellungsprozess der mikrobiellen Multisensoren mittels einer Kombination von Siebdruck, „Spin- und „Drop-Coating“ sowie Laminierung und die verwendeten Layouts zeigt Abbildung C.2.

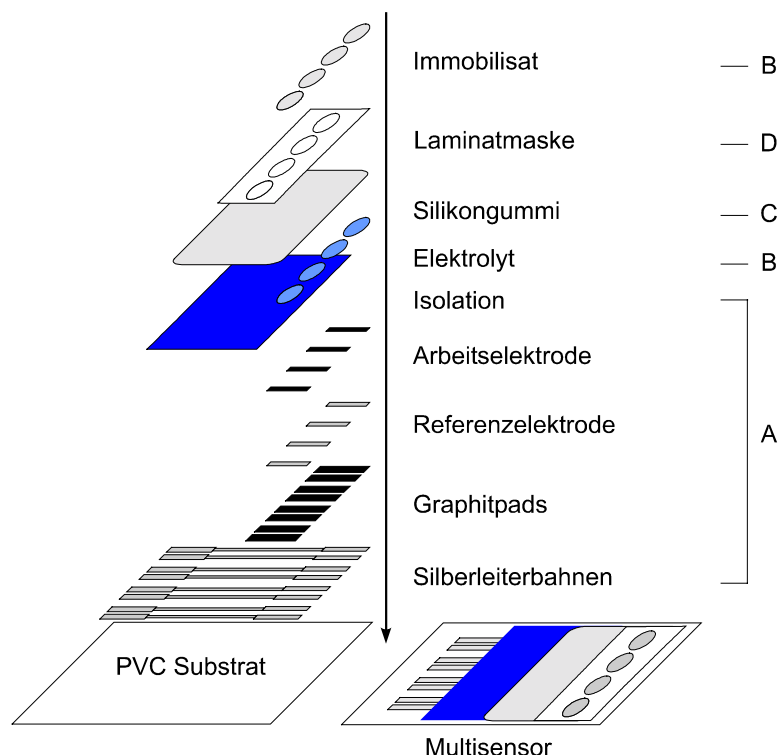


Abbildung C.2: Herstellung von mikrobiellen Multisensoren durch Siebdruck (A), Drop Coating (B), Spin Coating (C) und Laminierung (D)

## C.II Multianalyt-Detektion mit mikrobiellen Multisensoren

Als biologische Komponente für den Einsatz im „AOX“-Sensor kam *R.eutropha* JMP 134 zum Einsatz, da dieser Stamm ein hohes, vielfach beschriebenes Abbaupotential für halogenierte Aromaten besitzt. Um die für den Multisensor notwendigen differenzierten Signalmuster zu erhalten, wurde *R.eutropha* JMP 134 auf verschiedenen Substraten unter sonst gleichbleibenden Bedingungen kultiviert. Die einzelnen Wachstumssubstrate waren 2,4-Dichlorphenoxyessigsäure (2,4-D), 2-Methyl-4-chlorphenoxyessigsäure (MCPA), 2-MPA (2-Methylphenoxyessigsäure) und Phenol. Die Ernte der Zellen zur Immobilisierung erfolgte jeweils in der exponentiellen Wachstumsphase nach 6 Stunden (2,4-D; Phenol), 9 Stunden (2-MPA) und 24 Stunden (MCPA).

Das zur Bestimmung von 2,4-Dichlorphenol (2,4-DCP), 4-Chlorphenol (4-CP) und Phenol benötigte Induktionsmuster bei *R.eutropha* JMP 134 sollte durch Messung der Sauerstoffaufnahme nach Zugabe dieser Substanzen überprüft werden. Dabei zeigten auf 2,4-D gewachsene Zellen keine Respiration bei Zugabe von Phenol und umgekehrt Phenol kultivierte Zellen keine Reaktion auf Zugabe von 2,4-Dichlorphenol. MCPA und 2-MPA als Wachstumssubstrate führten zu Zellen, die ein Signalmuster aufwiesen, das sich in Kombination mit Ersteren zum Einsatz im Multisensor eignen sollte.

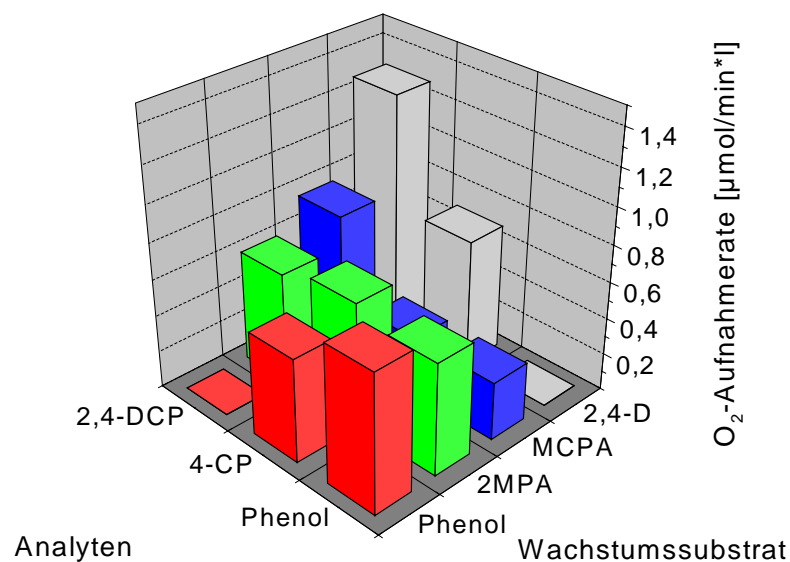


Abbildung C.3: Sauerstoffaufnahme suspendierter *R.eutropha* JMP 134 Zellen in Abhängigkeit vom Analyten (Cs = 16 µM) und Wachstumssubstraten (Cs = 2 mM).

Zur Multianalyt-Detektion von 2,4-DCP und Phenol oder 2,4-DCP und 4-CP wurden *R.eutropha* JMP 134 auf o.g. Substraten kultiviert und anschließend, wie in Abbildung C.4 gezeigt, immobilisiert.

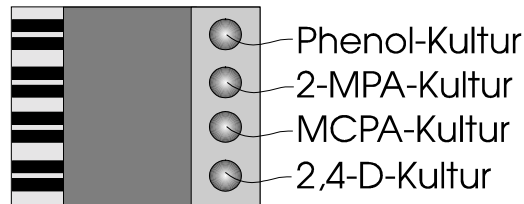
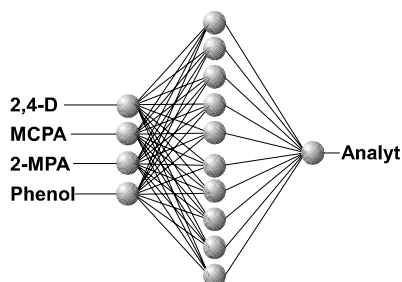


Abbildung C.4: Verteilung der *R.eutropha* JMP 134 - Kulturen auf dem Multisensor.

Bei Messungen binärer Gemische von 2,4-DCP und Phenol oder 2,4-DCP und 4-CP lagen diese Analyten in Konzentrationen von je 0 - 40  $\mu\text{M}$  vor. Die Verrechnung der dazugehörigen Messdaten, sowie der Aufbau und die Optimierung der künstlichen neuronalen Netze, erfolgte beim mikrobiellen Sensor in Analogie zum AChE-Multisensor. Ausgehend von einer Netztopologie von 4:10:1 wurde eine verbesserte Konfiguration für jeden Analyten getrennt generiert (Abbildung I.VII).

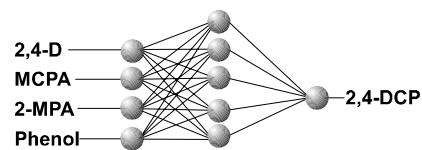
a.) Initiale Netzwerktopologie



Pruning A



b.) Optimierte Netzwerktopologie



Pruning B

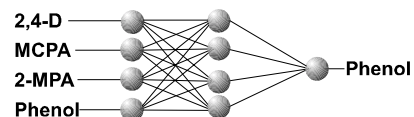


Abbildung C.5: Entwicklung künstlicher neuronaler Netze zur Prozessierung von Multisensordaten für die simultane Bestimmung von 2,4 Dichlorphenol (Pruning A) und Phenol (Pruning B) in binären Mischungen.

Die Topologie-optimierten neuronalen Netze wurden in weiteren Schritten erneut auf dem Datensatz trainiert und durch Kreuzvalidierung getestet. Abbildung I.VIII zeigt das Ergebnis der Netzwerkprozessierung.

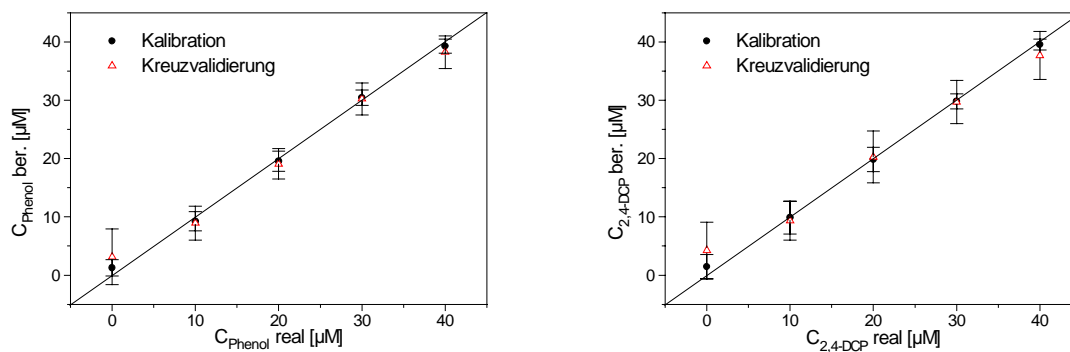


Abbildung C.6: Simultane Detektion von 2,4-DCP und Phenol in binären Gemischen. Auftragung der errechneten (ber.) gegen die tatsächliche (real) Analytkonzentration.

Wie in Abbildung I.VIII zu erkennen, ist mittels mikrobieller Multisensoren eine simultane Messung von zwei Analyten in binären Gemischen prinzipiell möglich. Durch den Einsatz von Datenreduzierung durch künstliche neuronale Netze konnte eine Bestimmung der beiden Analyten mit einer mittleren Abweichung von 4,5 µM für 2,4-DCP und 3,6 µM für Phenol in der Kreuzvalidierung erfolgen (0,62 und 0,34 mg/l).

In weiterführenden Versuchen wurden binäre Mischungen von 2,4-Dichlorphenol und 4-Chlorphenol im Konzentrationsbereich von 0 - 40 µM analysiert. Multisensormessung sowie Aufbau und Datenprozessierung mittels neuronaler Netze entsprachen dem ersten Multisensoransatz. Bei der selektiven Erfassung beider Analyten konnten Genauigkeiten von 5,1 µM für 2,4-DCP und 2,6 µM für 4-CP (0,33 und 0,7 mg/l) erreicht werden.

## D Fazit

Die Entwicklung von neuen Biosensorsystemen für eine simultane Mehrkomponentenbestimmung konnte erfolgreich aufgezeigt werden. Dazu wurden zum einen eine neuartige Multienzymelektrode und zum anderen eine sensitive Sauerstoffelektrode für den Einmalgebrauch und Einsatz im Multisensor entwickelt. Beide, auf die neuen Transducer aufbauenden Biosensoren, waren bereits in der Einzelstoffanalytik ausreichend sensitiv. In der Kombination dieser Multisensoren mit neuronalen Netzen konnten Zweistoffgemische chemisch verwandter Analyten mit hoher Auflösung und Sensitivität erfaßt werden. Zukünftige Untersuchungen sollten im Falle des mikrobiellen Sensors den Schwerpunkt auf die Stabilisierung des Induktionsmusters legen. Für eine tatsächliche Anwendung als Feldtest wären für beide Sensorsysteme weitere Verbesserungen hinsichtlich der Interferenz- und Matrixempfindlichkeit sowie eines erweiterten Analytspektrums empfehlenswert.

$\epsilon$	Extinction coefficient
2,4-D	2,4-Dichlorophenoxyacetic acid
2,4-DCP	2,4-Dichlorophenol
2-MPA	2-Methylphenoxyacetic acid
4-CP	4-Chlorophenol
4-MP	4-Methylphenol
AbsE	Mean absolute error
AChE	Acetylcholinesterase
ANN	Artificial neural network
APTS	4-Aminopropyl-triethoxysilane
ATCh	Acetylthiocholine
BSA	Bovine serum albumine
CF	Carbofuran
DTNB	5,5'-Dithio-bis(2-nitrobenzoic acid)
GA	Glutaraldehyde
HEC	Hydroxyethylcellulose
$k_i$	Inhibition constant
$K_m$	Michaelis Menten constant
MaxE	Maximal absolute error
MCPA	4-Chloro-2-methylphenoxyacetic acid
MX	Malaoxon
NC	Nitrocellulose
NEMO	Neural modelling
PBS	Phosphate buffered saline
PCS	Polycarbamoylsulfonate
PVA	Polyvinylalcohol
PVC	Polyvinylchloride
PVP	Polyvinylpyrrolidone
PX	Paraoxon-ethyl
PXmeth	Paraoxon-methyl
ReE	Mean relative error
RMSE	Root mean square error
RT	Room temperature
RTV	Room temperature vulcanisation
SPOE	Screen printed oxygen electrode
TBS	Tris buffered saline
TCNQ	7,7,8,8-Tetracyanoquinodimethane
TNB	2,4,6-Trinitrobenzenesulfonate
U	Units
$U_{pol}$	Polarisation potential
w/v	Weight per volume

Danksagung.....	I
Abstract.....	II
Zusammenfassung .....	III
Abbreviations .....	XIII
Table of contents .....	XIV

## 1 INTRODUCTION ..... 1

1.1 BIOSENSORS.....	1
1.1.1 <i>Thick film sensors</i> .....	2
1.1.2 <i>Thick film based biosensors</i> .....	4
1.1.3 <i>Biosensors for environmental monitoring</i> .....	5
1.1.4 <i>Multisensors</i> .....	6
1.2 ARTIFICIAL NEURAL NETWORKS .....	8
1.3 WORK OBJECTIVE.....	12
1.4 ACETYLCHOLINESTERASE MULTISENSORS .....	14
1.4.1 <i>Organophosphorus and carbamate insecticides</i> .....	14
1.4.2 <i>Detection of cholinesterase inhibiting insecticides</i> .....	15
1.5 DETECTION OF HALOGENATED AROMATICS.....	18

## 2 MATERIALS AND METHODS..... 22

2.1 AChE SENSORS .....	22
2.1.1 <i>Reagents</i> .....	22
2.1.2 <i>Enzymes</i> .....	22
2.1.2.1 AChE-sensor prototype .....	22
2.1.2.2 Wild-type AChE multisensor .....	22
2.1.2.3 Multisensor I and II .....	23
2.1.2.4 Enzyme activity test .....	23
2.1.3 <i>AChE sensor prototype</i> .....	24
2.1.3.1 Basic transducer fabrication .....	24
2.1.3.2 Variation of prototype manufacturing.....	25
2.1.3.3 Measurement set-up: AChE sensor prototype.....	27
2.1.4 <i>AChE multisensor</i> .....	28
2.1.4.1 Working electrode preparation .....	28
2.1.4.2 AChE immobilisation .....	28
2.1.4.3 Measurement set-up: AChE multisensor .....	30
2.1.5 <i>Data sets</i> .....	30
2.1.5.1 Wild-type AChE sensor .....	30
2.1.5.2 Multisensor I and II .....	31
2.1.6 <i>Artificial neural network performance</i> .....	31
2.2 MICROBIAL SENSORS .....	32
2.2.1 <i>Reagents</i> .....	32
2.2.1.1 Buffers .....	32
2.2.1.2 Growth substrates.....	32
2.2.1.3 Analytes.....	32
2.2.2 <i>Microbial strains and cultivation</i> .....	33
2.2.2.1 <i>Ralstonia eutropha</i> JMP 134, pJP4 ( <i>Alcaligenes eutrophus</i> ) .....	33

---

2.2.3 Determination of specific oxygen uptake rates.....	33
2.2.4 Development of microbial sensor prototypes .....	34
2.2.4.1 Screen printing of basic transducer .....	34
2.2.4.2 Working electrode.....	34
2.2.4.3 Electrolyte .....	35
2.2.4.4 Oxygen selective membrane: Spin coating / lamination .....	35
2.2.4.5 Immobilisation of micro-organisms .....	35
2.2.4.6 Monitoring of surface modification / TNB-test.....	38
2.2.4.7 Measurement set-up: Microbial sensor prototype.....	38
2.2.5 Microbial multisensors.....	39
2.2.5.1 Screen printing of the multisensor platform .....	39
2.2.5.2 Multisensor pretreatment.....	39
2.2.5.3 Cell harvesting .....	39
2.2.5.4 Immobilisation.....	39
2.2.5.5 Microbial multisensor equilibration.....	40
2.2.5.6 Storage .....	40
2.2.5.7 Measurement set-up: Microbial multisensor .....	40
2.2.6 Data sets .....	41
2.2.7 Artificial neural network performance .....	41
<b>3 RESULTS .....</b>	<b>42</b>
3.1 MULTIANALYTE AChE SENSORS.....	42
3.1.1 Development of AChE-sensor prototype.....	42
3.1.1.1 Stability of rhodium graphite electrode with drop-coated AChE.....	43
3.1.1.2 Printed AChE- rhodium graphite sensors .....	44
3.1.1.3 Stability of printed AChE-rhodium graphite sensors stored at 80 ° C ...	45
3.1.1.4 Coating of printed AChE-rhodium graphite -sensors with polyurethane	46
3.1.1.5 Drop-coated AChE-TCNQ-graphite-sensors .....	47
3.1.1.6 Printed AChE-TCNQ-graphite-sensors.....	48
3.1.1.7 Characterization of the final transducer format.....	49
3.1.2 Development of a wild type AChE multisensor .....	50
3.1.2.1 Basic characteristics of the AChE-multisensor .....	50
3.1.2.2 AChE-multisensor performance.....	51
3.1.2.3 Artificial neural network performance .....	53
3.1.2.4 Sample discrimination .....	54
3.1.2.5 Multisensor performance in real samples .....	55
3.1.3 Improved multisensors using <i>Drosophila</i> AChE mutants .....	56
3.1.3.1 Multisensor properties .....	56
3.2 MULTIANALYTE MICROBIAL SENSORS.....	66
3.2.1 Development of a planar oxygen electrode.....	66
3.2.1.1 Manufacturing of oxygen electrodes.....	66
3.2.1.2 Characterisation of SPOEs.....	69
3.2.2 Development of the microbial sensor .....	72
3.2.2.1 Preparation of the biological receptor: Cultivation of <i>Ralstonia eutropha</i> JMP 134 on different carbon sources.....	72
3.2.2.2 Determination of induction states .....	72
3.2.2.3 Immobilisation of the biological receptor.....	73
3.2.2.4 Basic biosensor characterisation .....	77
3.2.3 Multi-analyte detection I: Phenol and 2,4-dichlorophenol.....	83

---



---

3.2.3.1 Data generation .....	83
3.2.3.2 Data processing.....	84
3.2.3.3 Multianalyte detection results .....	85
3.2.3.4 Improving the multianalyte detection resolution.....	86
3.2.4 <i>Multi-analyte detection II: 4-Chlorophenol and 2,4-dichlorophenol</i> .....	89
3.2.4.1 Data generation .....	89
3.2.4.2 Data processing.....	90
3.2.4.3 Multianalyte detection results .....	91
3.2.4.4 Improving the multisensor resolution .....	91
<b>4 DISCUSSION .....</b>	<b>94</b>
4.1 MULTIANALYTE AChE SENSORS.....	95
4.1.1 <i>Development of the disposable sensor platform</i> .....	95
4.1.1.1 Manufacturing of the basic sensor.....	95
4.1.2 <i>The AChE multisensor approach</i> .....	99
4.1.2.1 Wild-type AChE multisensor .....	99
4.1.2.2 Mutant AChE multisensors I and II .....	100
4.1.3 <i>Artificial neural network performance</i> .....	103
4.1.4 <i>Real sample analysis</i> .....	103
4.1.5 <i>Conclusion</i> .....	104
4.2 MULTIANALYTE MICROBIAL SENSORS .....	106
4.2.1 <i>Screen printed oxygen electrodes</i> .....	106
4.2.1.1 Manufacturing of SPOE .....	106
4.2.1.2 Characteristics of SPOE .....	107
4.2.2 <i>The biological receptor</i> .....	111
4.2.3 <i>Microbial sensor manufacturing</i> .....	115
4.2.3.1 Immobilisation.....	115
4.2.3.2 Properties of the basic microbial sensor.....	117
4.2.4 <i>The microbial multisensor approach</i> .....	119
4.2.4.1 Multisensor properties .....	119
4.2.4.2 Judging the multisensor performance.....	119
<b>5 REFERENCES .....</b>	<b>123</b>

---

# 1 Introduction

## 1.1 Biosensors

Over thirty years after the first enzyme electrode was developed by Clark and Lyons in 1962 [1] an increasing number of biosensors were invented and commercial devices became available. A definition of the term „Biosensor“ was recently proposed by the International Union of Pure and Applied Chemistry in *Biosensors and Bioelectronics*: „A biosensor is a self-contained integrated device which is capable of providing specific quantitative or semi-quantitative analytical information using a biological recognition element (biochemical receptor) which is in direct spatial contact with a transducer element“ [2].



In simple words, the aim is to create a solid-state device analogue of the miner's canary, that serves as a real-live biosensor for oxygen which drops off in the presence of toxic gases. The photograph above shows two Welsh miners waiting to enter the mine with a canary caged in a crate.

In principle there are four transducer classes available for biosensors. These are potentiometric, amperometric, optical and other physicochemical probes which convert a biochemical signal into an electrical. Potentiometric electrodes, such as ion-selective field-effect transistors (ISFET) [3], measure the change of charge density. Amperometric sensors, i.e. dissolved oxygen electrodes [4], monitor currents originated by a biochemical reaction. Optical biosensors correlate changes in mass, concentration, or detect directly changes in light characteristics or intensity. As an important example, surface plasmon resonance (SPR) devices have to be mentioned [5]. Other physicochemical transducers monitor biological interactions via changes in conductance [6], mass [7] and enthalpy [8].

Biosensors are always of interest as soon as they offer advantages over standard laboratory equipment for an existing analyte in terms of specificity, sensitivity, assay speed or simplicity. In general, a biosensor is competitive if it helps to save costs by redundantizing trained personnel or avoiding consumables. As soon as biosensors detect parameters which are considered as equivalent to existing methods or rather

---

uncommon, certain hurdles in consumer perceptance and legislation have to be taken during commercialisation. The world-wide biosensor market is expected to grow significantly. By 1996 the biosensor sales volume was \$360 million and is estimated to become \$700 million by the year 2000 [9]. Biosensors are especially advantageous, when assay systems are required which can be used outside the laboratory for on-line, in-situ, in-field, or for point-of-care applications. In the latter case the glucose sensor ExacTech<sup>®</sup> by MediSense is especially successful having annual sales of about \$100 million [9]. This sensor is a ferrocene mediated glucose oxidase electrode strip which can be used in whole blood for diabetes control. This example was followed by several other companies, all on basis of portable devices and disposable sensors. The ExacTech<sup>®</sup> device, among many others, made use of thick film technology which is commonly used for manufacturing of electronic circuits. This technology enables mass production of cheap one-shot sensors for clinical, agricultural, veterinary and environmental applications. These areas are increasingly valid, particularly the environmental area, where major public awareness has been developed in recent years.

### 1.1.1 Thick film sensors

Thick film technology is used since the 1950s for the production of hybrid circuits in electronics. By composition of different materials it enables the formation of fine line conductor geometries. This technology allows a high packing density of microelectronic devices on a single substrate. The term „thick film“ refers to the thickness of layers (8 to 40  $\mu\text{m}$ ) related to thin-films which are vapour or sputter deposited and have a thickness of 0.02 to 2  $\mu\text{m}$ . Thick film devices consist of one or more layers of material on an insulating substrate, which are conventionally deposited by screen printing. Screen printing is a technique where viscous pastes or paints are pressed through apertures in stencils. The stencil is formed by a woven screen or a metal mask, having the layout of the desired device. While stencils in metal masks are usually laser carved, they can be formed photolithographically in screens which are covered with a photo cross-linkable coating [10]. A general description of the screen printing process can be seen in Figure 1.1.

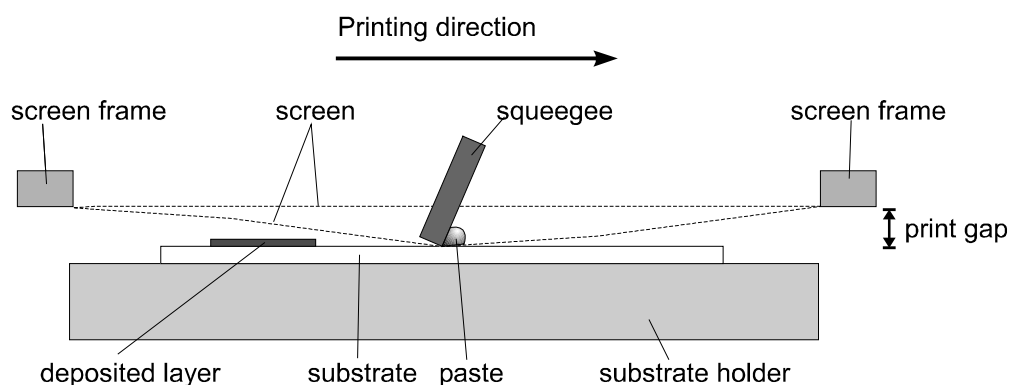


Figure 1.1: Schematic representation of the screen print process

Screen printing is performed by pressing paste through a screen by means of the moving rubber squeegee. The squeegee brings the screen into contact with the substrate surface dependent on screen tension and squeegee pressure, hardness and speed. The paste remaining in the screen aperture is then transferred to the substrate resulting in the desired layout. Whilst conventional screen printing inks have to be heated for curing, removal of solvents and tight fusion to the substrate, polymer based inks can be cured at temperatures below 100°C. As a result, low temperature curing inks are increasingly used. These inks enable the usage of plastic substrates, i.e. polyvinylchloride foils, making the whole process more suitable for mass production of disposable biosensors. Carbon is emerging as one of the favoured electrode materials and it is offered in a wide variety of paste formulations. An example of a commercial screen print machine is shown in Figure 1.2 below.



Figure 1.2: DEK 248, a semi-automatic, precision screen printer by DEK Printing Machines Ltd, UK.

In recent years there has been a growing interest in the use of screen printing technology for the production of biosensors. Although the major developments of thick film sensors were made in the field of physical parameters such as humidity, pressure, or tension, a considerable progress has been done in the development of chemical thick film sensors, which form the basic transducers for biosensors.

### 1.1.2 Thick film based biosensors

The leading example of biosensors using screen printed electrodes as transducers is the blood glucose sensor for the ExacTech® device by MediSense. While other manufactures participated in the success of biosensors for home use, such as Glucometer Elite® by Bayer Diagnostics or One Touch® by LifeScan, a large number of biosensors using screen printed disposable electrodes have been published in other application areas. A short overview on the literature is given in Table 1-1.

Table 1-1:

Selection of recent publications on disposable thick film biosensors

Analyte	Receptor	Reference
2,4-D	Antibody	[11]
2,4-D	Antibody	[12]
AChE inhibitors	AChE	[13]
AChE inhibitors	AChE	[14]
AChE inhibitors	AChE	[15]
Antibody	Progesterone	[16]
Atrazine	Antibody	[17]
Carbamates	AChE	[18]
DNA	DNA	[19]
DNA / Intercalators	DNA	[20]
<i>E. coli</i> DNA	DNA	[21]
Ethanol and Urea	Alcohol oxidase / urease	[22]
Ethanol	Alcohol dehydrogenase	[23]
Fatty acid-binding protein	Antibody	[24]
Formaldehyde	Formaldehyde DH	[25]
Glucose	Glucose oxidase	[26]
Heavy metal	Oxidases	[27]
Lactose	$\beta$ -Galactosidase / glucose oxidase	[28]
Lactose	Lactose oxidase	[29]
Maltose and glucose	Amyloglucosidase / glucose oxidase	[30]
Phenol	Tyrosinase	[31]
Phenol	<i>P.putida</i>	[32]
Progesterone	Antibody	[33]
Triazines	Antibody	[34]
Urea	Urease	[35]

Table 1-1 above gives an impression about the variability of screen printed electrodes. It is noteworthy that the selection does not reflect the number of publication in a certain field. Whilst a great number of reports on enzyme and DNA sensors has been published, the field of immuno or microbial sensors incorporating screen printed electrodes is still at the beginning. Additionally, it has to be kept in mind that most screen printed sensors for clinical diagnostics have been patented and do not occur in the literature. A specific situation, however, has to be concerned in case of biosensors for environmental monitoring. The reason for the success of glucose sensors was based on two main factors. First the high stability and

availability of the enzyme used, glucose oxidase and second, the mono-parametric detection mode. As only glucose has to be detected and the enzyme displays a narrow substrate specificity, glucose sensors succeeded. Moreover, blood as the medium to be investigated has a well defined composition which further focuses the analytical problem and eases the prevention of interferences such as hematocrit.

### 1.1.3 Biosensors for environmental monitoring

A completely different situation can be found for environmental monitoring. Here the analytical chemist faces samples of a highly variable, unknown content. Drinking water, as an example of key human nutrients, can contain hundreds of components of interest in trace concentrations. Especially the high number of crop protection pesticides which may be found in drinking water, cause considerable analytical effort. As an example, 1031 formulations on the basis of 257 active substances were registered for usage in Germany in 1998 (source: German Federal Environmental Agency). The challenging situation can be seen from the fact that for environmental monitoring thresholds for sum parameters are the general rule. In the case of pesticide monitoring, legislative action has focused on the definition of threshold levels of 0.5 µg/l for the sum and 0.1 µg/l for the individual concentration of pesticides [36]. Because for some of the analytes no compound-specific detection method exists, one has concentrated on the development of multi-residue methods based on Solid Phase Extraction in off-line with gas chromatography-mass spectrometry (GC-MS), high performance liquid chromatography-diode array detector (HPLC-DAD) and HPLC-MS [37]. Moreover, an European priority pollutant list is envisaged in order to narrow the analyte spectrum and give the possibility to set up sufficient standards [38]. Among possible priority pesticides compounds like atrazine, 2,4-dichlorophenoxy acetic acid, parathion and carbofuran are discussed to be added to the list. Alternative ways to overcome the lack of specific detection systems were the definition of sum parameters such as the AOX, which refers to the amount of adsorbable organic halogen detected by microcolourimetry [39]. Other examples are the chemical oxygen demand (COD) and the biological oxygen demand (BOD). The advantage of such sum parameters is the complete covering of a certain substance class.

Bioanalytical tests, especially biosensors, can be valuable tools for the detection of analytes in the presence of structurally related compounds which should not interfere. The diverse group of biosensors for environmental monitoring ranges from enzyme electrodes which use direct metabolism of the analyte, i.e. phenol sensors [40], enzyme inhibition, like it was shown in numerous cases for cholinesterase sensors [15] or the use of apoenzymes for heavy metal detection [41]. Other systems use microorganisms for the detection of environmental pollutants.

Microbial biosensors can be regarded as ideal sensors, because the biological component is readily available and the sensor works reagent free which gives the possibility to design devices at low cost. Microbial sensors have been oftenly used for the detection of single compounds like sulphite [42] or nitrate [43], but the main advantage of this kind of biosensors is the detection of sum parameters such as the biological oxygen demand (BOD). BOD sensors are one good example of

---

successfully commercialised biosensors. The most important are BOD 2000 from Central Kagaku, Tokyo, Japan and ARAS from Dr. Lange GmbH, Berlin, Germany. These sensors enable the determination of a parameter in few minutes which takes usually five days with conventional methods. Whilst the Japanese device has been widely distributed, ARAS in Germany has to gain acceptance against the standard operation [44].

Other powerful bioanalytical tools in the environmental field are immunosensors and immuno assays. On one hand they display a very high sensitivity and on the other a distinct selectivity. As an example, Richman *et al.* [45] used immunoassay techniques for the detection of 2,4-D in food samples with lower detection limits of 5 µg/l with a commercial assay kit (Ohmicron). However, in other cases like the detection of atrazine, a presence of metabolites and closely related compounds may be problematic due to the cross reactivity of the antibodies used. Wortberg *et al.* found no cross reactivities of an atrazine/simazine specific antibody for propazine [46] while Witmann *et al.* reported high cross reactivities for propazine for a different antibody [47]. Nevertheless, Wortberg *et al.* were able to detect simazine at lower detection levels of 0.05 µg/l.

As a common property most biosensor sensors show a characteristic, diminished selectivity towards cross-reacting analytes. Therefore, with most of the biosensors a specific quantification of a single compound is not possible and only sum parameters of related compound families can be obtained.

### 1.1.4 Multisensors

Sensing with receptors that have a broad specificity is a common motif in nature. The human nose, as an example, uses only a limited number of odour sensitive receptors for a sensitive detection at the parts per trillion level in combination with the discrimination of thousands of different odours. Upon action of certain odour molecules with olfactory ligands a signal cascade and neural transmission is started which amplifies and processes the response leading to a neural activity reflecting the smelled odour. The olfactory pathway reaches thereby its sensitivity and selectivity by using large arrays of cross-reactive receptors instead of using highly compound specific sensors [48].

Based on the principle of olfactory recognition various concepts for pattern recognition and multisensing with chemosensors have been described. The most known is the electronic nose [49]. Electronic noses use arrays of sensing elements, such as metal oxide sensors [50] or sensitive polymers [51] [52], which display a relatively wide and overlapping specificity. These chemical sensor arrays are combined with an automated data analysis system (i.e. artificial neural networks (ANN)) to identify vapours. As an example, chemical sensor arrays have been used for the detection of mixtures of chlorinated hydrocarbons using bulk acoustic wave transducers [53].

In the field of biosensors multianalyte detection has been an emerging area of interest in the last decade. With the developing technologies for nucleic acid

---

processing, a new perspective of biosensors has been opened. Recent developments focused for example on the use of fibre optic sensor arrays for analysis of gene expression [54]. The major progress of array technologies, however, has been made with DNA-chips. For a recent review see [55] and others in the same issue.

As another, in particular advantageous biological receptor, antibodies have been repeatedly used for multisensing approaches. Monoclonal antibodies from different origin display certain overlapping sensitivities which are related to the initial design of the immunogen. Especially for the detection of triazine herbicides several approaches have been undertaken. For a different set of enzyme tracers, characteristic cross-reactivity patterns can be found for each investigated mono- or polyclonal antibody [56]. Using these properties, Wittmann *et al.* [57] detected three different triazines (atrazine, terbuthylazine and terbutryn) using ELISA techniques with four different monoclonal antibodies followed by artificial neural network data processing. Optical biosensors, equipped with antibodies of different specificities to detect up to 14 substances in river water were reported by Brecht *et al.* [58;59]. Another promising approach for the detection of triazines was described by Winkelmaier *et al.* [60]. Here, the samples were analysed in a parallel affinity sensor array (PASA). Using this immunoarray the detection and identification of atrazine, terbuthylazine, simazine and deethylatrazine at a lowest level of 0.1 µg/l. Jinag *et al.* [61] described an immunosensor employing five quartz crystal microbalances (QCM) for the detection of immunoglobuline M and C-reactive protein. Each QCM was covered with a different antibody mixture exhibiting different response patterns which were analysed by linear regression methods (i.e. partial least squares).

Other approaches for multi-analyte detection for process control used multi-channel devices based on flow injection analysis employing a different enzyme per channel [62]. Flow injection analysis has also been employed for multi-analyte detection using field effect transistors (FET) by Hitzmann *et al.* They evaluated penicillin concentrations at various medium conditions by means of a signal processing of pH-FETs using artificial neural networks [63]. In further applications a similar system was expanded to the simultaneous detection of glucose and urea [64].

Disposable multi biosensors have been rarely published up to date. Wang and Cheng reported a screen printed micro disk array for the detection of glucose and lactate [26]. The electrochemical signals, however, were not further processed as the enzymes used displayed an absolute selectivity for the desired analytes. Starodub *et al.* reported a micromachined multi-enzymatic electrochemical sensor for field measurements [65]. The authors employed cholinesterases, urease and glucose oxidase, which were individually immobilised in a multichannel sensor chip, but only poor information is given on the selectivity of the system.

The predominant motivation for using multielectrode sensors were attempts to improve the statistical relevance of a measurement by a multi shot measurement. Successful examples have been shown for ethanol [23] and 2,4-D [66]. Other authors reported screen printing as a useful method to fabricate integrated chemical

---



sensor arrays [67] or microelectrode arrays with up to 3000 electrodes on an area of 5 x 5 mm [68].

Screen printing has proved essentially successful for the production of disposable multisensors. Although pattern recognition has been often performed with chemosensors, the combination of different enzymes or antibodies on thick film sensors followed by chemometric data evaluation is still lacking.

## 1.2 Artificial neural networks

Chemosensor arrays have been repeatedly used in combination with back-propagation artificial neural networks (BP-ANN) as it was shown for electronic noses [69]. Other possibilities are probabilistic neural networks (PNN), learning vector quantitation neural networks (LVQ), soft independent modelling of class analogy (SIMCA), Bayesian linear discriminant analysis (BLDA), Mahalanobis linear discriminant analysis (MLDA), and the nearest neighbour pattern recognition algorithms (NN) [70]. In a comparison of the methods mentioned above for the classification of multisensor data, the artificial neural network approaches gave the best results [69]. Other authors describe multivariate calibration techniques such as linear regression, multiple linear regression (MLR), and principal component analysis (PCA) for the chemometric analysis of multisensor array data [71]. Seemann *et al.* compared classical multivariate regression with BP-ANN analysis for the processing of chemosensor array data. Here, the backpropagation artificial neural networks performed best [51]. As a general rule, sensor data which display overlapping clusters and multimodality require non-linear classifiers. If a sensor array should display pattern vectors which are normally distributed around the mean vector, the neural network perform as accurately as linear classifiers. The clear advantage of neural network approaches is that the main computational effort can be done prior the actual test. Nevertheless for both ways of regression, successful examples can be given, either linear regression [72] or non-linear [57].

A short introduction in the theory and terminology of artificial neural networks is given in the next section, for more detailed information see recent reviews of Zupan and Gasteiger [73] or Zell [74].

Artificial neural networks (ANN) are programs which are intended to act in a similar way a simple biological brain operates. They are based on virtual „nerve cells“ called neurons, units or nodes. These nodes are connected among each other in multiple ways to build up networks. In ANN terminology these simulated „axons“ are called connections. Such networks have the capacity to learn, memorise and create relationships amongst data sets. The most oftenly used artificial neural network is the Back Propagation ANN. The term „back propagation“ refers to the learning mode of the network and is explained below. This type of ANN is suited for prediction and classification questions. Other examples are Kohonen Networks or Self Organising Maps which are more applicable for finding relationships of complex data.

---

The architecture of artificial neural networks is conventionally built up out of layers. These contain a number of interconnected nodes or units bearing an activation and output function (Figure 1.3). A model representation of an unit is given in Figure 1.4.

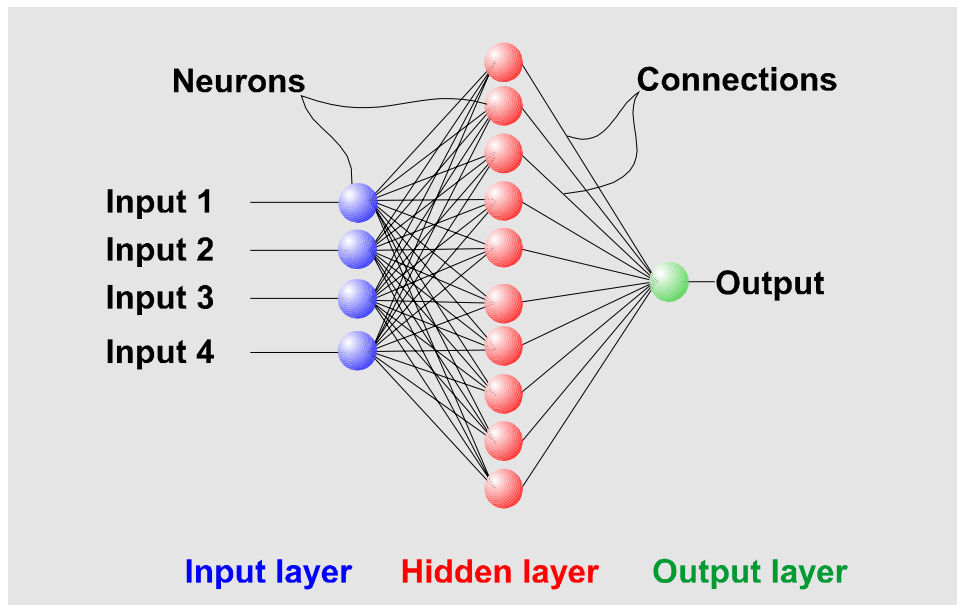


Figure 1.3: General architecture of a 3 layer, feed forward artificial neural network

One can distinguish three types of units: input units, hidden units, and output units. Each unit can be defined by the activation function  $f_{act}$ :

$$a_j(t) = f_{act}(net_j(t) - \theta_j)$$

$a_j(t)$	activation function of unit $j$ in step $t$
$net_j(t)$	net input in unit $j$ in step $t$
$\theta_j$	threshold of unit $j$

In most cases the sigmoidal activation function is used, which leads to a logistic activation function:

$$f_{act}(x) = (1 + e^{-x})^{-1}$$

The output function of a unit is defined as:

$$o_j(t) = f_{out}(a_j(t))$$

$a_j(t)$	activation function of unit $j$ in step $t$
$o_j(t)$	output in unit $j$ in step $t$
$j$	unit index in the net

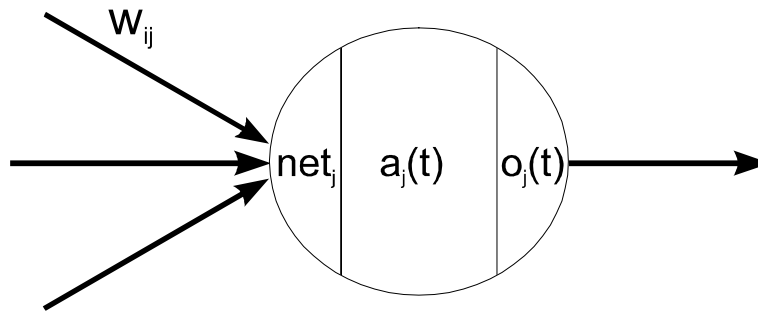


Figure 1.4: Components of an unit:  $a_j(t)$  activation function, the value  $net_j(t)$ , and an output function  $o_j(t)$ . The weighted connection is  $w_{ij}$ , which connects units.

The generalisation ability of a neural network is dependent on the training of the network using a data set. Training of ANN means setting the weights of the connections between the neurons. For this purpose and for validation of the network ability a data set is usually divided in three parts:

1. Training data: Uses the biggest part of the available data. The network error is minimised using this data set.
2. Validation data: Used for testing the networks ability to generalise a data set which was never used for training.
3. Test data: Similar to validation data, but usually obtained by a novel series of tests with the analysis system. Used for checking the overall performance of the system.

A special feature of several ANN modelling softwares is the possibility to use cross validation [51]. Cross validation was also implemented in NEMO, the software which was used in this work. This procedure is essentially useful for systems which produce rather small data sets. This is especially the case for biosensors, as they often exhibit complicated and time consuming test procedures. During the cross validation procedure the neural network is trained in a data set leaving a certain number of data out of the training. These data are used for validation in the same training cycle. In the next round, another set of data is left out for the same purpose. Within one complete training session the program uses all available data for cross validation. Especially for smaller data sets this procedure is more efficient, than validating the network performance with a statistically not significant number of independent test data.

The training of feed forward neural networks is performed by a defined set of steps:

Propagation phase:

- Randomizing of network weights and activation functions
- Presentation of an input pattern to the network
- Propagation to the output layer

Backward propagation phase

- Comparison of output  $o_j$  with input pattern  $i_j$
- Calculation of link changes  $w_{ij}$  for unit  $j$  using the error  $\delta_j$  between output  $o_j$  with teaching input  $t_j$
- Proceeding backwards using already calculated units as teaching units

The most widely used formula for this backpropagation of the network error is the Standard Backpropagation:

$$\Delta_p w_{ij} = \eta o_{pi} \delta_{pj}$$

$o_{pi}$  output of unit  $i$  for the pattern  $p$

$\delta_{pj}$  difference between calculated output and teaching input

$\eta$  constant learning factor

Other methods of network training are variations of the standard backpropagation: Backpropagation with momentum term, backpropagation with weight decay or Rprop (resilient propagation) and Cascade correlation. A detailed description of available algorithms is found in [74].

## 1.3 Work objective

The aim of this work was to develop two novel systems for multi-analyte detection in environmental monitoring. The systems should comprise of

1. a disposable multi electrode biosensor,
2. a suitable data processing tool.

The data analysis should be performed with the neural modelling software NEMO 1.15.02 [75]. Thus, the development of the novel multisensor format was the essential part of this work. The intended combination of multisensor and artificial neural network is shown in Figure 1.5. First a set of data is generated by the use of a number of disposable multisensors. This data set („sensor signal“) is then used for training of the ANN. In a second step sensors from the same batch as the training sensors are used to analyse unknown samples. Finally, with the aid of the previously trained ANN the correct concentrations of the target analytes can be calculated.

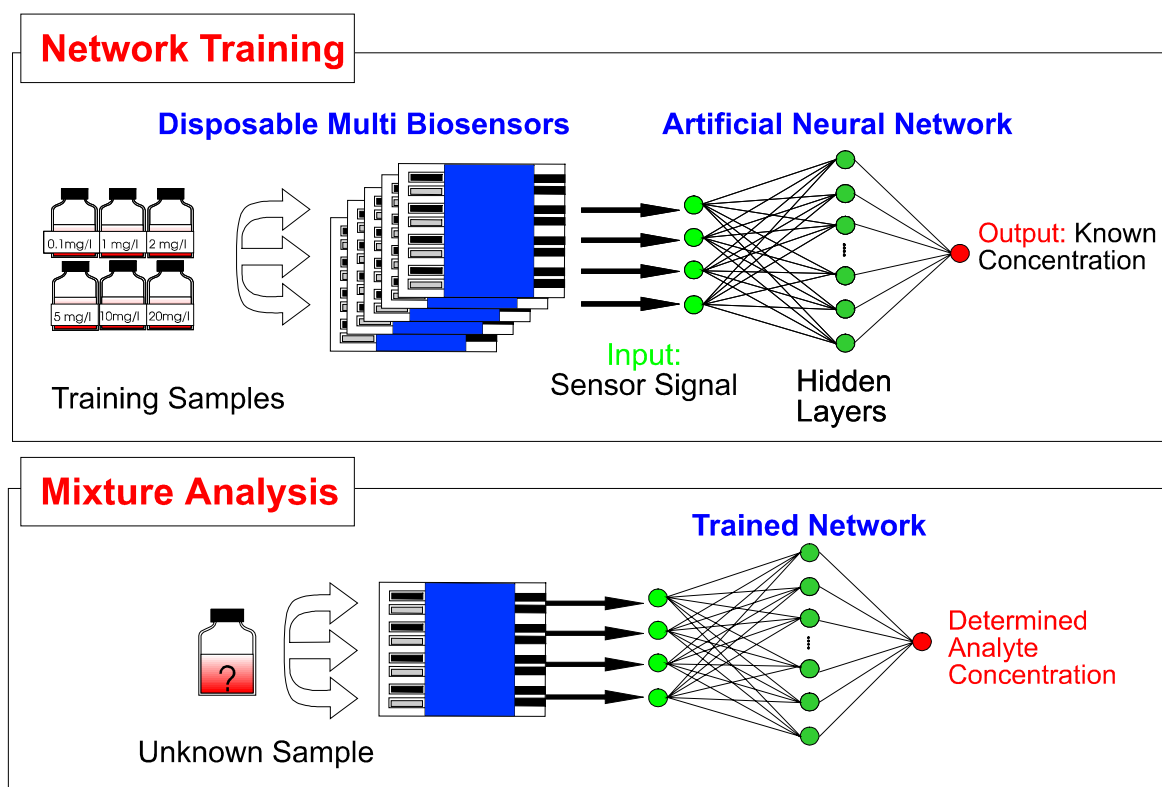


Figure 1.5: Combination strategy of multielectrode biosensors with ANN data processing for simultaneous multi-analyte detection in unknown samples.

The feasibility of the project concept should be demonstrated for two basically different biosensor systems: enzyme and microbial biosensors. From this tasks the following project progression was envisaged:

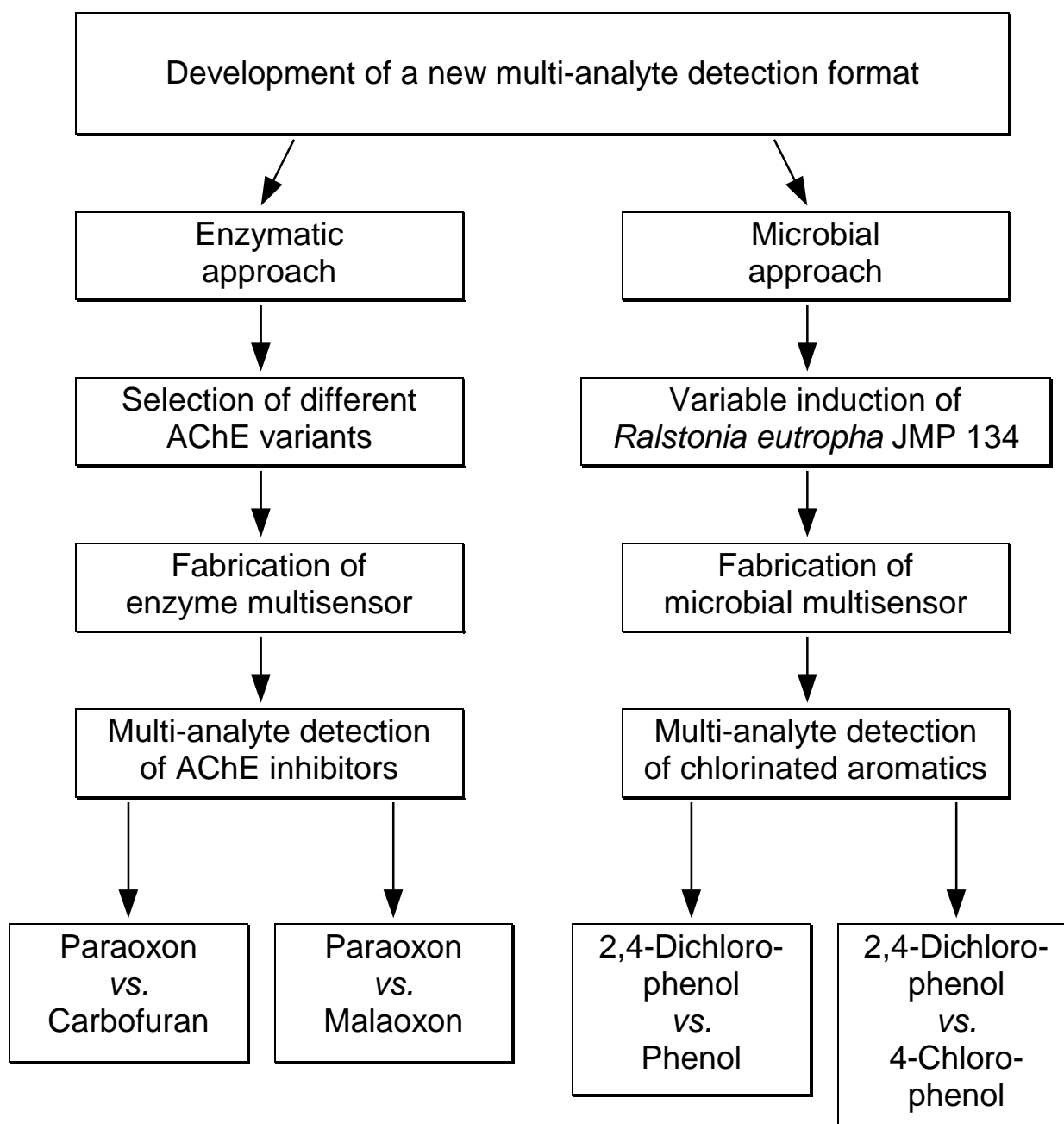


Figure 1.6: Project progression

## 1.4 Acetylcholinesterase Multisensors

### 1.4.1 Organophosphorus and carbamate insecticides

The extensive use of pesticides to protect agricultural crops necessitates reliable tools for the detection of residues in food and water, thus ensuring environmental protection and consumer safety. Organophosphates, such as paraoxon, and carbamates, such as carbofuran, are widely used in agriculture because of their high insecticidal activity and their rapid mineralisation in the environment [76]. In 1996 nearly three quarters of all insecticides used in Germany belonged to the group of cholinesterase inhibitors.

Figure 1.7 shows the distribution of compound classes on the insecticides used in Germany 1996 (source: Industrieverband Agrar, Germany).

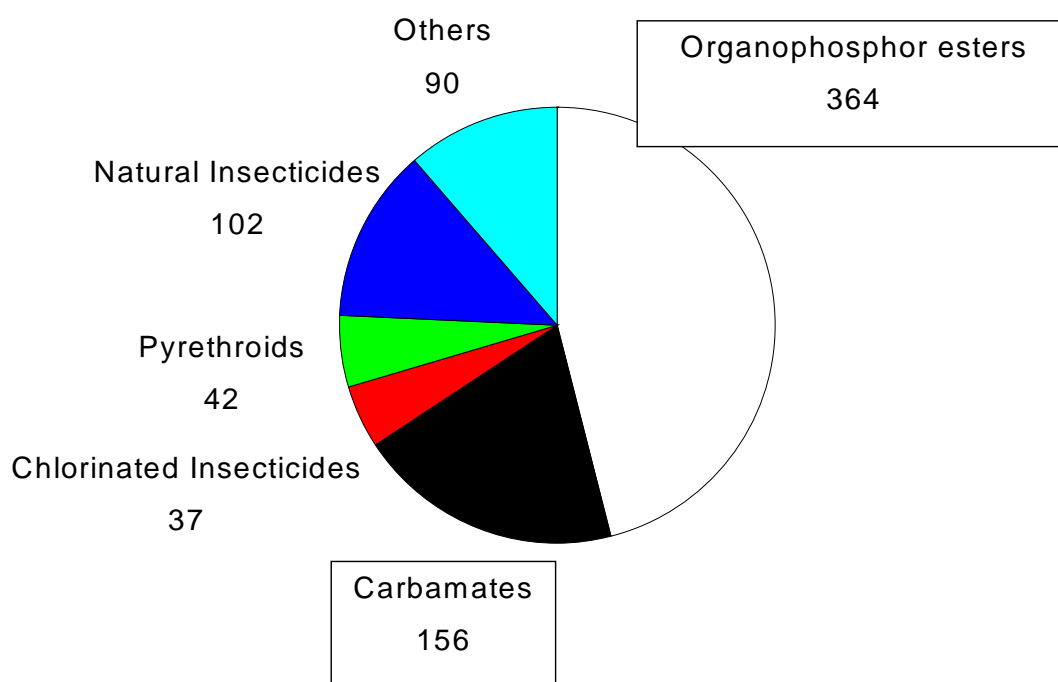


Figure 1.7: Insecticide usage in Germany 1996. (numbers refer to tons)

Since organophosphates and carbamates not only inhibit insect acetylcholinesterase (AChE), but also interfere with neural transmission in other organisms, including humans, they represent a potential hazard for human health and environmental food chains, and thus require continuous assessment [36]. Recent reports on organophosphate contamination in baby food [77;78] have for example initiated the reassessment of residual concentrations of these compounds permitted in view of the US Food Quality Protection Act [79].

### 1.4.2 Detection of cholinesterase inhibiting insecticides

Highly sensitive and specific chromatographic detection methods, such as HPLC, GC, GC-MS or LC-MS/MS, are available for the detection of organophosphate and carbamate insecticides in food and environmental samples, but these are expensive and time-consuming and currently not suitable for field use [80;81]. Alternatively, a relatively simple spectrophotometric assay for organophosphate and carbamate detection based on cholinesterase inhibition has been standardised but is rather laborious and unsuitable for the detection of mixtures or for on-site analysis [44].

A model of the structure of AChE is shown in Figure 1.8. The active site including acetylcholine, the natural substrate is shown in Figure 1.9. The mode of acetylcholinesterase inhibition by paraoxon and carbofuran is described in Figure 1.10.

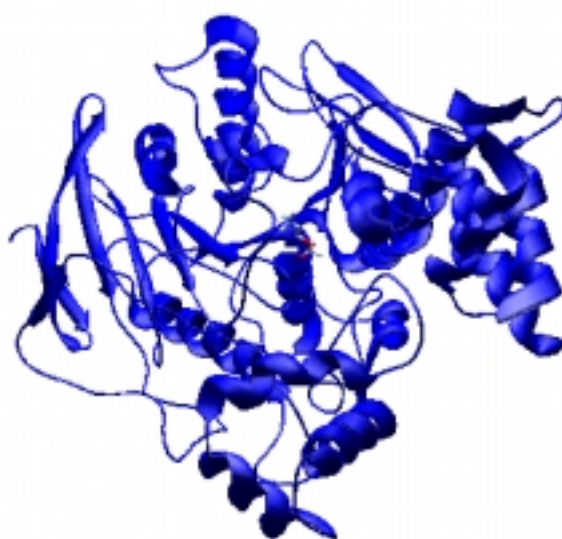


Figure 1.8: Model structure of *Torpedo californica* acetylcholinesterase

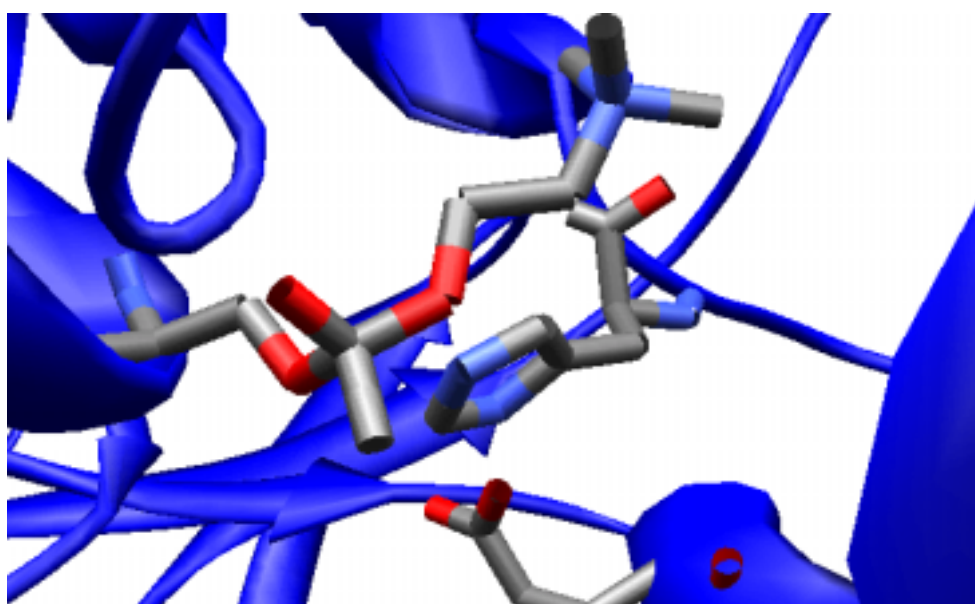


Figure 1.9: Active site structure of *Torpedo californica* acetylcholinesterase



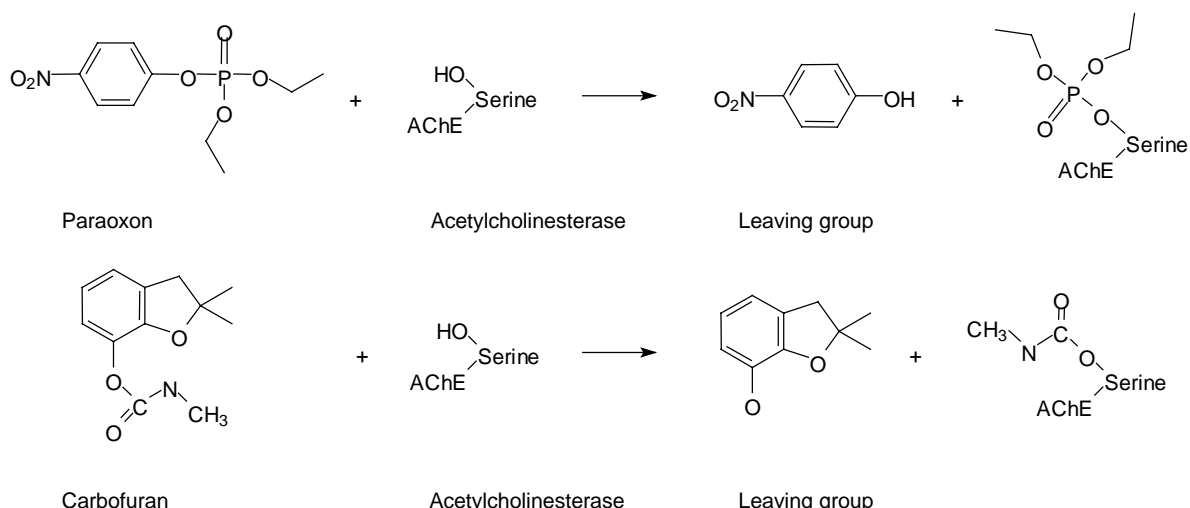


Figure 1.10: Schematic view on AChE inhibition by paraoxon and carbofuran

A number of biosensors that function according to the principle of AChE inhibition have been proposed. In addition to a commercial AChE-based sensor (Cide Lite from Charm Sciences, Malden, USA [82]), numerous prototypes have been developed that are based on potentiometric [83;84], amperometric [85-87] and piezoelectric [88;89] transducers. Since enzymatic activity in AChE-based biosensors is destroyed upon calibration or in the presence of the analyte, the sensor must either be discarded after evaluation [15;14] or the enzyme must be replaced [90-93]. A severe drawback of all methods described previously based on cholinesterase inhibition emerge from the fact that various organophosphates and carbamates inhibit this enzyme to a different extent, rendering calibration for an unknown mixture virtually impossible. In practice, calibration with paraoxon is still used, but the value of such an assay for the quantitative determination of AChE inhibitors of unknown composition does raise doubts. All biosensors described so far are based on the same mechanism, thus giving a sum parameter expressed as total anti-acetylcholinesterase activity using paraoxon as reference.

Multianalyte detection can benefit from different inhibitory properties. Cholinesterase inhibitors can reveal the individual binding properties and the origin and structure of the cholinesterase itself can also define its affinity [94]. A reliable detection system should be capable of discriminating and quantifying several inhibitors in a mixture. Based on the combination of different enzymes, one approach has been described by Schäfer *et al.* [95] using a microtiter plate assay for the differentiation of cholinesterase inhibitors. In this case, acetylcholinesterases from electric eel and bovine erythrocytes and butyrylcholinesterases from human and horse serum were used in procedures involving sample oxidation, enzyme inhibition and reactivation, followed by chemometric analysis. Similarly, Danzer *et al.* [96;97] developed a test method for the identification of aldicarb, trichlorofon and mercury in ternary mixtures with concentrations of 1 mg/l of each compound. Accordingly, acetylcholinesterases from electric eel and acid- and alkaline-phosphatase were immobilised on three standard commercial pH-electrodes prior to performing data analysis by standard multivariate analysis. Although both methods allowed analyte discrimination in principle, their suitability for on-site analysis or for being marketed commercially

seems doubtful on account of the expense involved in terms of equipment, chemometric analysis and time.

The target of this work was to apply a multianalyte biosensor based on a disposable, thickfilm multielectrode for highly sensitive insecticide detection. The intention of this project was to take previous work one stage further [95-97] by focusing on cholinesterase inhibition and advanced data processing only. Using a combination of different enzymes on one sensor and ANN data evaluation a reliable, and simple test method should be developed.

The first strategy was based on the use of either commercially available acetylcholinesterases from natural sources or recombinant acetylcholinesterases, all of which differ both in sensitivity and specificity. As such variants display a desirable cross-reactivity towards both analytes, the multisensor signals can be subjected to chemometric analysis [98].

In a second approach, an improved sensor performance should be possible by employing recombinant AChE mutants with the relevant properties, which up until now has not been reported. In particular, specific and high inhibition constants for the desired analytes were expected to improve the sensor's capacity in terms of assay duration, enhanced sensitivity, and analyte range. Earlier investigations into AChE mutagenesis were performed to determine the properties of the enzyme and its hydrolytic mechanism [99-102]. For analytical purposes, the highly sensitive AChE from *Drosophila melanogaster* and rat brain AChE were genetically engineered to increase their suitability for a possible biosensor application [103-105]. The production of recombinant AChEs is a well-established method [106-108] that provides a supply of good quality enzyme in sufficient amounts in contrast to purification from natural sources. Here, for the first time the use of recombinant proteins for multisensors is described. Four different mutants of *Drosophila melanogaster* AChE, which were adapted specifically by protein engineering for enhanced sensitivity [104], should be used for the rapid multianalyte detection of binary mixtures of paraoxon with malaoxon or carbofuran using disposable multisensors.

---

## 1.5 Detection of halogenated aromatics

Organohalogene substances are generally regarded as problematic or frightening in the modern and ecologically aware society. In this respect, legislative action was demanded. As a result with the 5th modification of the German Federal Water Resources Act the AOX as an additional parameter for water monitoring was introduced in 1986. AOX refers to adsorbable organic halogen and includes all halogenated substances which can be adsorbed from water samples to activated carbon. The adsorbed substances are then detected microcolourimetrically. This method follows a standard operation according to DIN 38409-14. Since the implementation of this parameter it became well established for screening and supervision of industrial effluents. However, the AOX is usually identified in an unjustified way with spectacular cases of highly toxic chlorinated compounds such as DDT.

Additional problems may arise within the detection procedure from the fact that AOX can be formed by various states of compounds. The AOX can contain particle bound, dissolve, dispersed, or volatile substances. Other misinterpretations can result from high salt concentrations in the samples. Nevertheless, AOX is a useful parameter for the assessment of industrial waste water clean up. In contrast to the general public opinion, the rating of AOX as a synonyme for toxicity can not be confirmed. A study of industrial relevant compounds carried out by Voelskow in [109] showed that toxicity could not directly be correlated to the AOX. As an example, this report demonstrated that the  $EC_{50}$  values of the majority of substances belonging to the AOX ranked in the upper concentration range (Figure 1.11).

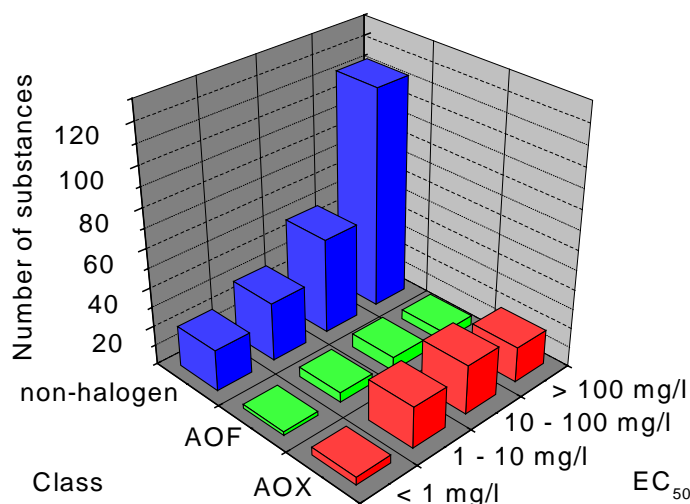


Figure 1.11: Rating of industrially relevant chemicals according to the fish test  $EC_{50}$ .

Although this data can only be taken as a general trend, they demonstrate that the mere suspicion of toxicity of organohalogens is not justified. Similar results were found for persistence and accumulation in the food chain.

For this reason a test additional to the AOX, which would be capable to detect organohalogenes individually and in presence of other less toxic compounds, would be helpful. In order to develop such a test system for this purpose, chlorinated phenols were chosen as model analytes for chlorinated aromatic hydrocarbons.

Chlorinated phenols are important intermediates and products of the chemical industry. They are considered to cause environmental problems if liberated into the biosphere. It is estimated that from a yearly world-wide production of 40.000 t monochlorinated phenols (1990), 10 % or 4000 t are released into the environment [110]. Chlorination of drinking water is a further source of chlorinated aromatic compounds in the water cycle [111]. Thus, the detection of these chemicals is an essential part of environmental monitoring, and HPLC and GC-MS are currently the methods of choice [112;113].

For rapid on-site analysis of water and soil samples it would be desirable to have simpler and portable analytical equipment available. Various enzyme sensors based on mushroom phenolase and tyrosinase have been proposed for phenol and chlorophenol detection, but leave much to be desired in terms of their narrow substrate specificity which is limited to phenol derivatives [114;115]. Microbial sensors are an interesting alternative to specifically detect chlorinated aromatic compounds, as many microbial strains have developed pathways along which aromatic compounds including halogenated xenobiotics are oxidized [116]. Isolated enzymes from these pathways are not suitable for biosensor use as they are usually instable after purification and depend on cofactor regeneration [117]. Microbial sensors for phenol and chlorophenols, which have been described to date were all based on conventional Clark-type oxygen electrodes [118-121].

An investigation of the suitability of microbial strains for biosensor use has been described by Beyersdorf-Radeck *et al.* [122]. Amongst the tested strains *Ralstonia eutropha* JMP 134 proved to be favourable for the use in a microbial biosensor. The degradative potential of *R.eutropha* JMP 134 is one of the best described for halogenated xenobiotics. These capabilities are mainly related to the presence of the plasmid pJP4 which harbours the information for the mineralisation of 2,4-dichlorophenoxy acetic acid and 3-chlorobenzoate as well as mercury resistance [123;124]. *R.eutropha* JMP 134 seemed to be especially suitable for a multisensor approach as this strain harbours three phenolhydroxylases. Pieper *et al.* proposed the existence of three different phenol hydroxylating activities in *R. eutropha* JMP 134 [125]. This property would make pattern recognition possible, if four differently induced *R. eutropha* JMP 134 cells are used for the multisensor. Based on literature data, the following substrates were chosen to create specific induction patterns: 2,4-dichlorophenoxyacetic acid (2,4-D), 4-chlor-2-methylphenoxyacetic acid (MCPA), 2-methylphenoxyacetic acid (2-MPA), and phenol. The degradation pathways in *R.eutropha* JMP 134 for the four substrates until aromatic ring cleavage are shown in Figure 1.12. While MCPA and 2,4-D are oxidised via the chloroaromatic degradation pathway leading to an ortho cleavage, 2-MPA and phenol can be degraded either via the ortho or the meta pathway. The inducing agent, however is not the carbon source itself, but a degradation intermediate. Filer *et al.* discovered dichloromuconate as the inducing agent of the 2,4-D degradation pathway using transposon mutagenesis and reporter assays [126].

---

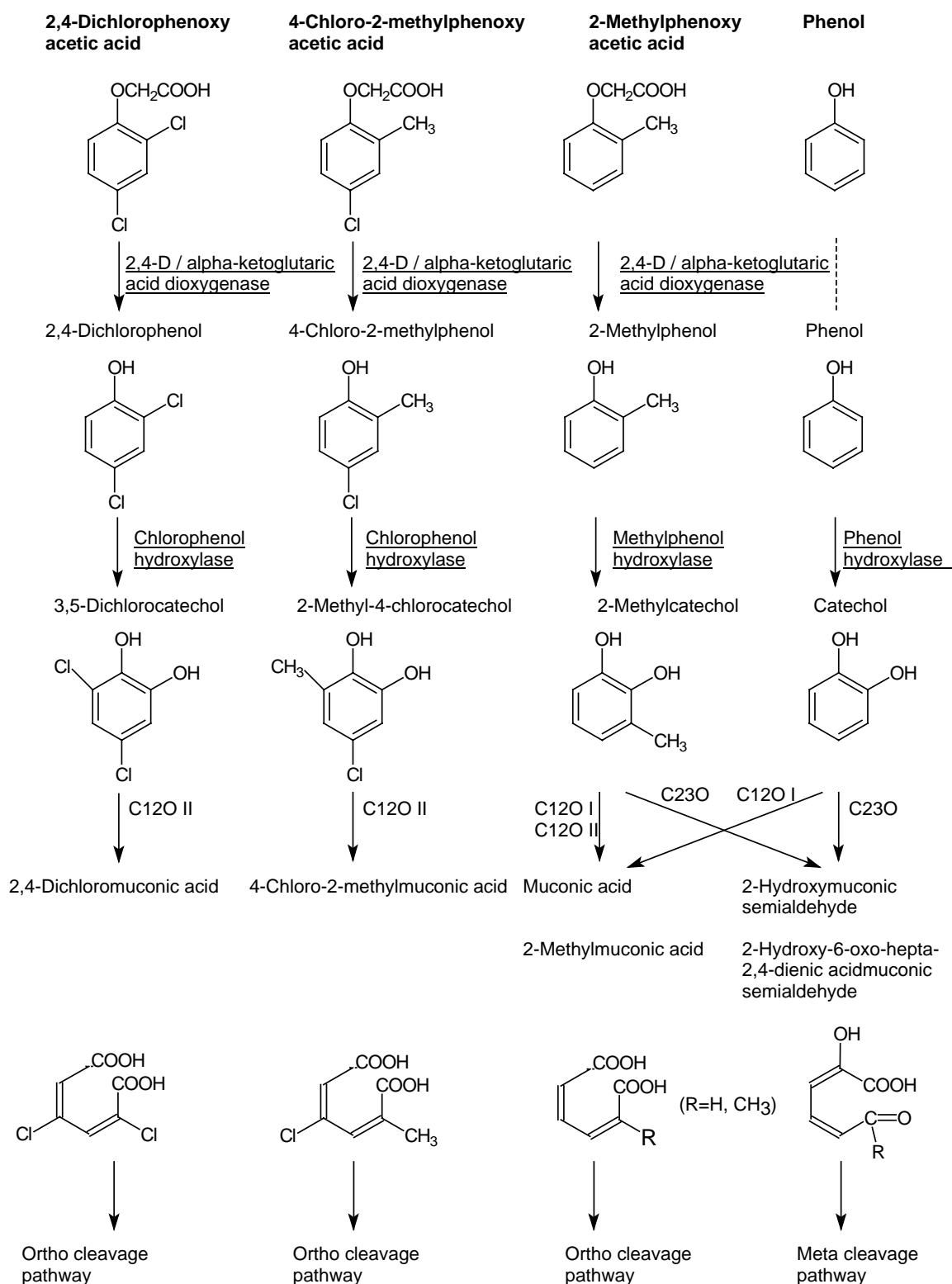


Figure 1.12: Degradation pathways for 2,4-D, MCPA, 2-MPA and phenol in *R. eutropha* JMP 134 [127;124]. (C12O-II: catechol 1,2-dioxygenase type II, (3,5-dichlorocatechol 1,2-dioxygenase), C12O-I: catechol 1,2-dioxygenase type I, C23O: catechol 2,3-dioxygenase)

The ideal end product of this multisensor development would be a hand-held device requiring minimal operator training. The device should be used at the site of analysis and give immediate information. It should be furthermore highly specific, reliable and cheap to produce. To meet these demands, a transducer had to be developed, which was capable to measure cell respiration upon analyte addition and was preferably miniaturised and disposable.

Most of previously described microbial biosensors [128;118-121;129] used conventional Clark-type oxygen electrodes as transducers [130]. These electrodes are, however, far too expensive to be disposable and attempts to use disposable microbial membranes in commercial devices such as the ARAS (Dr. Lange GmbH, Berlin) for BOD measurement are not favourable. A schematic view on a membrane covered oxygen electrode with immobilised microorganisms is shown in Figure 1.13.

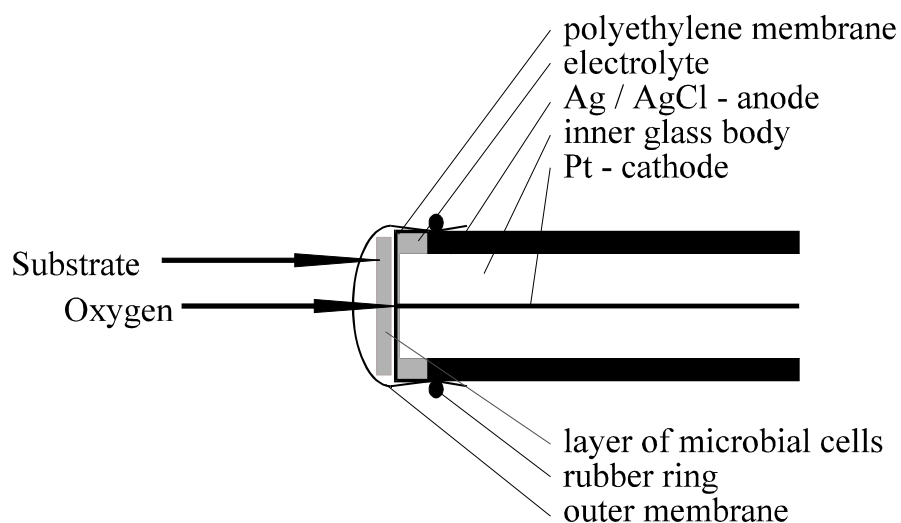


Figure 1.13: Cross section of a Clark type oxygen electrode which was used for a microbial biosensor [122].

Attempts to develop miniaturised oxygen electrodes [131;132;4;133-137] mostly followed the design proposed by Clark [130]. Microbial biosensors incorporating miniaturised oxygen electrodes were described for the detection of BOD [138] and inhibition of nitrification [139]. To date there are no reports available about the use of microbial multisensors for pattern recognition. One approach to employ microorganisms for multi-analyte detection was reported by Slama *et al.* [72]. In this case the dynamic response of a single sensor upon analyte mixtures was evaluated by means of linear regression methods.

Consequently, the objectives of this project part were :

- Developement of a novel transducer (multi oxygen electrode)
- Set-up and performance of a microbial mutlisensor for multi-analyte detection of chlorophenol mixtures

## 2 Materials and Methods

### 2.1 AChE sensors

#### 2.1.1 Reagents

All insecticides were purchased from Riedel de Haën (Seelze, Germany). in Pestanal quality. Insecticide stock solutions were prepared as 1 g/l solutions in ethanol and stored at - 20 °C. Dilutions for sensor measurements were made daily and stored at - 4 °C. All other reagents were of analytical grade as supplied by Sigma-Aldrich (Deisenhofen, Germany), unless stated otherwise.

Table 2.1:

Insecticides used as analytes for AChE sensor measurements

Abbrev.	Real name	Molecular weight [g/mol]
PX	Paraoxon-ethyl	275.20
CF	Carbofuran	221.26
MX	Malaoxon	314.30
PXmeth	Paraoxon-methyl	247.14
AC	Aldicarb	190.27

#### 2.1.2 Enzymes

##### 2.1.2.1 AChE-sensor prototype

The development of the AChE-sensor prototype was performed using the acetylcholinesterase (E.C. 3.1.1.7) from electric eel („eeAChE“) (Type V-S, 1580 U/mg) which was obtained from Sigma-Aldrich (Deisenhofen, Germany).

##### 2.1.2.2 Wild-type AChE multisensor

The wild-type AChE-multisensor was equipped with the following AChEs: Acetylcholinesterase (E.C. 3.1.1.7) from electric eel; AChE from bovine erythrocytes („beAChE“) (2 U/mg) was purchased from Boehringer Mannheim (Mannheim, Germany). Recombinant AChE from rat brain („rbAChE“) and *Drosophila melanogaster* wild-type AChE („dmAChE“) were expressed in a baculovirus/insect cell system as described before [140;106].

## 2.1.2.3 Multisensor I and II

*Drosophila melanogaster* wild-type acetylcholinesterase („dmAChE“) and AChE mutants Y408F (330) , F368L (290), F368H (290) and F368W (290) were produced as described previously [107;104] (numbers in brackets correspond to *Torpedo* AChE numbering.).

## 2.1.2.4 Enzyme activity test

The determination of enzymatic activity of dissolved AChE was performed according to the method of Ellmann *et al.* [141] using acetylthiocholine iodide as substrate and DTNB as chromogen.

Table 2.2:

Parameters for spectrophotometric determination of AChE activity

Test parameter	Value
Photometer	Pharmacia Biochrom 4060
Wavelength	412 nm
Light path	1 cm
Temperature	25°C
Assay time	20 min
Test volume	0.5 ml
$\epsilon$ DTNB	13600 l mol <sup>-1</sup> cm <sup>-1</sup>
$C_{\text{ACh}}$	$2.5 \cdot 10^{-3}$ mol/l
$C_{\text{DTNB}}$	$6 \cdot 10^{-4}$ mol/l

Volumes for assay	
ATCh solution	0.40 ml
DTNB solution	0.40 ml
AChE solution	0.20 ml

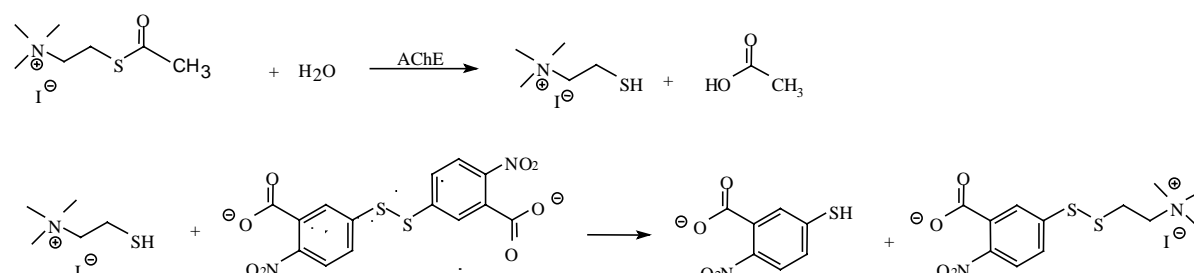


Figure 2.1: Reaction scheme of acetylthiocholine hydrolysis to thiocholine and acetate and subsequent reaction of thiocholine with DTNB forming 5-thio-2-nitrobenzoate.



## 2.1.3 AChE sensor prototype

### 2.1.3.1 Basic transducer fabrication

The transducers for this work were produced by screen printing as illustrated in Figure 2.2 on flexible polyvinylchloride sheets from SKK (Denzlingen, Germany) using a DEK 249 screen printer (DEK Ltd., Weymouth, England) and polyester screens that were purchased from Steinmann GmbH (Stuttgart, Germany). Screen printing inks (Electrodag PF-410, Electrodag 423 SS, Electrodag 6037 SS) were obtained from Acheson (Scheemda, Netherlands). Marastar SR 057 purchased from Marabu (Tamm, Germany) was used as insulation ink. The electrodes were cured for 30 min at 90°C after each printing step before enzyme immobilisation. All further developed sensors based on this prototype of electrode. The electrodes were printed in sets of 4 or 8 x 4 electrode pairs. Table 2.3 and Table 2.4 give the detailed parameters of the printing process of the basic transducer and Figure 2.3 displays the dimensions of the completed electrode.

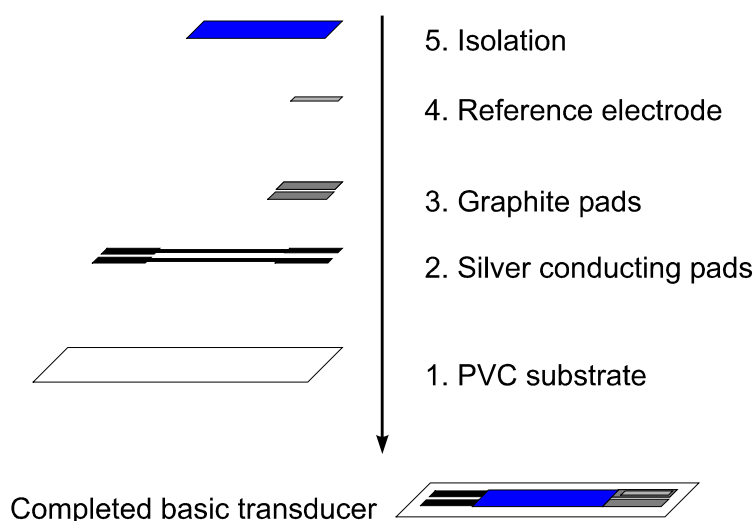


Figure 2.2: Screen printing of basic transducer.

Table 2.3:

Screen printing parameters for production of basic transducers.

Printing step	Paste	Squeegee pressure	Print mode	Gap [mm]	Squeegee speed [mm/s]
1 - Silver conducting tracks	Electrodag PF-410	4	flood/print	1.7	50/50
2 - Graphite pads	Electrodag 423 SS	5	flood/print	1.8	70/70
3 - Reference electrodes	Electrodag 6037 SS	4.5	flood/print	2.1	70/70
4 - Isolation	Marastar SR 057	5	flood/print	2.3	70/70

Table 2.4:  
Screens used for production of basic transducer

Printing step	Screen material	Mesh angle	Screen thickness	Screen coating	Screen mesh
1	polyester	45°	55 $\mu\text{m}$	Monolen Plus	120 T
2	polyester	45°	55 $\mu\text{m}$	Monolen Plus	80 T
3	polyester	45°	55 $\mu\text{m}$	Monolen Plus	100 T
4	polyester	45°	55 $\mu\text{m}$	Monolen Plus	100 T

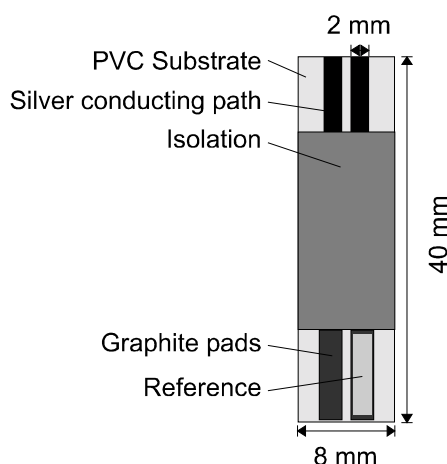


Figure 2.3: Basic transducer components and dimensions.

#### 2.1.3.2 Variation of prototype manufacturing

During the development of the AChE sensor prototype, the following working electrode compositions were tested:

Table 2.5:  
Parameters for AChE sensor production - Variation 1

Component	Paste	Protocol
Working electrode	Rhodium graphite <i>printed on basic transducer (Figure 2.3)</i>	1. 10% rhodium graphite in 3 % HEC (15 min homogenised at 24000 rpm Ultraturrax (Ika, Staufen, D,model T-25))
		2. 30 min drying at 80 °C
Immobilisate 1	AChE/BSA <i>drop-coated on working electrode</i>	3a. 5 U/ml, 10 mg BSA, 2.5 % GA 30 $\mu\text{l}$ , 3 $\mu\text{l}$ / electrode
		4a. 30 min drying
Immobilisate 2	AChE <i>drop-coated on working electrode</i>	3b. 10 $\mu\text{l}$ of 5 U/ml AChE solution
		4b. 60 min drying
Polarisation	$U_{\text{pol}} = + 410 \text{ mV vs. Ag/AgCl}$	

Table 2.6:

Parameters for AChE sensor production - Variation 2

Component	Paste	Protocol	
Working electrode +immobilisate	Rhodium graphite + AChE / BSA <i>printed on basic transducer (Figure 2.3)</i>	1.	10% rhodium graphite in 3 % HEC (15 min homogenised at 24000 rpm Ultraturrax (Ika, Staufen, D,model T-25))
		2.	Mixing with AChE 1 U/ml in 5 % BSA
		3.	Screen printing
	cross-linking	4a.	0 - 22 h GA vapour, 4 ° C
		4b.	0 - 2 h GA vapour, 20 ° C
Polarisation		$U_{pol} = + 410 \text{ mV vs. Ag/AgCl}$	

Table 2.7:

Parameters for AChE sensor production - Variation 3

Component	Paste	Protocol	
working electrode +immobilisate	TCNQ-Graphite + AChE / BSA <i>printed on basic transducer (Figure 2.3)</i>	1.	15 % TCNQ-graphite* in 3 % HEC (manually mixed),
		2.	Mixing with AChE 1 U/ml in 5 % BSA
		3.	Screen printing
	cross-linking	4a.	0 - 22 h GA vapour, 4 ° C
		4b.	0 - 2 h GA vapour, 20 ° C
Polarisation		$U_{pol} = + 100 \text{ mV vs. Ag/AgCl}$	

Table 2.8:

Parameters for AChE sensor production - Variation 4

Component	Paste	Protocol	
Working electrode	TCNQ-Graphite <i>printed on basic transducer (Figure 2.3)</i>	1.	15 % TCNQ-graphite* in 3 % HEC (manually mixed),
		2.	30 min drying at 80 ° C
Immobilisate	AChE solution <i>printed on working electrode</i>	3.	1 -5 U/ml AChE, 1 -5 % BSA, 1 - 3 % HEC
		4.	Screen printing
Cross-linking		4a.	0 - 22 h GA vapour, 4 ° C
		4b.	0 - 2 h GA vapour, 20 ° C
Polarisation		$U_{pol} = + 100 \text{ mV vs. Ag/AgCl}$	

TCNQ-graphite\* (see Table 2.7): Investigated graphites (Lonza, Basel, CH):

- T15 graphite
- KS 6 graphite
- PWA Carbon Chemvion
- Fine Coke Chemvion

Preparation of TCNQ-graphite:

- (1) Dissolving 100 mg TCNQ in 300 ml acetone or toluene.
- (2) Mixing with 4 g graphite.
- (3) Evaporation of solvent using rotary evaporator.

### 2.1.3.3 Measurement set-up: AChE sensor prototype

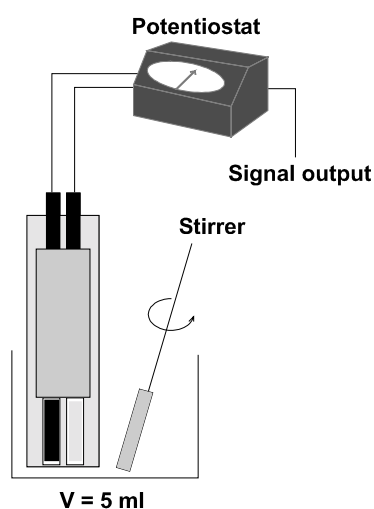


Figure 2.4: Measurement set-up of AChE sensor prototype. Measurements were performed in stirred solutions (5 ml) using an overhead stirrer (RW 10, Ika, Staufen, Germany) with plastic pad.

All sensor experiments were carried out in stirred solution (0.01 M potassium phosphate buffer, 0.05 M NaCl, pH 7.5) (PBS) at room temperature unless stated otherwise (Figure 2.4). Activity of immobilised enzymes was determined by monitoring thiocholine formed by enzymatic hydrolysis of acetylthiocholine chloride (ATCh) [87]. Thiocholine was determined by oxidation at  $U_{\text{pol}} = +100 \text{ mV}$  vs the printed Ag/AgCl reference electrode for TCNQ graphite working electrodes and at  $U_{\text{pol}} = +410 \text{ mV}$  for rhodium graphite working electrodes. Therefore, the AChE sensors were connected to a potentiostat (641 VA-Detektor, Metrohm, Herisau, Switzerland) and output signals were monitored with a recorder (L200E, Linseis, Selb, Germany). The reaction scheme of thiocholine oxidation is shown in Figure 2.5.

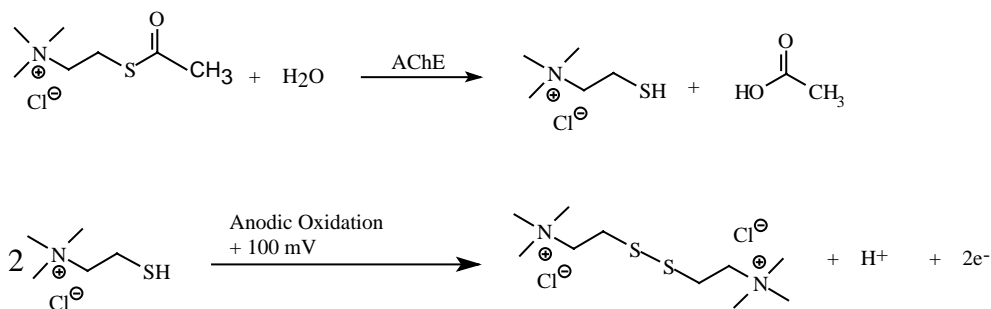


Figure 2.5: Reaction scheme of acetylthiocholine hydrolysis and subsequent amperometric choline oxidation.

The enzymatic activity was quantified from the difference of the steady state currents before and after substrate addition (Equation 1).

Equation 1

$$a = \Delta I \text{ [nA]} = I_1 \text{ [1 mM ATCh]} - I_0 \text{ [0 mM ATCh]}$$

a	enzyme activity
$I_1$	steady state current after substrate addition
$I_0$	steady state current before substrate addition

## 2.1.4 AChE multisensor

### 2.1.4.1 Working electrode preparation

The paste for the working electrodes was prepared and printed according to chapter 2.1.3.2, variation 4. (3 % (w/v) HEC, 15 % (w/w) TCNQ - T15 graphite.)

### 2.1.4.2 AChE immobilisation

For each AChE listed in section 2.1.2.2 a separated printing paste was prepared according to the multisensor used. Printing immobilisation parameters are given in Table 2.10. Wild-type AChE sensors were cross-linked in glutaraldehyde vapour after printing (15 min, 22 °C) [142]. The screen printing inks for multisensors I and II contained 0.02 g/ml or 0.04 g/ml of photocrosslinkable polyvinyl alcohol (PVA-SbQ) from Toyo Gosei (Tokyo, Japan) [143] respectively and 1 U/ml AChE in 1 % (w/w) hydroxyethylcellulose aqueous solution (Table 2.9). Electrodes with printed enzyme solution were subsequently illuminated for cross-linking immobilisation for 12 h at 4 °C (model T-88, Luxo, Hildesheim, Germany). Table 2.11 gives the distribution of the cholinesterases on the different multisensors.

Table 2.9:  
Printing paste composition for AChE multisensors

Multisensor	Paste
„wild-type“	BSA 5% (w/w), HEC 1%(w/w) , AChE 1 U/ml
I	0.04 g/ml PVA-SbQ , AChE 1 U/ml
II	0.02 g/ml PVA-SbQ , AChE 1 U/ml

Table 2.10:  
Printing parameters for preparation of AChE multisensors

Printing step	Paste	Squeegee pressure	Print mode	Print gap [mm]	Squeegee speed [mm/s]
5- Working el.	HEC/TCNQ-graphite	7	flood/print	1.7	70/70
6- AChE sln.	see Table 2.10	5	flood/print	2.3	50/50

Table 2.11:  
Distribution of AChE variants on electrode positions of each multisensor

Multisensor	Position 1	Position 2	Position 3	Position 4
„wild-type“	rbAChE	dmAChE	beAChE	eeAChE
I	dmAChE	Y408F	F368L	F368H
II	dmAChE	Y408F	F368L	F368W

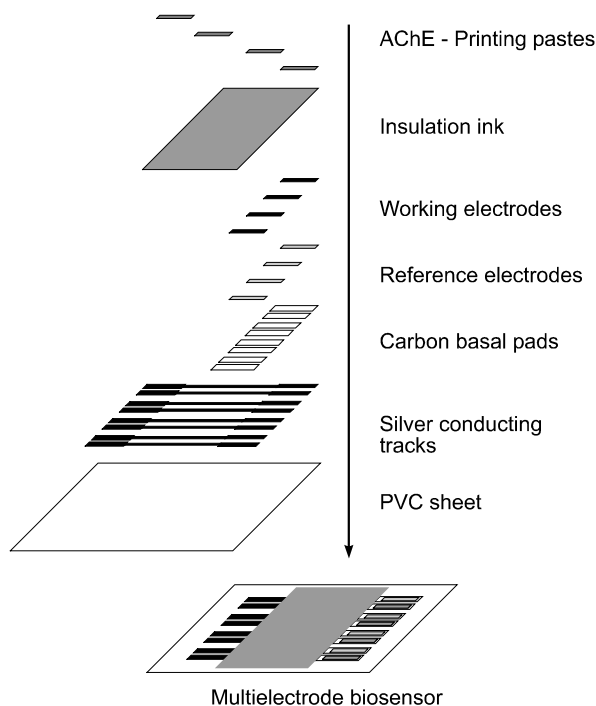


Figure 2.6: AChE multisensor assembly by screen printing.

### 2.1.4.3 Measurement set-up: AChE multisensor

The multisensors were connected to a four-channel potentiostat (MCP 94) from Bank-Wenking (Clausthal-Zellerfeld, Germany) and output current was recorded by a multichannel recorder from Kipp & Zonen (Solingen, Germany). AChE activity was calculated as  $\Delta I$  from steady state currents monitored at acetylthiocholine concentrations of 0 and 1 mM. For inhibition experiments, the multisensors were incubated with a sample for 20 min at room temperature. Percent inhibition was calculated as  $\text{inhibition [\%]} = ((a_0 - a_i) / a_0) * 100$ . ( $a_0$  = activity without inhibition,  $a_i$  = enzyme activity after incubation with sample.)

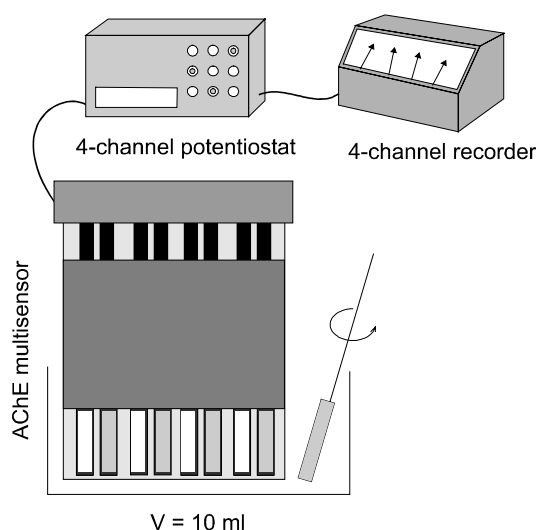


Figure 2.7: Experimental set-up for AChE multisensor measurements.

## 2.1.5 Data sets

### 2.1.5.1 Wild-type AChE sensor

Paraoxon and carbofuran were analysed individually and in binary mixtures using the AChE-multisensor. For the neural network training, a data set was used comprising 50 detections of both analytes in concentrations of 0-20  $\mu\text{g/l}$  in standard buffer solutions (0.01 M potassium phosphate buffer, 0.05 M NaCl, pH 7.5). Analysis of real samples was performed using 15 data sets compiled from measurements of waste water samples. The latter were taken from a municipal sewage treatment plant (Stuttgart-Büsnau, Germany). Real samples were also spiked with 5  $\mu\text{g/l}$  of paraoxon and/or carbofuran. For inhibition studies, the multisensor was incubated for 20 min directly in the samples.

### 2.1.5.2 Multisensor I and II

To train and test the neural networks, three different data sets were generated by sensor inhibition analysis of analyte mixtures. These were first, binary mixtures of paraoxon and carbofuran in the concentration range 0-5 µg/l of each analyte, analysed using multisensors I and II (50 data sets). Second, real samples analysed with multisensor II. The surface water samples were taken from the river Neckar, Stuttgart, Germany. All real samples were spiked with 0-2.5 µg/l of paraoxon and carbofuran (10 data sets). Third, malaoxon and paraoxon analysed in binary mixtures in the concentration range 0-5 µg/l of each analyte using multisensor II (36 data sets).

### 2.1.6 Artificial neural network performance

Processing of inhibition data was done using feed forward neural networks generated with NEMO 1.15.02 [75]. Network training was carried out with the resilient backpropagation algorithm (Rprop) [144] using the data sets described in chapter 2.1.5. The inputs (% inhibition) were normalised and centred and the output values were scaled in a range of -0.9 to 0.9 to be accessible for the neural net according to Seemann et al. [51].

Manual and automatic topology optimisation was monitored by comparing the root mean square error (RSME) of the optimised networks. Manual topology set-up was investigated for the following network configurations: input layer, 1 - 4 input nodes (one AChE variant per input); hidden layer, 5 or 10 nodes; output layer, one node (equals the analyte concentration); all nodes fully interconnected. Automatic optimisations by pruning algorithms were performed starting from the following initial network topology: input layer, 4 input nodes; hidden layer, 10 nodes; output layer, one node. The nodes were fully interconnected, including shortcut connections (not shown in Fig. 4 a for greater clarity). For each insecticide, the network topologies were optimised separately by pruning algorithms (MagPruning and Skeletonisation [145]) [51]. (Ten times pruning per 10 separate runs). The networks with the best RSME for calibration and cross-validation were chosen to undergo another 10 separate runs for 3000 epochs until no further change of the network error was observed.

All network results given represent mean values of 10 individual training runs. Evaluations of the networks were made by full cross-validation [51] for all training data sets and by validation using data obtained by real sample analysis as independent test sets.



## 2.2 Microbial sensors

### 2.2.1 Reagents

All reagents were purchased at analytical grade by Sigma-Aldrich, Deisenhofen, if not stated otherwise.

#### 2.2.1.1 Buffers

Tris buffer (TBS)	10 mM Tris/HCl
	10 mM NaCl
	0.5 mM CaCl <sub>2</sub>
	pH 7.5

#### 2.2.1.2 Growth substrates

Carbon source stock solutions (50 mM) were prepared in 1 mM NaOH and sterile filtrated (0.2 µM):

- |   |                |
|---|----------------|
| • 2,4-D (2,4-dichlorophenoxy acetic acid)     | (221.04 g/mol) |
| • MCPA (2-methyl-4-chlorophenoxy acetic acid) | (200.62 g/mol) |
| • 2-MPA (2-methylphenoxyacetic acid)          | (166.16 g/mol) |
| • Phenol                                      | (94.11 g/mol)  |
| • Benzoic acid                                | (122.12 g/mol) |

#### 2.2.1.3 Analytes

Additionally to the growth substrates, the following analytes were investigated for microbial sensor response:

- |                                |                |
|--------------------------------|----------------|
| • 2-CP (2-chlorophenol)        | (128.56 g/mol) |
| • 4-CP (4-Chlorophenol)        | (128.56 g/mol) |
| • 2,4-DCP (2,4-dichlorophenol) | (163.01g/mol)  |

Analyte stock solutions (50 mM) were prepared in 1 mM NaOH and diluted in the measurement buffer to 1 mM before measurement.

---

## 2.2.2 Microbial strains and cultivation

### 2.2.2.1 *Ralstonia eutropha* JMP 134, pJP4 (*Alcaligenes eutrophus*)

Full medium:	(LB Medium)	
	tryptone	10 g
	yeast extract	5 g
	NaCl	5 g
		ad 1 l aqua dem.
		pH 7.5
Mineral medium:	[123]:	
	K <sub>2</sub> HPO <sub>4</sub>	1.6 g
	KH <sub>2</sub> PO <sub>4</sub>	0.4 g
	(NH <sub>4</sub> ) <sub>2</sub> SO <sub>4</sub>	1 g
	MgSO <sub>4</sub>	0.05 g
	FeSO <sub>4</sub>	0.01 g
		ad 1 l aqua dem.
		pH 7.5
Agar plates	tryptone	10 g
	yeast extract	5 g
	NaCl	5 g
	Agar	15 g
		ad 1 l aqua dem.
		pH 7.5

Cultivations were performed on a rotary shaker in 0.5 - 3 l fluted Erlenmeyer flasks with 20 % filling at 30 ° C and 180 rpm with 2 mM of a sole carbon source (2.2.1.2). (Infors, Basel, CH).

## 2.2.3 Determination of specific oxygen uptake rates

The determination of oxygen uptake rates by non-immobilised cells was performed by polarimetric oxygen monitoring using a Biological Oxygen Monitor YSI model 5300 (Yellow Springs Instrument Co. Inc., Yellow Springs, Ohio, USA).

For this purpose, 2.85 ml of oxygen saturated TBS-II at 30 °C were filled in the measurement chamber and the system was equilibrated. Then 100 µl of washed cell suspension ( $OD_{580nm}=2$ ) were added and the endogenous respiration was determined. The reaction was started by addition of 50 µl of 1 mM analyte solution. The decreasing current signal was subsequently monitored and the specific oxygen uptake calculated from an oxygen saturation concentration of 7.5 mg/l (234 µM) at 30 °C.

## 2.2.4 Development of microbial sensor prototypes

### 2.2.4.1 Screen printing of basic transducer

Basic transducers were produced according to Figure 2.2 and chapter 2.1.3.1. For fabrication of oxygen electrodes the screen printing parameters were changed as listed in Table 2.12:

Table 2.12:

Screen printing parameters for production of basic oxygen electrode.

Printing step	Paste	Squeegee pressure	Print mode	Gap [mm]	Squeegee speed [mm/s]
1- Silver conducting tracks	Electrodag PF-410	4	flood/print	2.8	50/50
2- Graphite pads	Electrodag 423 SS	4	flood/print	2.8	70/70
3- Reference electrodes	Electrodag 6037 SS	4	flood/print	2.8	70/70
4- Isolation	Marastar SR 057	5	flood/print	2.8	70/70
5- Working electrode	Graphite suspension (2.2.4.2)	7	flood/print	1.9	50/50

### 2.2.4.2 Working electrode

- The printing paste for working electrodes was prepared by homogenising of an aqueous solution of 3 % (w/w) hydroxyethylcellulose (HEC, medium viscosity, Fluka) containing 15 % (w/w) rhodium graphite using an Ultraturrax homogeniser (Ika, Staufen, Germany, model T-25)) at 24000 rpm. The electrodes were subsequently dried at 80 °C for 15 min.
- For stabilisation the working electrodes were drop-coated by approx. 2 µl 0.5 % (w/v) cellulose acetate / acetone solution.

### 2.2.4.3 Electrolyte

For the development of the basic oxygen sensor, various electrolyte compositions were investigated:

Table 2.13:  
Investigated electrolytes

Electrolyte	Application	Composition
1	Screen printing	12 % PVP (K30, Fluka), 0.4 M KCl
2	Screen printing	12 % PVP (K90, Fluka), 0.4 M KCl
3	Screen printing	12 % PVP (PVP-10, Sigma), 0.4 M KCl
4	Screen printing	30 % PVP (K90, Fluka), 1 M KCl
5	Drop-coating	3 % PVP (K30, Fluka), 0.1 M KCl, 5 - 20 $\mu$ l
6	Drop-coating	6.6 % PVP (K30, Fluka), 0.3 M KCl, 5 - 20 $\mu$ l, pH 7.5 (adjusted with $K_2HPO_4$ )
7	Drop-coating	6.6 % PVP (K30, Fluka), 3 M KCl, 5 - 20 $\mu$ l, pH 7.5 (adjusted with $K_2HPO_4$ )

- After deposition of the electrolyte, the electrodes were dried for 6 h at room temperature.
- For better formation of a salt bridge, the PVC sheet between working electrode and reference electrode was treated with 0.5 % cellulose acetate (w/v in acetone).

### 2.2.4.4 Oxygen selective membrane: Spin coating / lamination

- (1) To achieve oxygen selectivity the electrodes with dried electrolyte were covered with a layer of silicon rubber (1 Component RTV, KE4895T, Shin Etsu Ltd., Tokyo, Japan). The silicon rubber was applied by spin coating using an in-house constructed spin-coater (2500 rpm, 30 s).
- (2) Directly after spin-coating the active area of the electrodes was laminated with a mask (Scotch 550, 3M France, Cergy-Pontoise, France) forming a circular, oxygen permeable area (4 mm diameter) at each electrode pair.
- (3) The electrodes were cured for 12 h at room temperature.

### 2.2.4.5 Immobilisation of micro-organisms

For the immobilisation of the micro-organisms on the oxygen electrode several methods and protocols were investigated. Table 2.14 gives details of materials and conditions used for immobilisation. Figure 2.8 shows the design of the microbial sensor prototype.

Table 2.14:

Immobilisation matrices and protocols investigated for *R.eutropha JMP 134*

Matrix	Supplier	Protocol
PU3	Provided by Prof. Tanaka, Kyoto University, Japan	<ol style="list-style-type: none"> <li>1. Mixing of PU3 with chilled bacterial suspension (1 - 20 % PU3 (w/v)).</li> <li>2. Immediate application of suspension on electrode.</li> <li>3. Curing for 6 h at RT.</li> </ol>
PU6	see PU3	see PU3
Ca-Alginate	Sigma	<ol style="list-style-type: none"> <li>1. Mixing of bacteria (pellet) with 1 - 4 % Na-alginate (w/v in aqua dem.).</li> <li>2. Drop-coating / screen printing on electrode (5 - 30 µl).</li> <li>3. Gelation in 0.2 M CaCl<sub>2</sub> for 20 min, RT.</li> </ol>
Al-Alginate	Sigma	<ol style="list-style-type: none"> <li>1. Mixing of bacteria (pellet) with 1 - 4 % Na-alginate (w/v in aqua dem.).</li> <li>2. Drop-coating on electrode (10 - 20 µl).</li> <li>3. Gelation in 5 % AlK(SO<sub>4</sub>)<sub>2</sub> or Al(SO<sub>4</sub>)<sub>3</sub> (w/v in aqua dem.) for 20 min at RT.</li> </ol>
PVA-SbQ	Toyo Gosei	<ol style="list-style-type: none"> <li>1. Mixing of bacterial suspension (0.9 % NaCl) with PVA-solution (50 - 100 g/l).</li> <li>2. Drop-coating on electrode.</li> <li>3. Illumination for 12 h at 4 °C.</li> </ol>
PCS	SensLab	<ol style="list-style-type: none"> <li>1. Mixing of 100 mg PCS with 120 µl water (pH 1).</li> <li>2. Adjusting pH to 6 - 7 with polyethylene imine (2.5% in aqua dem.).</li> <li>3. Mixing of PCS with bacterial suspension (1:1).</li> <li>4. Drop-coating on electrode (5 µl)</li> <li>5. Curing for 2 h at 4°C.</li> <li>6. 30 s curing in polyethylene imine solution (0.5% w/v in aqua dem.).</li> </ol>
Silicon rubber RTV KE4895T	Shin Etsu	<ol style="list-style-type: none"> <li>1. Mixing of silicon rubber as 1 - 20 % with bacterial suspension (w/v).</li> <li>2. Immediate drop-coating of suspension on electrode (approx. 20 µl).</li> <li>3. Curing for 1 h at RT.</li> </ol>
Sylgard 184	Dow Corning	<ol style="list-style-type: none"> <li>1. Mixing of basic fluid with 10 % (w/w) curing catalyst.</li> <li>2. Mixing of silicon fluid with bacterial suspension (1:2 - 1: 10).</li> <li>3. Drop-coating on electrode (5 - 30 µl).</li> <li>4. Curing for 12 h at RT.</li> </ol>

NC-Filter	Sartorius		<ol style="list-style-type: none"> <li>1. Drop bacterial suspension on NC filter (pore size 0.4 <math>\mu\text{m}</math>).</li> <li>2. Remove liquid by applying gently vacuum.</li> <li>3. Attachment of filter via silicon rubber to electrode.</li> </ol>
Ca-Alginate / NC-Filter	Sigma / Sartorius		<ol style="list-style-type: none"> <li>1. Attachment of filter via silicon rubber to electrode.</li> <li>2. Mixing of bacteria (pellet) with 1 - 4 % Na-alginate (w/v in aqua dem.).</li> <li>3. Drop-coating on electrode (5 - 30 <math>\mu\text{l}</math>).</li> <li>4. Gelation in 0.2 M <math>\text{CaCl}_2</math> for 20 min, RT.</li> </ol>
PVA-SbQ / NC-Filter	Toyo Gosei / Sartorius		<ol style="list-style-type: none"> <li>1. Attachment of filter via silicon rubber to electrode.</li> <li>2. Mixing of bacterial suspension (0.9 % NaCl) with PVA-solution (50 - 100 g/l)</li> <li>3. Drop-coating on electrode (20 <math>\mu\text{l}</math>).</li> <li>4. Illumination for 12 h at 4 <math>^{\circ}\text{C}</math>.</li> </ol>
Ca-Alginate / Nylon nets	Sigma		<ol style="list-style-type: none"> <li>1. Attachment of net via silicon rubber to electrode.</li> <li>2. Mixing of bacteria (pellet) with 1 - 4 % Na-alginate (w/v in aqua dem.).</li> <li>3. Drop-coating on electrode (10 <math>\mu\text{l}</math>).</li> <li>4. Gelation in 0.2 M <math>\text{CaCl}_2</math> for 20 min, RT.</li> </ol>
Ca-Alginate / KE4895T	Sigma / Shin Etsu		<ol style="list-style-type: none"> <li>1. Mixing of bacteria (pellet) with 1 - 4 % Na-alginate (w/v in aqua dem.).</li> <li>2. Mixing of silicon fluid with bacterial suspension (1:2 - 1:10).</li> <li>3. Drop-coating on electrode (10 <math>\mu\text{l}</math>).</li> <li>4. Gelation in 0.2 M <math>\text{CaCl}_2</math> for 20 min, RT.</li> <li>5. Curing for 1 h at RT.</li> </ol>
Ca-Alginate / Sylgard 184	Sigma / Dow Corning		<ol style="list-style-type: none"> <li>1. Mixing of bacteria (pellet) with 1 - 4 % Na-alginate (w/v in aqua dem.).</li> <li>2. Mixing of silicon fluid with bacterial suspension (1:2 - 1:10).</li> <li>3. Drop-coating on electrode (10 <math>\mu\text{l}</math>)</li> <li>4. Gelation in 0.2 M <math>\text{CaCl}_2</math> for 20 min, RT.</li> <li>5. Curing for 12 h at RT.</li> </ol>

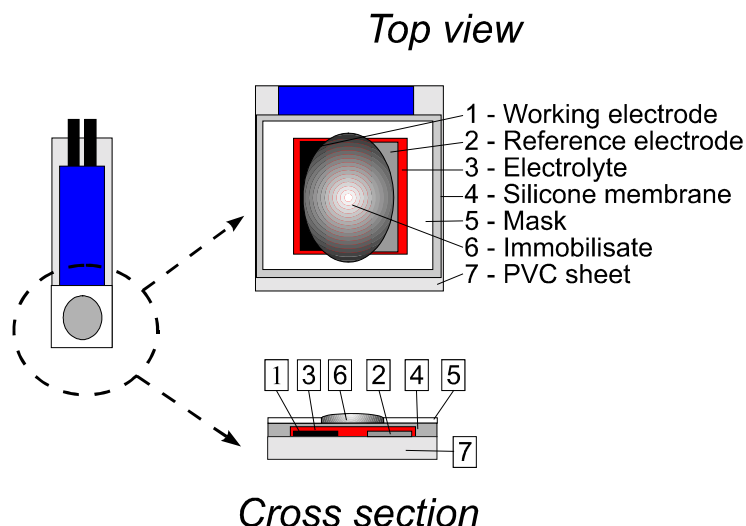


Figure 2.8: Construction scheme of planar oxygen electrode. Numbers for „cross section“ refer to „top view“.

The adhesion of Ca-alginate and PVA-SbQ membranes was investigated depending on the pretreatment of the silicon rubber membrane. Prior to hydrogel drop-coating, the electrodes were treated with:

- 10% APTS (w/v in demineralised water), 30 min.
- 98% APTS (as supplied by Sigma), 1 - 4 min.

#### 2.2.4.6 Monitoring of surface modification / TNB-test

The TNB-test was carried out according to Cutraceasas [146]. 20 µl of saturated  $\text{Na}_2\text{B}_4\text{O}_7$  containing 0,03 % TNB were incubated per electrode. After 10 min the colour development was visible. An orange colour indicated the presence of free amino groups on the surface.

#### 2.2.4.7 Measurement set-up: Microbial sensor prototype

The experimental set-up was prepared according to chapter 2.1.3.2. and Figure 2.4. The potential was set to  $U_{\text{pol}} = -300 \text{ mV}$  vs. Ag/AgCl for oxygen reduction using a potentiostat (641 VA-Detektor, Metrohm, Herisau, Switzerland) and output signals were monitored with a recorder (L200E, Linseis, Selb, Germany). Measurements were performed in 5 ml stirred solution of TBS-II at 22 °C unless stated otherwise. The signal (sensor response) was calculated according to Equation 2:

Equation 2

$$r = \Delta I [\text{nA}] = I_1 - I_0$$

$r$	sensor response
$I_1$	steady state current after analyte addition
$I_0$	steady state current before analyte addition

## 2.2.5 Microbial multisensors

Chapters 2.2.5.1 - 2.2.5.4 give details of the protocol for microbial multisensor fabrication, Figure 2.9 shows the microbial sensor assembly.

### 2.2.5.1 Screen printing of the multisensor platform

The disposable oxygen electrodes were screen printed as described for the basic transducer described in chapter 2.2.4.1. Building up on this platform, rhodium graphite working electrodes were printed according to chapter 2.2.4.2. The printing layout is shown in Figure 2.9.

### 2.2.5.2 Multisensor pretreatment

- (1) 1 min incubation in 98 % APTS.
- (2) Rinsing with aqua dem..
- (3) 20 min incubation in GA vapour.
- (4) 10 min incubation with 5 % BSA aqueous solution.
- (5) Rinsing with demineralised water.

### 2.2.5.3 Cell harvesting

Cells were harvested at the late exponential growth phase.

- (1) Centrifugation (30 min, 4°C, 9000 g).
- (2) Resuspension (0.9% NaCl) in 50 ml.
- (3) Centrifugation (30 min, 4°C, 9000 g).
- (4) Resuspension (0.9% NaCl) in 1 ml.
- (5) Centrifugation (4 min, 4°C, 9000 g).

### 2.2.5.4 Immobilisation

- (1) Mixing of 2 % Na-alginate aqueous solution with cell pellet (biomass concentration = 100 mg/ml).
  - (2) Drop-coating of 10 µl of cell/alginate suspension on active surface of electrode.
  - (3) 20 min gelation in 0.2 M CaCl<sub>2</sub>
  - (4) Rinsing with demineralised water.
-



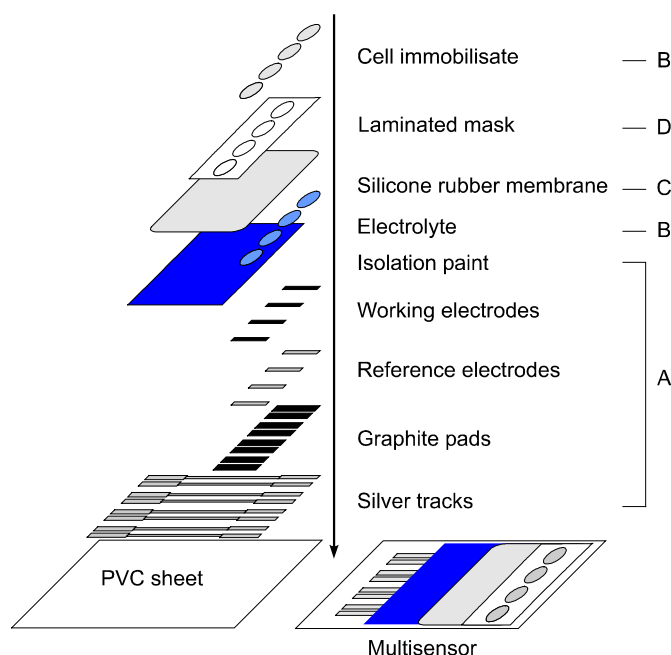


Figure 2.9: Assembly of microbial multisensor by screen printing (A), drop-coating (B), spin coating (C) and lamination (D).

#### 2.2.5.5 Microbial multisensor equilibration

Prior to the measurements, the microbial multisensors were immersed for 40 min in demineralised water to hydrate the electrolyte.

#### 2.2.5.6 Storage

Completed multisensors were stored at 4 °C in moisture-saturated atmosphere until usage.

#### 2.2.5.7 Measurement set-up: Microbial multisensor

The experimental set-up was designed according to chapter 2.1.4.3. Measurements were performed in 10 ml TBS-II according to chapter 2.2.4.7. Positions 1 - 4 of the multisensor were equipped with cells which were grown on the following sole carbon sources according to Figure 2.10:

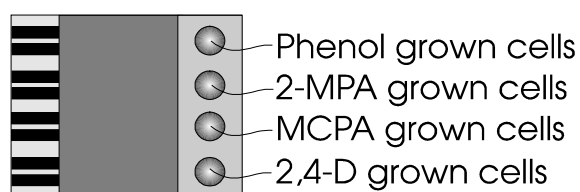


Figure 2.10: Distribution of differently grown cells of *R.eutropha* JMP 134 on microbial multisensor.

## 2.2.6 Data sets

The microbial multisensors were applied for different binary mixture analysis. Table 2.15 shows the data sets generated with the microbial multisensors M1 - M4.

Table 2.15:  
Data sets generated with microbial multisensors

Data sets	Analytes	Concentration range	N
M 1	2,4-Dichlorophenol / Phenol	0 -40 $\mu$ M (each)	55
M 2	2,4-Dichlorophenol / Phenol	0 -40 $\mu$ M (each)	30
M 3	2,4-Dichlorophenol / 4-Chlorophenol	0 -40 $\mu$ M (each)	30
M 4	2,4-Dichlorophenol / 4-Chlorophenol	0 -40 $\mu$ M (each)	30

## 2.2.7 Artificial neural network performance

Processing of inhibition data was done according to chapter 2.1.6. Network training was performed with the resilient backpropagation algorithm (Rprop) [144]. Network topology was optimised using MagPruning, Skeletonisation and Non-contributing Units methods [145] [147] and consisted of 10 times pruning in 10 separate runs. Starting from an initial network topology of 4:10:1, one hidden layer (10 nodes) and one output node for each analyte concentration, all nodes were fully interconnected including shortcut connections (not shown in Figure 2.11 for better clarity).

After the pruning, the networks with the best root mean square error (RSME) for calibration and cross-validation were selected to undergo 10 separate runs for 3000 epochs until no further change of the network error was observed. All network results given in this report represent mean values of 10 individual training runs. Network assessment was carried out by full cross-validation for all training data sets [51].

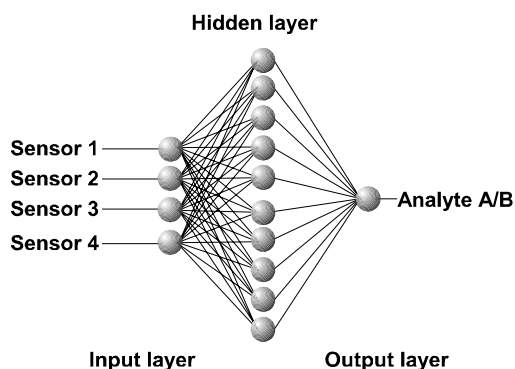


Figure 2.11: Initial network topology for processing of microbial multisensor data prior pruning procedure.

## 3 Results

### 3.1 Multianalyte AChE sensors

The strategy to develop a new sensing tool for multianalyte detection of acetylcholinesterase inhibitors followed five steps until the final goal was achieved:

1. Basic transducer	Development of a disposable AChE sensor.
2. AChE multisensor	Set-up of a multisensor prototype using wild type acetylcholinesterases. Performing of initial mixture analysis.
3. Data processing	Generation, adaptation and usage of artificial neural networks for data processing.
4. Multisensor improvement	Set-up of an improved multisensor AChE mutants. Performing of mixture analysis.
5. Data processing	Generation, adaptation and usage of artificial neural networks for data processing.

#### 3.1.1 Development of AChE-sensor prototype

Several thick-film sensors based on AChE have already been described [15;92], but none of them have been used for the discrimination of analyte mixtures by monitoring several AChE variants in parallel. For the design of the AChE-multisensor it was therefore necessary to develop first of all a suitable multielectrode sensor platform. In order to optimise the transducer and the procedure for enzyme immobilisation, eeAChE was used as a reference enzyme. Its hydrolytic action on acetyl thiocholine was determined by amperometric measurement of thiocholine. Studies were carried out with the following aims:

1. To develop a sensor system with strong signals but short response time.
2. To obtain highly reproducible signals among up to 4 electrodes on one multisensor and between different sensors.
3. To follow a simple procedure of preparation.

Therefore a sensor was designed which could be fully fabricated by screen printing. Besides the optimisation of the general parameters for screen printing of the single

---

electrode elements, the key points of development of a stable AChE-sensor were the optimisation of the working electrode and of the immobilisation of the AChE. Rhodium-graphite and TCNQ were investigated as mediators in various paste formulations for facilitated electron transfer during thiocholine oxidation. Furthermore, the immobilisation of the acetylcholinesterase by drop-coating and screen printing was investigated.

### 3.1.1.1 Stability of rhodium graphite electrode with drop-coated AChE

The motivation for immobilisation by drop-coating was to achieve maximum reproducibility. Therefore the simple adsorption of AChE to activated carbon and the cross-linking by glutaraldehyde were investigated and compared. Figure 3.12 shows results for the operational signal stability for sensors from two electrode preparations with different ways of immobilisation. Cholinesterase sensors with adsorbed AChE displayed on one hand a severe decrease of the signal height by each measurement and a high sensor-to-sensor variation. Therefore the use of this protocol was discarded in the following. In contrast, electrodes with cross-linked AChE were much more stable and displayed a significantly reduced sensor-to-sensor error as indicated by the error bars in Figure 3.12.

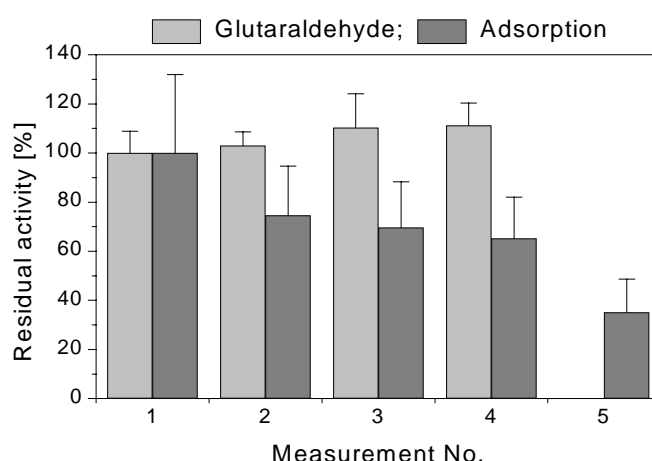


Figure 3.12: Signal stability of AChE sensors with differently immobilized AChE. 1. Immobilisation by cross-linking using glutaraldehyde (activity 100 % = 226 nA), 2. direct adsorption (100 % = 241 nA) ( $C_{\text{ATCh}} = 1.1 \text{ mM}$ .) Each curve represents mean values of three different electrodes.

Sensors with AChE immobilised by cross-linking were further investigated in view of their kinetic parameters. Figure 3.13 represent data of three different sensors. As can be seen from these data, these sensors displayed a significant variation. As a further drawback, mean apparent  $K_m$  value for acetylthiocholine exceeded 1 mM. As the sensor was intended to be used as a disposable sensor in pattern recognition, the minimal variation of each sensor and the ease of production were main tasks to be reached in the course of the AChE-multisensor development. The high apparent  $K_m$  value furthermore indicated diffusion problems. For this reasons, investigations dealing with this manual and unreliable immobilisation protocol were stopped. The

main focus was hence laid on immobilisation processes with a higher potential for automatization.

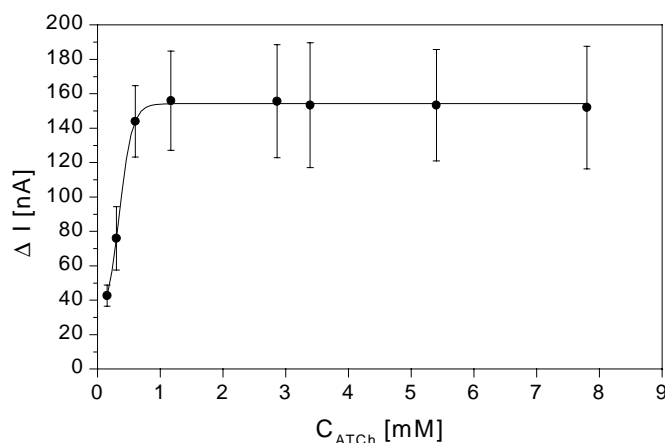


Figure 3.13: AChE-sensor signal at different concentrations of acetylthiocholine. The immobilisation was performed by glutaraldehyde cross-linking. (n= 3 electrodes.)

### 3.1.1.2 Printed AChE- rhodium graphite sensors

As already discussed in section 3.1.1.1, the automation of immobilisation was one of the major tasks for developing the new multisensor. Therefore a protocol was investigated where the printing step of the active layer of the working electrode was combined with the immobilisation of the enzyme. Immobilisation by screen printing was thought to minimize variation of absolute signal heights.

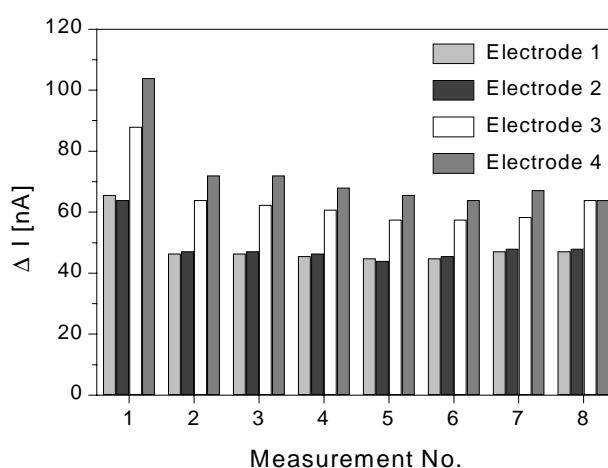


Figure 3.14: Signal stability of printed AChE-Sensors (19 h cross-linking in GA vapor, 4 °C). Measurements were performed with 4 different electrodes. ( $C_{ATCh} = 1.1$  mM.)

As can be seen from Figure 3.14, a full stabilization of the sensor signals could not be realized. A severe drop of the signal from the first to the second measurement

was observed for all 4 electrodes followed by a more or less stable development of the last 7 measurements. Possible reasons for this behaviour were suspected: a.) a dissolving of rhodium graphite, b.) loss of enzyme (activity or protein) or c.) a change in electrode performance due to heavy current load. At first, the impact of the incubation time of glutaraldehyde cross-linking on the signal stability was investigated. As shown in Figure 3.15 no activity was found after immobilisation for up to 6 hours incubation time. Starting from this point an increasing enzyme activity was monitored up to 14 hours. Further prolonged incubations had adverse effects in reduced activity, presumably due to inhibitory effects caused by the glutaraldehyde. Surprisingly no effect of the incubation time on the signal stability could be found.

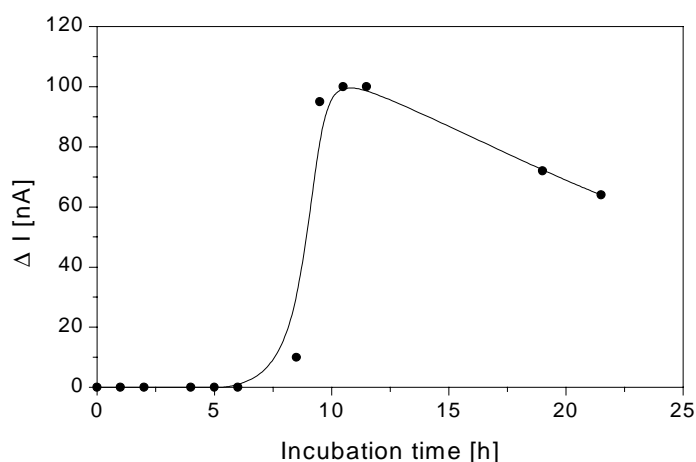


Figure 3.15: Influence of the exposure time of AChE-sensors to glutaraldehyde vapor at 4 °C on signal height. ( $C_{\text{ATCh}} = 1.1 \text{ mM}$ .)

In further experiments the influence of the following parameters was investigated: preincubation of the electrodes in buffer, intensive rinsing of the electrode prior the first measurement and variation of the current load. However, in non of the experiments any effects of these parameters could be observed (data not shown). In contrast, a certain impact of air humidity during storage of the sensors was found. Sensors stored in humid environments displayed a reduced stability and signal performance. Following these observations, the sensors were dried over silica at room temperature or in an oven up to 80 °C for several hours and remaining activity and signal stability was investigated.

#### 3.1.1.3 Stability of printed AChE-rhodium graphite sensors stored at 80 °C

Drying after immobilisation of electrodes which were produced according to section 3.1.1.2 had positive influences on equilibration behaviour and on signal stability as demonstrated in Figure 3.16. In this context a surprising high stability of the dry AChE sensors at elevated temperatures was discovered. Figure 3.17 shows the

residual activity of sensors stored at 80° C. After 24 hours incubation still 50 % of the initial activity were detected.

Results of operational stability investigations of these electrodes are shown in Figure 3.16. The drop of signal height between first and second measurement could be reduced but was still noticeable. Because of this circumstance and the continuous loss of activity during 4 measurements, it was tried to stabilize the sensor by addition of a covering membrane.

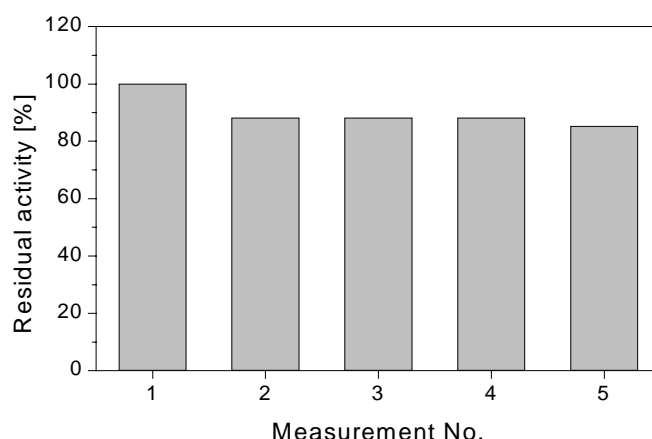


Figure 3.16: Operational stability during five measurements of AChE sensors stored dry at 80°C. ( $C_{\text{ATCh}} = 1.1 \text{ mM.}$ )

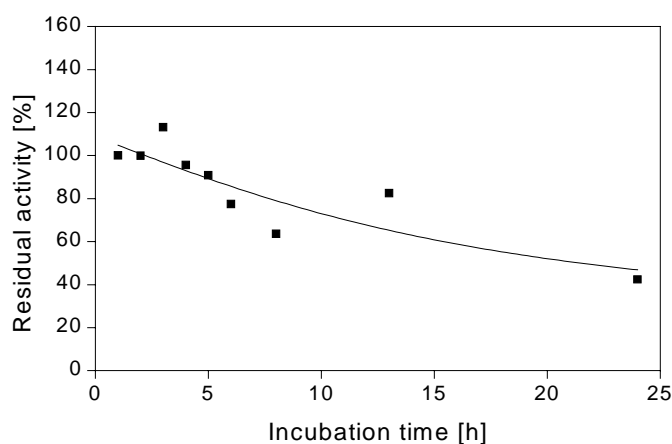


Figure 3.17: Residual activity of AChE sensors stored dry at 80°C. Each point represents one different electrode. ( $C_{\text{ATCh}} = 1.1 \text{ mM.}$ )

#### 3.1.1.4 Coating of printed AChE-rhodium graphite -sensors with polyurethane

One possible reason for the decrease in sensor signal upon addition of acetylthiocholine was supposed to be a loss of active electrode material, either enzyme or graphite itself. In order to preserve the working electrode an additional

membrane was added. The membranes were applied by dip coating of complete sensors in different dilutions of the polyurethane prepolymer PU6. Figure 3.18 shows the results of the coating experiments.

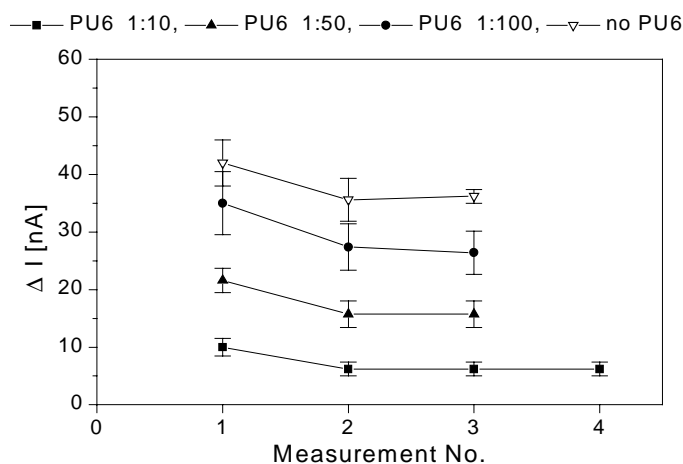


Figure 3.18: Operational stability of printed rhodium graphite AChE sensors coated with different PU6 dilutions. ( $C_{\text{ATCh}} = 1.1 \text{ mM}$ ,  $n = 4$ )

As can be seen in Figure 3.18, the coating of the cholinesterase sensors with additional membranes had one major effect, the reduction of the signal itself. Despite this unwanted effect, no positive influence was found on the operational stability. Consequently, a change of the working electrode itself was aimed in the following experiments.

#### 3.1.1.5 Drop-coated AChE-TCNQ-graphite-sensors

As it was outlined in the preceeding chapters, all attempts of using rhodium graphite as catalyst for thiocholine oxidation failed because of the instability of the electrode signal at repeated measurements. Visible changes of the electrodes and results from heating and drying of the sensors indicated problems with adhesion of the working electrode material. For this reason, the composition of the anode material was completely changed. Instantly, electrodes were produced as described in chapter 2.1.3.1 using TCNQ-graphite. The immobilisation solution was then drop-coated on the working electrode and cross-linked in the same way as described for chapter 3.1.1.1.

These sensors were stored at 4°C and could be used for several weeks. Figure 3.19 gives a typical example of one set of sensors used for repeated measurements using 1.1 mM ATCh. All sensors were stable for 6 rounds of analysis. For the final goal of the multianalyte sensor project, a manufacturing of a large number of multisensors was envisaged. For this reason, a full production of the AChE multisensors by screen printing was demanded. Therefore, the possibility to include AChE immobilisation into the screen printing process was again investigated and is described below.



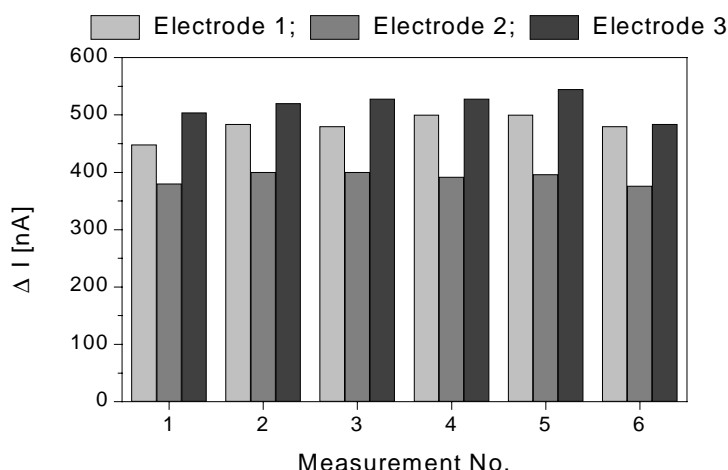


Figure 3.19: Operational stability of drop-coated TCNQ-graphite-AChE-sensors. ( $C_{\text{AChE}} = 1.1 \text{ mM}$ .)

#### 3.1.1.6 Printed AChE-TCNQ-graphite-sensors

In order to achieve a minimal number of printing steps and to reduce the number of diffusion boundaries, the AChE was mixed with the TCNQ-graphite paste and printed. Cross-linking was performed subsequently in glutaraldehyde vapor. As electrode materials several graphite variants were investigated (activated carbon, fine coke, T15 graphite). The mediator TCNQ was loaded on the carbon as solution in acetone or toluene and following evaporation.

In none of the cases any activity of the AChE could be detected. Inhibitory effects by the solvent could be excluded as the graphite was dried in the rotary evaporator over night at  $60^\circ\text{C}$  and 50 mbar. Furthermore the graphite was subsequently washed with demineralized water. A suspected inhibitory effect caused by TCNQ was also excluded effectively. AChE solutions with an activity of 1mU/ml were incubated in saturated TCNQ solutions and residual activity was measured. No inhibition in the enzyme activity test was monitored after an incubation for 4 hours as compared to the blanc.

As reasons for the complete inactivation were not discovered, the printing steps of working electrode and enzyme layer were investigated separately. In this case, good enzymatic activity could be monitored after immobilisation. This time, cross-linking of the enzyme layer was performed at room temperature within 15 min. Prolonged exposition to the glutaraldehyde vapor at room temperature resulted in complete loss of enzymatic activity (data not shown). The cross-linking for 15 minutes at room temperature resulted in even higher activities as they were found with cross inking at  $4^\circ\text{C}$  for 10 hours. As shown in Figure 3.20, these sensors were stable over three measurements with a slight signal decrease beginning from the third detection.

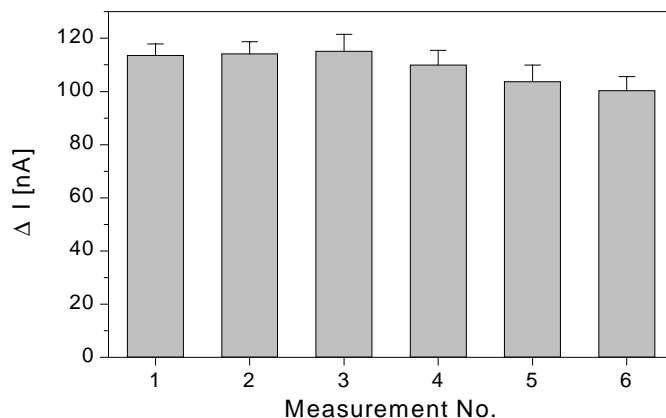


Figure 3.20: Operational stability of two step printed AChE + TCNQ-graphite-sensors.  $C_{\text{ATCh}} = 1.1 \text{ mM}$ . ( $n = 3$ )

It can be concluded, that the best working electrode production and enzyme immobilisation method was the separate printing of TCNQ-graphite and a AChE/BSA/HEC solution followed by subsequent cross-linking in glutaraldehyde vapor. Consequently, this method was used in all following sensor experiments.

#### 3.1.1.7 Characterization of the final transducer format

After the optimal conditions were found for sensor production, a test series of eeAChE sensors was manufactured and characterised. Sensors produced with this method displayed an equilibration time to reach a stable base current of 10 min. After the addition of 1 mM ATCh, a mean current output of 50 nA could be monitored. Within 60 seconds after substrate addition, 90% of the full signal was reached. Repeated measurements of the same ATCh concentration revealed a maximal signal error of  $\pm 1.7\%$ . The apparent  $K_m$  value determined for the acetylthiocholine sensor was 0.08 mM. Investigation of the sensor-to-sensor inhibition error using 10  $\mu\text{g/l}$  paraoxon resulted in a mean error of  $\pm 11.5\%$  when comparing complete multisensors comprising 4 single sensors, and  $\pm 13.1\%$  for the error related to the sensor position in different multisensors. Using the method described above, the aim of producing a suitable AChE-sensor platform was achieved. However, sensor-to-sensor inhibition errors close to 10% still present difficulties and have to be considered separately in the final multisensor production and performance.

### 3.1.2 Development of a wild type AChE multisensor

#### 3.1.2.1 Basic characteristics of the AChE-multisensor

For the discrimination experiments, a set of 100 four-electrode multibiosensors containing four AChE variants each was produced according to the optimal conditions determined in experiments using eeAChE for sensor platform development. For the AChE-multisensor the following enzymes were used rbAChE, dmAChE, beAChE, and eeAChE.

The mean current outputs at 1 mM acetylthiocholine for the individual sensors in nA were  $74 \pm 21$ . The pH-dependency of the sensors was investigated over a range of pH 6 - 10 and revealed enhanced activity for all sensors on the AChE-multisensor in the alkaline range (Figure 3.21). However, a pH of 7.5 was selected because signals at a pH greater than 8.5 tended to be unstable in terms of noise and steady state current.

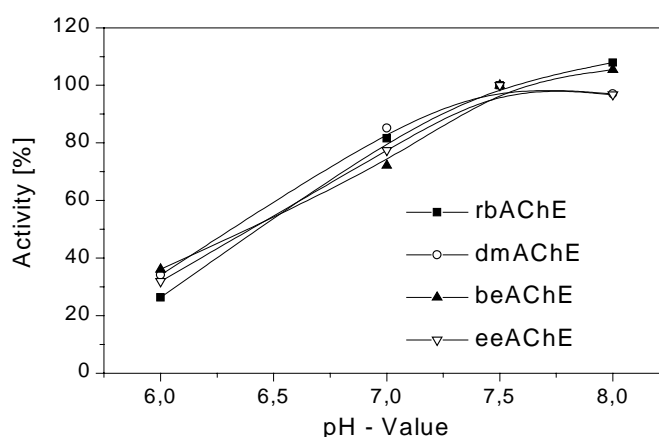


Figure 3.21: Influence of pH value on AChE sensor signal using four different immobilized AChE variants. ( $C_{\text{ATCh}} = 1.1 \text{ mM}$ .)

In inhibition experiments to determine the reproducibility of the sensors, the electrode-to-electrode errors using  $10 \mu\text{g/l}$  paraoxon were: rbAChE 2.3%, dmAChE 3.6%, beAChE 4.7%, eeAChE 23.4%. Again, a high variation in the case of the eeAChE-electrode in the AChE-multisensor was found but this obviously did not have a negative effect on the overall assay performance after data processing, as shown in Figure 3.22. The linear ranges for paraoxon or carbofuran detection were up to  $10 \mu\text{g/l}$  except for the highly sensitive dmAChE and carbofuran. Here, maximum inhibition was already reached at  $5 \mu\text{g/l}$ . The lowest concentration with a detectable effect was  $0.2 \mu\text{g/l}$  for both analytes. Table 3.16 gives all experimentally determined inhibition constants of the immobilised cholinesterase variants for each single pesticide. The correlation between data quoted in the literature for inhibition constants ( $k_i$  values) of AChEs in solution [94;106] and immobilised enzymes (this work, Table 3.16) could be confirmed. Differences were lower than one order of

magnitude and can be accounted for by variations in experimental conditions and the immobilisation process.

Table 3.16:

Inhibition constants for paraoxon and carbofuran of AChEs in solution<sup>a</sup> [106] [94] [104] and immobilised on the AChE-multisensor.

Enzyme	ki [ $10^6 \cdot \text{M}^{-1} \text{min}^{-1}$ ]		ki [ $10^6 \cdot \text{M}^{-1} \text{min}^{-1}$ ]	
	paraoxon		carbofuran	
	solubilised <sup>a</sup>	immobil.	solubilised <sup>a</sup>	immobil.
rbAChE	0.8	2.2	0.3	0.4
dmAChE	1.5	1.5	5.1	4.9
beAChE	0.6	0.6	0.9	0.4
eeAChE	0.2	0.3	1.8	0.7

### 3.1.2.2 AChE-multisensor performance

Training of artificial neural networks requires a sufficient number of data sets for network calibration. Binary mixtures of paraoxon and carbofuran in a concentration range of 0 - 20  $\mu\text{g/l}$  were used for this purpose, and inhibition data of the AChE-multisensors were analysed. Figure 3.22 shows results for each electrode of the AChE-multisensor.

The relationship between concentration and inhibition observed for binary mixtures was not linear. Furthermore, each electrode displayed individual inhibition patterns, depending on the identity and concentration of the analyte investigated. The ratio of sensitivity among the four electrodes corresponded to values deduced from the respective inhibition constants. Thus, sensors loaded with rbAChE were more sensitive to paraoxon, sensors containing dmAChE and eeAChE were more sensitive to carbofuran, and sensors based on beAChE displayed equal sensitivity towards both inhibitors, if with less sensitivity in general.

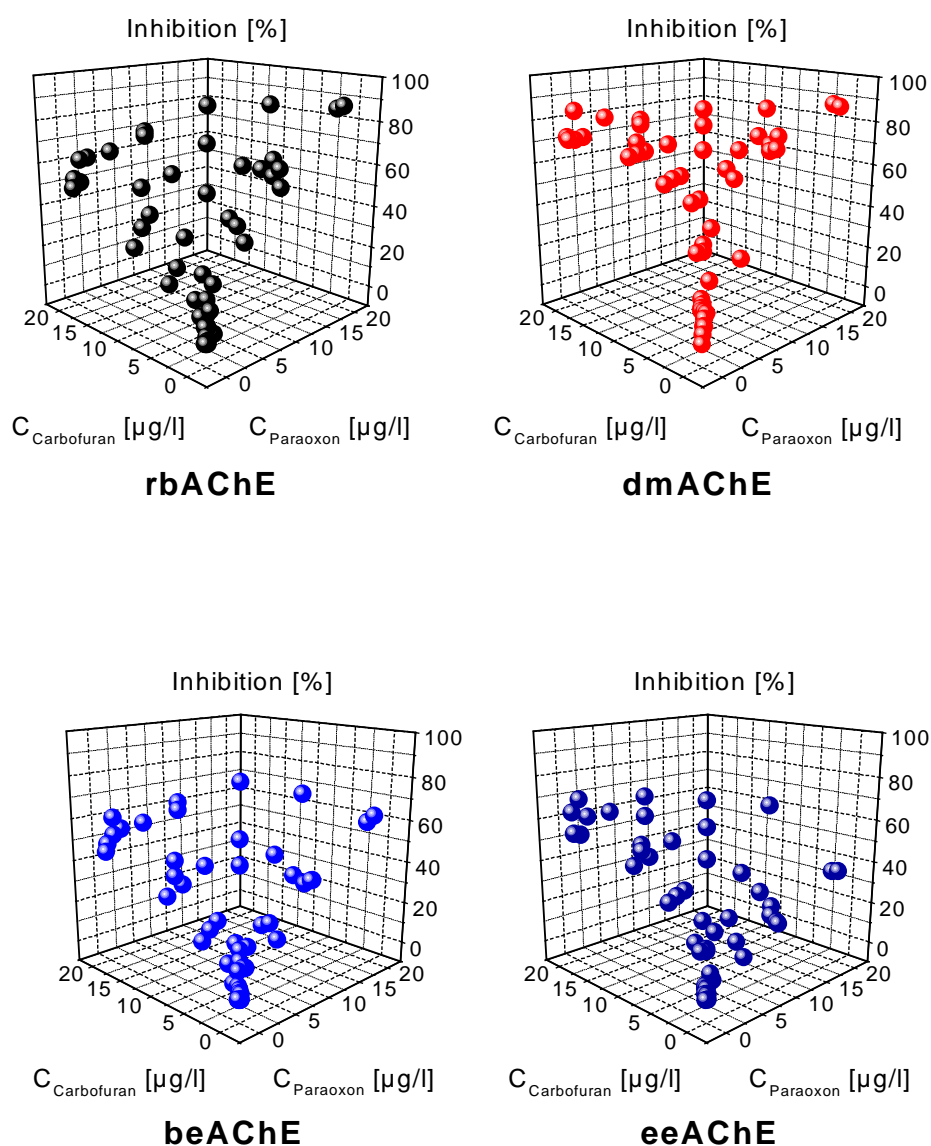


Figure 3.22: Inhibition values for each enzyme of the AChE-multisensor toward binary mixtures of carbofuran and paraoxon (0 - 20 µg/l). AChE partition on the AChE-multisensor: Position 1, rbAChE; position 2, dmAChE; position 3, eeAChE; position 4, beAChE. AChE-inhibition in [%] plotted for each single electrode position vs. concentrations of carbofuran (x-axis) and paraoxon (y-axis) in binary mixtures.

### 3.1.2.3 Artificial neural network performance

The discrimination of the two analytes was carried out by data processing on artificial neural networks generated with the software NEMO. Prior to automatic network optimisation the effect of input numbers on the network's discrimination ability was investigated. Figure 3.23 shows the results for network configurations set manually with different numbers of inputs. Each EOP (error of prediction) value represents the mean value of network errors calculated from all possible AChE combinations. As expected, optimal results were obtained using all four AChE variants. However, in the case of carbofuran, for three inputs the prediction error was already rather low as compared to four input neurons.

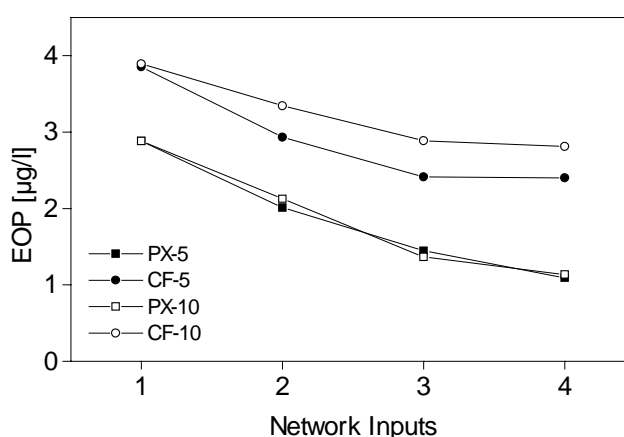


Figure 3.23: Artificial network error (EOP) depending on the number of used inputs. (PX-5: paraoxon, 5 hidden neurons), (PX-10: paraoxon, 10 hidden neurons), (CF-5: carbofuran, 5 hidden neurons), (CF-10: carbofuran, 10 hidden neurons).

To further improve the performance of the network, the optimal combination of inputs, hidden neurons and connections was developed by the network pruning methods MagPruning and Skeletonisation [145]. As shown in Figure 3.24, the network size was reduced from the original number of 10 hidden nodes to 6 hidden nodes in the case of paraoxon and three for carbofuran. The best performing networks used rbAChE, beAChE and eeAChE for paraoxon and dmAChE, beAChE and eeAChE for carbofuran discrimination.

Interestingly, inputs which seemed to be significant were also removed, and the reason for this action is unclear. One explanation might be their low contribution to the network performance or to a reduction of the network calibration error by their removal. On the other hand, inputs from sensors with a higher error, such as the eeAChE sensor, remained for both analytes. Although the inhibition constants were the key factor in choosing the AChEs for the multisensor approach alone, they were not sufficient to recommend the use of a cholinesterase after pruning or not.

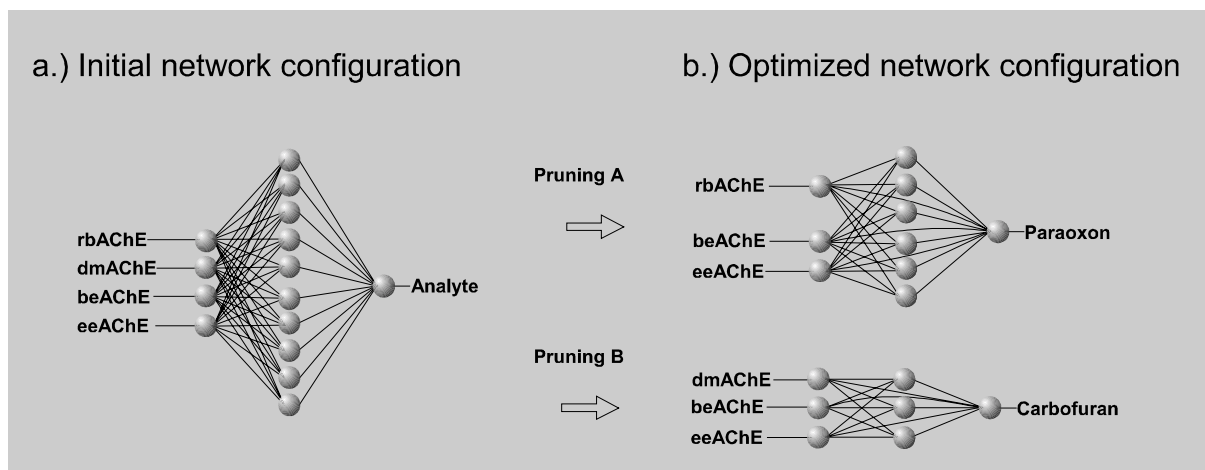


Figure 3.24: Initial network configuration (a) and results of pruning for each analyte (b). (pruning A = paraoxon, pruning B = carbofuran).

The neural networks shown in Figure 3.24 were generated by training on the data set which was obtained with the wild-type AChE multisensor (Figure 3.22). The course of development of the network error is displayed in Figure 3.25. It is obvious, that the paraoxon data set performed slightly better than carbofuran. Nevertheless, both network errors converged rapidly towards zero and no overtraining effects were observed even at higher cycle numbers.

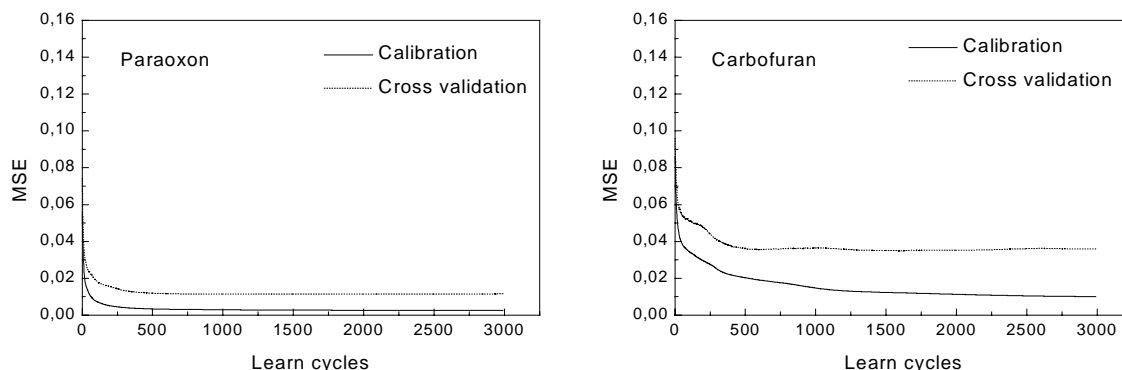


Figure 3.25: Development of network errors from artificial neural networks shown in Figure 3.24 for paraoxon and carbofuran, while training on data set generated with wild-type AChE multisensor.

#### 3.1.2.4 Sample discrimination

In order to test the ability of the AChE-multisensor to discriminate between different AChE inhibitors, two sets of experiments were carried out. These involved first, the discrimination of standard samples of paraoxon and carbofuran by cross-validation and second, the discrimination of paraoxon and carbofuran in spiked waste and river water samples serving as an independent test set.

In the first set of experiments, a the combination of AChE-multisensor and optimised neural network (Figure 3.24b) was used to discriminate mixtures of paraoxon and carbofuran in standard buffer solutions. The analyte concentration of the samples ranged from 0 to 20  $\mu\text{g/l}$  for each compound. In total, 50 samples were analysed and included in the network calculations. As illustrated in Figure 3.26, discrimination was possible over the total concentration range. The mean errors of prediction were 0.9  $\mu\text{g/l}$  for paraoxon and 1.4  $\mu\text{g/l}$  for carbofuran (see Table 3.17 for further details).

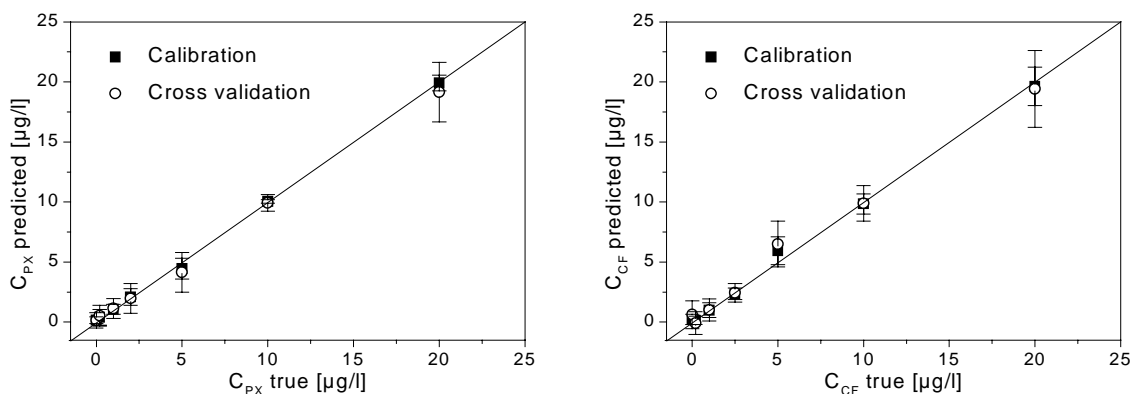


Figure 3.26: True vs. predicted plots for neural network calculations of multisensor responses to binary inhibitor mixtures. The figures represent the mean results of ten network training runs.

Table 3.17:

Results for neural network evaluation of sample discrimination using the AChE-multisensor.

			Paraoxon	Carbofuran
Calibration	RMSE	[ $\mu\text{g/l}$ ]	0.6	1.0
	AbsE	[ $\mu\text{g/l}$ ]	0.4	0.8
	MaxE	[ $\mu\text{g/l}$ ]	1.8	3.9
	ReIE	[%]	49	64
Cross Validation	RMSE	[ $\mu\text{g/l}$ ]	1.3	2.0
	AbsE	[ $\mu\text{g/l}$ ]	0.9	1.4
	MaxE	[ $\mu\text{g/l}$ ]	3.2	6.6
	ReIE	[%]	78	118

### 3.1.2.5 Multisensor performance in real samples

To demonstrate the ability of the system to carry out real sample analysis, waste water samples from the influent of a local sewage treatment plant were investigated. The samples were analysed directly and after spiking with 5  $\mu\text{g/l}$  of paraoxon or carbofuran, or with a mixture of both. The unspiked waste water revealed no inhibitory effect. As in the case of the standard solutions, the concentrations of each analyte was determined using the AChE-multisensor in combination with the optimised neural networks (Figure 3.24 b). The networks were calibrated with the 50



data sets obtained by analysis of standard solutions. Using the inhibition data from waste water samples as independent test sets, discrimination was possible with mean errors of prediction calculated at 1.8 µg/l for each analyte. The recovery rates in spiked waste water samples were 67% for paraoxon and 118% for carbofuran. Although the performance of the sensor was obviously disturbed by the problematic sample matrix ( $\text{BOD}_5 > 100 \text{ mg/l}$  [148]), an identification of the analyte was still possible with the aid of neural network data processing.

### 3.1.3 Improved multisensors using *Drosophila* AChE mutants

#### 3.1.3.1 Multisensor properties

In order to improve the sensor as far as assay duration and accuracy is concerned a set of highly sensitive *Drosophila* AChE variants was used and the immobilisation method was modified. The sensor described previously exhibited a signal equilibration within 10 min and a variation of the basic sensor signal of up to 25 %. By printing the enzymes in a matrix containing photosensitive PVA-SbQ, the sensors equilibrated in 5 min. The mean current outputs for multisensors I and II were 58 and 35 nA at 1 mM acetylthiocholine, respectively (multisensor I, dmAChE  $31.6 \pm 2.8$ , Y408F  $62.8 \pm 4$ , F368L  $40 \pm 3.2$ , F368H  $96.6 \pm 3.4$ ; multisensor II, dmAChE  $38 \pm 4$ , Y408F  $35 \pm 2.8$ , F368L  $27 \pm 3$ , F368W  $39 \pm 2.6$  (all values given in nA). These data demonstrate that the use of PVA-SbQ as an immobilisation matrix led to highly reproducible signals with 6.7 % and 9.7 % variation, respectively, of the mean response current. The change of the PVA-SbQ content from multisensor I to II did not improve the sensor performance any further.

In inhibition experiments using 5 µg/l paraoxon, the electrode-to-electrode errors for each enzyme were as follows: dmAChE,  $\pm 8.6 \%$ ; Y408F,  $\pm 1.2 \%$ ; F368L,  $\pm 1.3 \%$ ; F368H, not determined; F368W,  $\pm 18.7 \%$ . The determination limit in multisensor II was 0.5 µg/l for paraoxon ( $1.8 \times 10^{-9} \text{ M}$ ) and carbofuran ( $2.3 \times 10^{-9} \text{ M}$ ), with a mean signal-to-noise ratio of 6.3 and 3.0, respectively.

The lowest concentration for each analyte with a detectable effect was 0.1 µg/l. Depending on the AChE used, different linear ranges of sensor response to analyte concentration was observed. In the case of dmAChE, a linear relationship was observed for both analytes from 0 - 5 µg/l. For mutants F368L and F368H (multisensor I), the linear range of detection for either analyte was 0 - 10 µg/l. When the most sensitive mutant Y408F was used (multisensors I and II), a linearity was found of up to 3 µg/l carbofuran and 5 µg/l paraoxon. For F368W, inhibition over the whole range investigated was rather low and did not exceed 40 %, not even at a high concentration either of paraoxon or carbofuran.

Figure 3.27 shows the inhibition constants of the immobilised cholinesterase variants for each individual pesticide in comparison to the values in solution. Both multisensors for the three enzyme variants that were used repeatedly but with a different PVA-SbQ concentration for immobilisation were found to match well.

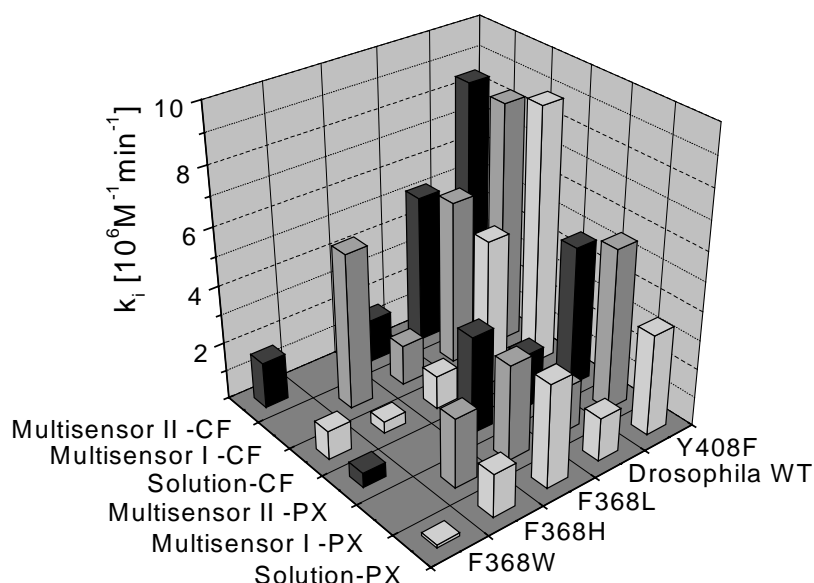


Figure 3.27: Comparison of inhibition constants for paraoxon and carbofuran of AChEs used for multisensors I and II before and after immobilisation on multisensors I and II. (CF, carbofuran; PX, paraoxon)

These observations confirmed that the modifications of the immobilisation matrix were successful in shortening the assay duration and reducing signal variation. However, in the case of F368H, the difference was rather extreme and this mutant was therefore replaced by F368W. As for the remaining variants, the correlation between  $k_i$  values in solution [104] [149] and immobilised enzymes was confirmed with respect to the modified experimental conditions (Figure 3.27).

### 3.4 Sample discrimination

In order to test the sensors for their capacity to discriminate between different AChE inhibitors, three sets of experiments were carried out.

1. Discrimination of standard samples of paraoxon and carbofuran by multisensors I and II using cross-validation.
2. Discrimination of paraoxon and carbofuran in spiked river water samples using multisensor II.
3. Discrimination of binary mixtures of malaoxon and paraoxon using cross-validation as the basic approach for multisensor II.

#### 3.4.1 Discrimination of paraoxon and carbofuran in standard solutions

Multisensors I and II which differ in the AChE variants F368L and F368W immobilised on sensor position 4, were compared for their ability to discriminate standard mixtures of paraoxon and carbofuran. (Figure 3.28 and 3.29)

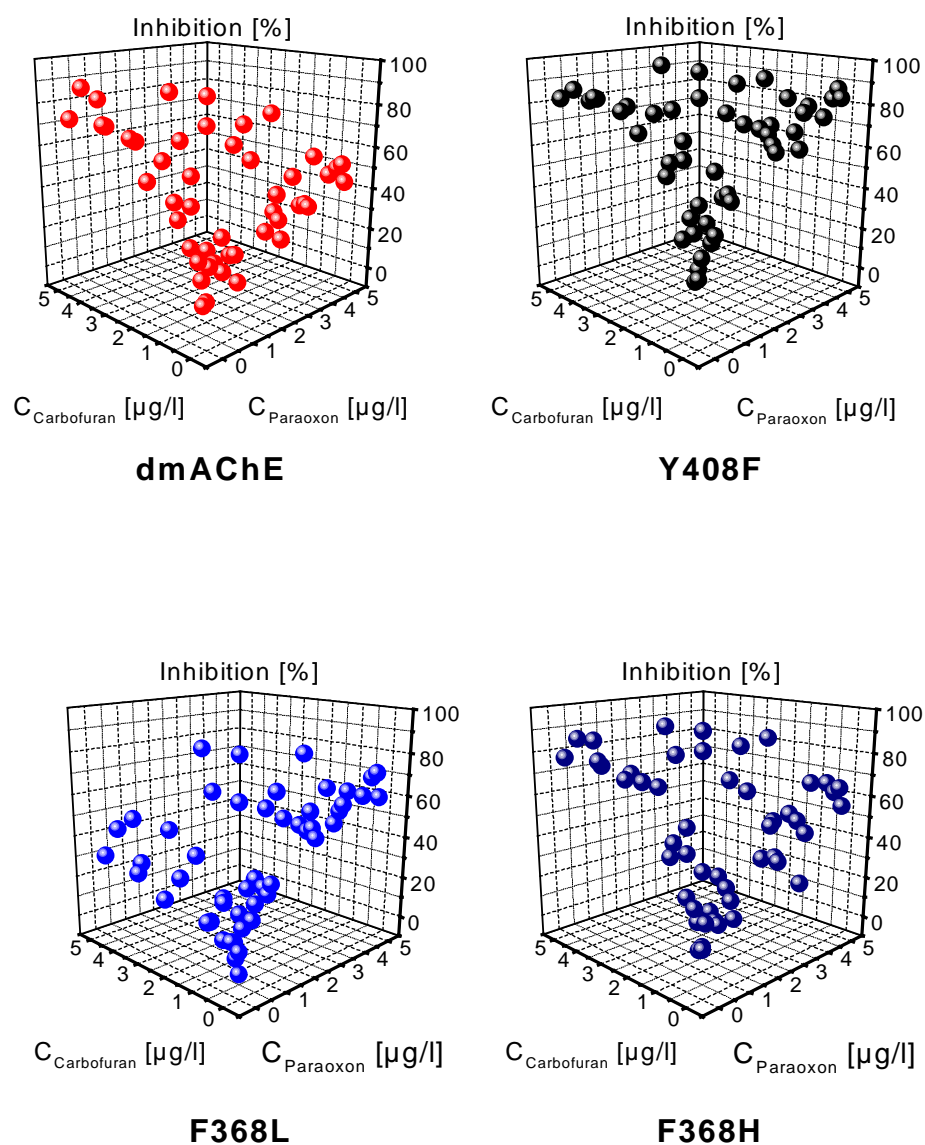


Figure 3.28: Multisensor I inhibition values by binary mixtures of carbofuran and paraoxon (0 - 5  $\mu\text{g/l}$ ). AChE partition on multisensor I: Position 1, dmAChE; position 2, Y408F; position 3, F368L; position 4, F368H. (AChE-inhibition in [%] plotted for each single electrode position *versus* concentrations of carbofuran (x-axis) and paraoxon (y-axis) in binary mixtures.)

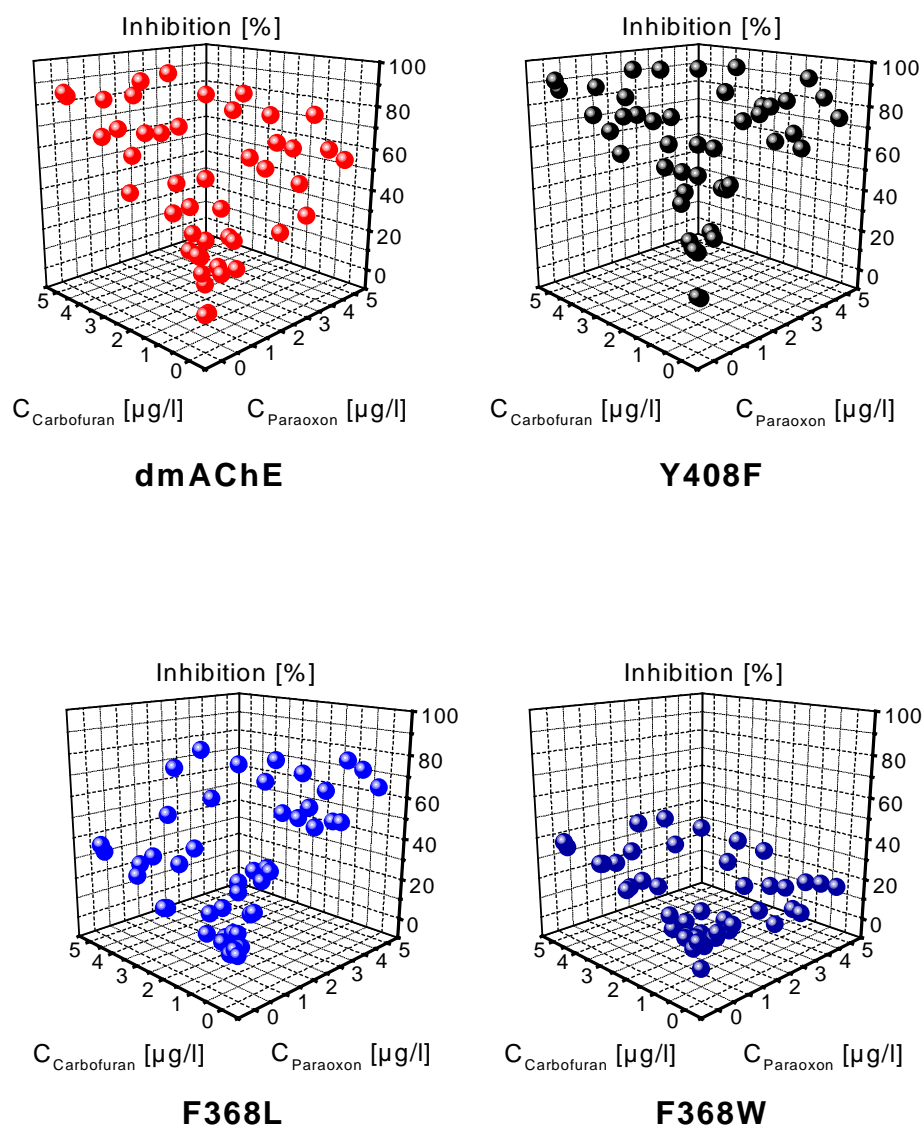


Figure 3.29: Multisensor II inhibition values by binary mixtures of carbofuran and paraoxon (0 - 5 μg/l). AChE partition on multisensor II: Position 1, dmAChE; position 2, Y408F; position 3, F368L; position 4, F368W. (AChE-inhibition in [%] plotted for each single electrode position *versus* concentrations of carbofuran (x-axis) and paraoxon (y-axis) in binary mixtures.)

### 3.3 Artificial neural network (ANN) set-up

For each multisensor and analyte, the optimal neural network configuration was chosen individually. As shown in Figure 3.30, network pruning was carried out starting from a 4:10:1 configuration. This resulted in the topology shown in Figure 3.30 b for each analyte.

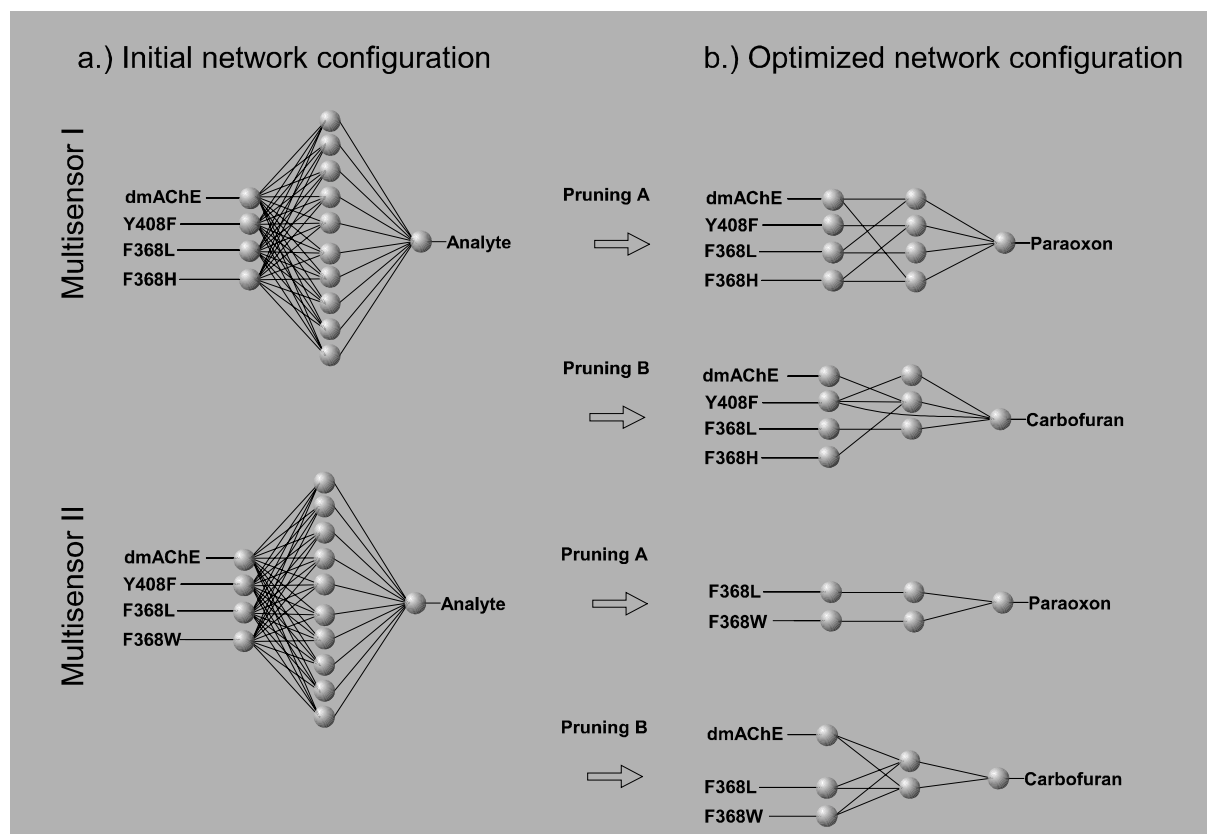


Figure 3.30: Initial network configurations (a) and results of pruning for each of the two analytes (b). For each analyte, separate pruning was performed (pruning A, pruning B)

The number of inputs for multisensor I remained the same, but hidden nodes were reduced to four for paraoxon and three for carbofuran discrimination. In the case of multisensor II, which employed resistant mutant F368W, the number of nodes was further minimised. For paraoxon discrimination, an optimal configuration of 2:2:1 was found using F368L and F368W as inputs. Interestingly, neither dmAChE nor Y408F were used as network inputs. For carbofuran analysis, a 3:2:1 configuration was preferred, using dmAChE to F368L and F368W. For both analytes, the highly sensitive mutant Y408F was removed. Nevertheless, the goal of reducing the number of enzymes necessary for discrimination of paraoxon and carbofuran from multisensor I to II could be achieved, thus paving the way for expanding the analyte spectrum even further.

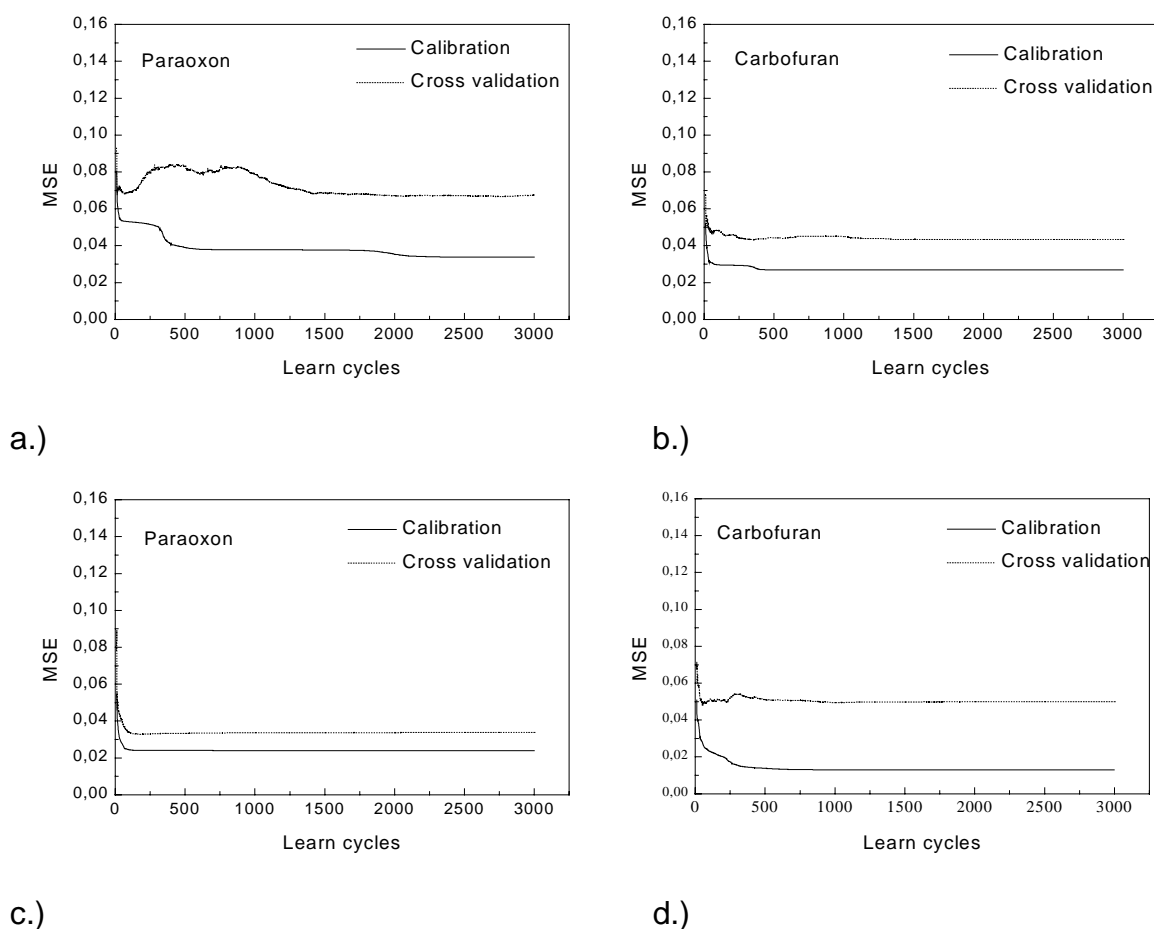
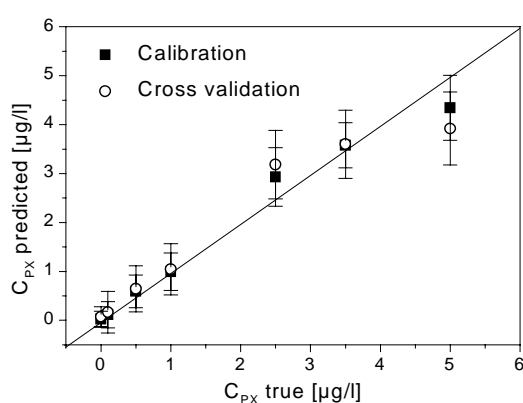
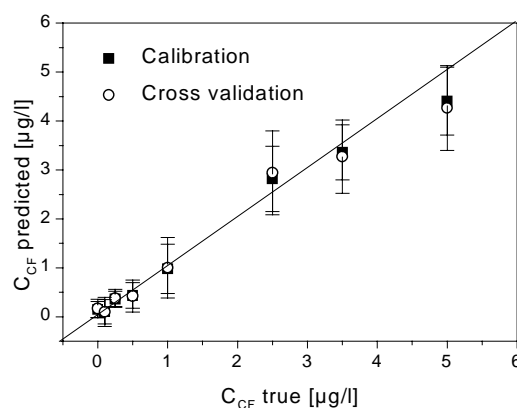


Figure 3.31: Development of neural networks shown in Figure 3.30 for paraoxon and carbofuran, while training on data set generated with multisensor I (a-b) and II (c-d).

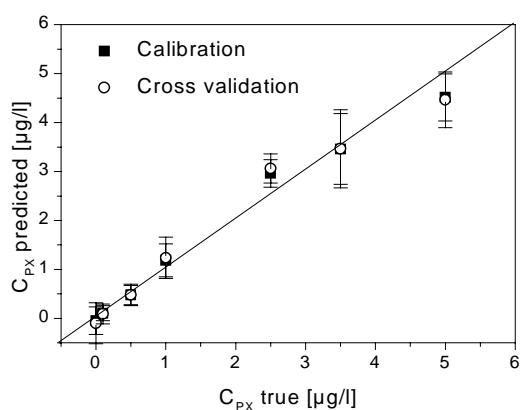
The training results for multisensor I and II and their corresponding artificial networks are given in Figure 3.31. As it was the case for the wild-type multisensor, the network error converged rapidly towards zero and no overtraining effect, indicated by an increased cross validation error was found. These network data were used for calculating the multi-analyte detection data and the results are shown in Figure 3.32. As illustrated in this figure, both sensor-network systems allowed the discrimination of paraoxon and carbofuran at high resolution.



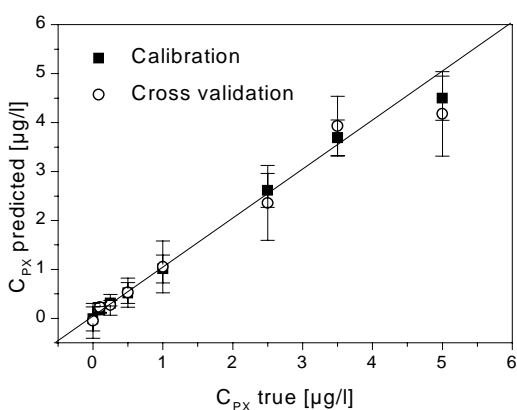
a.)



b.)



c.)



d.)

Figure 3.32: True *versus* predicted plots for neural network calculations of multisensor I (a-b) and II (c-d) responses to binary inhibitor mixtures. The figures represent the mean results of ten network training runs.

Multisensors I and II displayed a similar ability to detect both insecticides in the entire concentration range, but multisensor II required less inputs to reach the same result. The prediction errors for paraoxon/carbofuran mixtures in the range of 0 - 5 µg/l were significantly below 1 µg/l, namely 0.6 µg/l paraoxon and 0.5 µg/l carbofuran for multisensor I.

The integration of F368W into multisensor II further reduced prediction errors to 0.4 µg/l paraoxon and 0.5 µg/l carbofuran, determined by full cross-validation. Table 1-3 gives the detailed results for both multisensors.

Table 3.18:

Results of the neural network evaluation of mixture analysis using multisensors I and II.

			Multisensor I		Multisensor II	
			PX	CF	PX	CF
Calibration	RMSE	[ $\mu\text{g/l}$ ]	0.5	0.5	0.4	0.4
	AbsE	[ $\mu\text{g/l}$ ]	0.6	0.4	0.4	0.3
	MaxE	[ $\mu\text{g/l}$ ]	1.7	1.3	1.0	1.3
	RelE	[%]	42	57	38	31
Cross-Validation	RMSE	[ $\mu\text{g/l}$ ]	0.8	0.6	0.5	0.7
	AbsE	[ $\mu\text{g/l}$ ]	0.6	0.5	0.4	0.5
	MaxE	[ $\mu\text{g/l}$ ]	2.7	1.7	1.3	2.8
	RelE	[%]	67	71	45	54

The detection limit of multisensor II has been determined to 0.5  $\mu\text{g/l}$ . Consequently, the performance of the sensor-neural network system was also investigated for insecticide concentrations at this detection limit in the presence of one analyte and absence of the other.

A data set comprising triple determinations of 0.5  $\mu\text{g/l}$  paraoxon or carbofuran was used as an independent test set for evaluation of the neural networks shown in Figure 3.30. It could be demonstrated that multisensor II, in combination with neural networks and using only three AChE variants, was capable of discriminating the two insecticides paraoxon or carbofuran at the detection limit with mean errors of prediction of 0.25 and 0.17  $\mu\text{g/l}$ , respectively.

### 3.4.2 Discrimination of paraoxon and carbofuran in real samples

Samples of river surface water were spiked with paraoxon and carbofuran in the range of 0 - 2.5  $\mu\text{g/l}$ . The mean inhibition by the real sample itself was 28 % and neural network calculation of the blank data indicated theoretical concentrations of 0.4  $\mu\text{g/l}$  paraoxon and 0.2  $\mu\text{g/l}$  carbofuran. However, analysis of the fortified samples with multisensor II, and neural network processing of the sensor data, confirmed the spiked concentrations with a mean error of prediction of 1.1  $\mu\text{g/l}$  paraoxon and 0.67  $\mu\text{g/l}$  carbofuran.

### 3.4.3 Discrimination of paraoxon and malaoxon in standard solutions

As the results for multisensor II indicated a certain redundancy of the AChE mutants that were used for the discrimination of carbofuran and paraoxon, a higher resolution potential of this sensor was assumed. Its discrimination ability was therefore investigated for a two organophosphates containing mixture comprising paraoxon and malaoxon. The detection limit of multisensor II for malaoxon alone was determined to 0.5  $\mu\text{g/l}$  with a mean signal-to-noise ratio of 6.2. Multisensor II was investigated for the discrimination of paraoxon-malaoxon mixtures in the range of 0 - 5  $\mu\text{g/l}$  of each compound using a total of 36 samples (Figure 3.33).



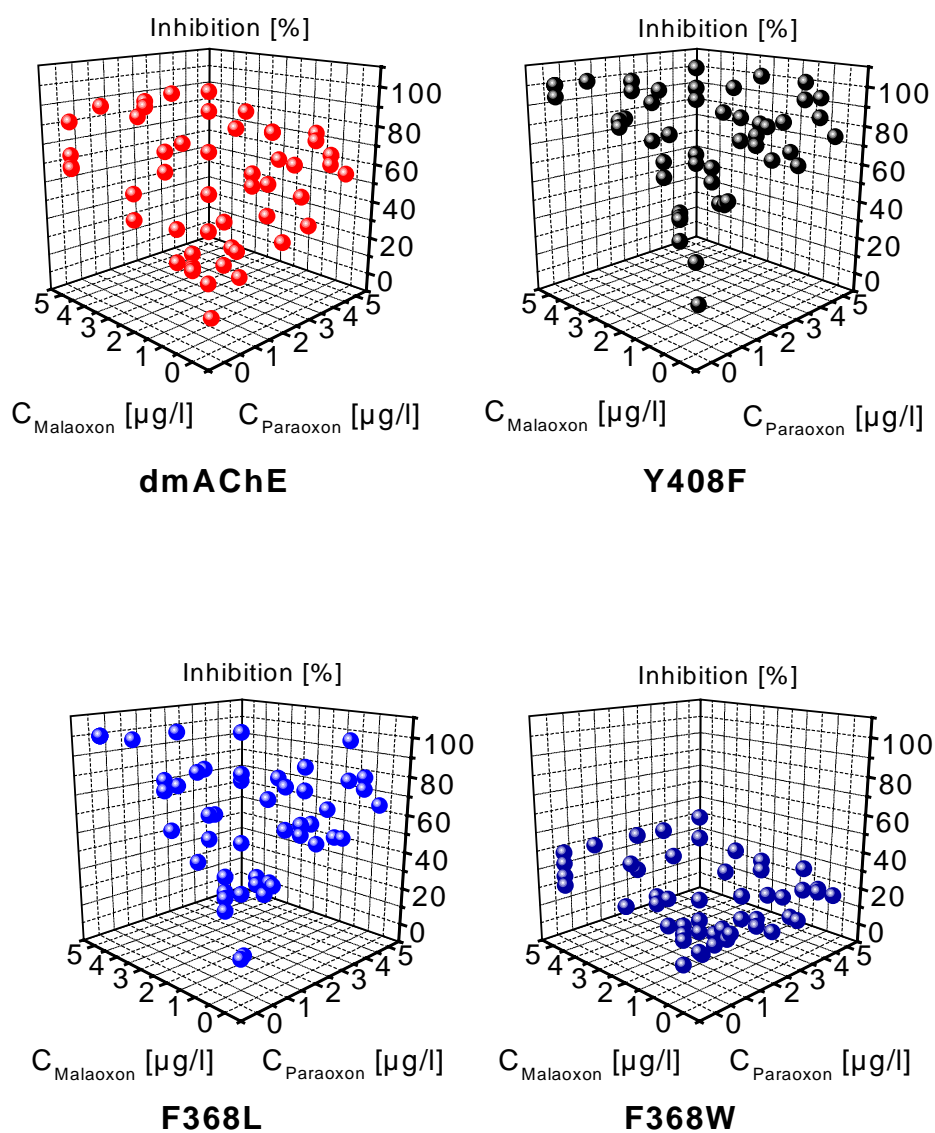


Figure 3.33: Multisensor II inhibition values by binary mixtures of malaoxon and paraoxon (0 - 5 μg/l). AChE partition on multisensor II: Position 1, dmAChE; position 2, Y408F; position 3, F368L; position 4, F368W.

The  $k_i$  values of the AChE variants used for multisensor II in the case of malaoxon were dmAChE 2.5, Y408F 8.7, F368L 9.3, F368W 0.3 (all in  $(10^6 \text{M}^{-1} \text{min}^{-1})$ ) [104;149]. This pattern of  $k_i$  values showed a strong similarity to that observed for paraoxon. This approach involving the discrimination of two closely related analytes belonging to the same compound family with a similar inhibition behaviour was therefore expected to be particularly difficult to perform. Following the same procedure described for paraoxon-carbofuran mixtures, which included pruning and cross-validation, the optimal networks for discrimination of the two organophosphates could be determined. As with multisensor I, all four AChE variants were used as inputs for the neural network (net topology for paraoxon 4:5:1, malaoxon 4:4:1). As a result, discrimination was possible using the optimised networks and cross-validation with a mean error of prediction of 1.6  $\mu\text{g/l}$  for paraoxon and 0.9  $\mu\text{g/l}$  for malaoxon (see Table 3.19 for details). The ability of the multisensor to discriminate two organophosphates was thus confirmed and the variability of the multisensor - artificial network combination could be demonstrated.

Table 3.19:  
Results of the neural network evaluation of mixture analysis using multisensor II.

			Multisensor II	
			PX	MX
Calibration	RMSE	$[\mu\text{g/l}]$	0.7	0.6
	AbsE	$[\mu\text{g/l}]$	0.5	0.4
	MaxE	$[\mu\text{g/l}]$	2.0	1.5
	RelE	$[\%]$	38	38
Cross-Validation	RMSE	$[\mu\text{g/l}]$	2.2	1.4
	AbsE	$[\mu\text{g/l}]$	1.6	1.0
	MaxE	$[\mu\text{g/l}]$	6.5	3.8
	RelE	$[\%]$	112	66

## 3.2 Multianalyte microbial sensors

The development of microbial sensors for multianalyte detection was performed in three steps:

- |                        |   |  |
|------------------------|---|--|
| 1. Basic transducer    | → | Planar disposable oxygen electrode.                                  |
| 2. Biological receptor | → | <i>Ralstonia eutropha</i> JMP 134, cultivation and characterisation. |
| 3. Biosensor           | → | Set-up and performance of microbial multisensor.                     |

### 3.2.1 Development of a planar oxygen electrode

Prior to the development of disposable microbial multisensors, a disposable transducer had to be designed for amperometric oxygen measurement. Starting from the fundamental electrode set-up as described in chapter 2.1.3.1, the transducer was developed and characterised. To use this electrode for microbial sensors the following points had to be considered specifically:

- For amperometric oxygen detection the polarisation of the electrode had to be set to negative values. Oxygen reduction is performed at -800 mV vs. Ag/AgCl in Clark type electrodes if platinum cathodes are used. In contrast, the screen printed oxygen electrode used rhodium graphite as cathode material. Therefore optimal polarisation and electrolyte conditions had to be found.
- High overpotentials cause unspecific electrochemical reactions. The microbial sensor was developed to be used predominantly in waste water. For this reason, specific precautions to prevent interfering electrochemical reactions had to be undertaken. This could be reached by the use of oxygen selective membranes.
- The use of planary structured electrodes complicate the immobilisation of microbial membranes. Therefore provision of immobilisation-compatible surfaces for sufficient adhesion of micro-organism membranes was essential for the sensor development.

#### 3.2.1.1 Manufacturing of oxygen electrodes

The preparation of the planar screen printed oxygen electrodes (SPOE) was performed in three steps. 1.) The basic transducer was screen printed, 2.) the electrolyte was drop-coated on the electrode surface, and 3.) the gas selective silicon rubber membrane was spin-coated over the electrolyte layer. In order to form a distinct immobilisation area for the microbial membrane, the electrodes were finally laminated using a tape mask.

---

### Basic transducer platform

The screen printing of the transducer platform was performed using the semi-automatic screen printer as described in chapter 2.1.3.1. A sufficient reproducibility of the SPOE was highly desired to provide optimal preconditions for multianalyte detection later with the microbial multisensor. This was achieved by production of batches of electrodes with exactly the same printing parameters. Oxygen electrodes were produced in batches of 500 - 2500 electrodes. Figure 3.1 shows scans of the five separately printed layers for the basic transducer platform.

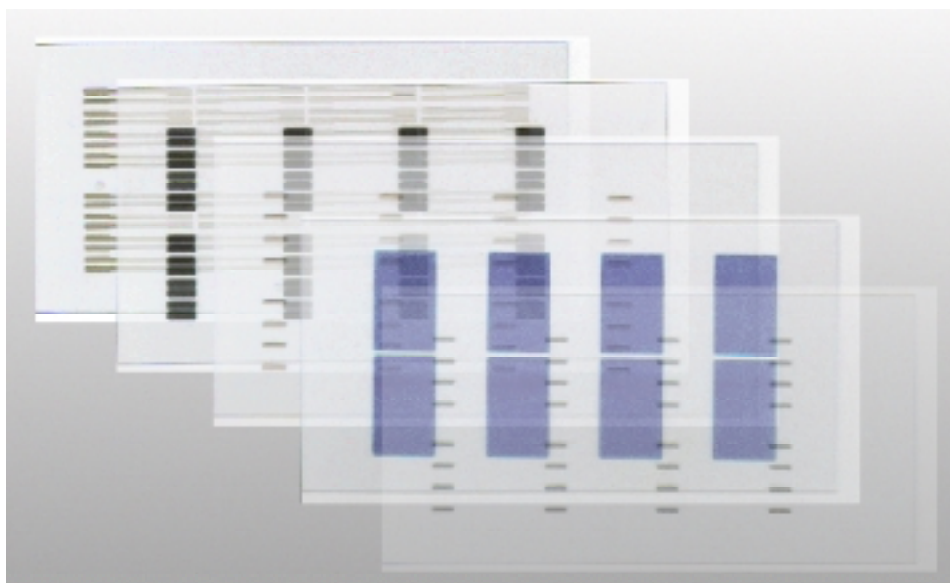


Figure 3.1: Overlay of five separately printed layers of the basic transducer. Each PVC sheet contained 36 single electrode pairs in sets of 4 each. (From left: silver conducting tracks, graphite pads, Ag/AgCl reference electrodes, insulation, working electrodes)

### Electrolyte

To simplify the production process, the deposition of the electrolyte was first performed by screen printing. Technically, this was only possible using solutions with sufficient viscosity. Therefore three different PVP types with different molecular weights (10, 40 and 360 kD) and different viscosities (K 12-18, 30, and 90) were investigated. In all cases the electrolyte layer was not homogenous after drying. Moreover the connection (salt bridge) over the gap between working electrode and reference electrode was not reproducible. Due to the hydrophobicity of the PVC substrate the electrolyte solution did not remain in the gap during the drying process. Increasing salt concentrations by printing of electrolyte containing 3 M KCl and K90 PVP did also not perform in the desired way.

Thus, the deposition of the electrolyte via drop-coating was used in further experiments. For the purpose of reliable salt bridge formation, the working/reference electrode gap was modified with approx. 0.5  $\mu\text{l}$  of 0.5 % cellulose acetate in acetone. Three electrolyte compositions were tested in volumes from 5 - 20  $\mu\text{l}$ . Only 20  $\mu\text{l}$  depositions gave the best results considering homogeneity of the electrolyte layer. As the reduction of oxygen forms hydroxide ions, the control of the electrolyte pH is

essential for the reaction equilibrium. Consequently, the non buffered electrolyte led to instable electrode signals. For this reason, the next two electrolytes were phosphate buffered and adjusted to pH 7.5. Two buffered electrolytes were investigated with KCl concentrations of 0.3 and 3 M. The electrolyte containing 3 M KCl led to inhomogeneous cristallisation although the PVP dried to homogeneous films on the electrode. The electrolyte which performed best contained 6.6 % PVP (K30, Fluka) and 0.3 M KCl.

### Selective membrane

For mass production reasons the deposition of a gas permeable membrane on the electrode with dried electrolyte layer was performed firstly by screen printing. Although the resulting electrodes showed a promising behaviour, this method had to be discarded as the silicon rubber was unremovable from screens after the process. As an alternative, spin-coating proved to be a fast and convenient method for the application of the silicon rubber membrane. The sensors were spin-coated for 20 seconds at 2500 rpm resulting in a 0.1 mm thick silicon rubber layer (determined using a fine caliper). Longer spinning times or higher rpm values did not significantly effect the layer thickness and electrode performance.

### Conditioning

As the electrolyte was dried prior to deposition of the silicon rubber membrane, the electrodes had to be rehydrated prior to use. To achieve this, the electrodes were immersed in demineralised water for one hour. The water uptake was determined by the weight of the electrodes before and after the incubation. As a result each electrolyte gained 36  $\mu\text{l}$  ( $\pm 5 \mu\text{l}$ ) of water during this procedure. The final electrolyte concentration can therefore be calculated as 2 M KCl and 9.9 % PVP.

---

### 3.2.1.2 Characterisation of SPOEs

The performance characteristics of the disposable SPOEs were investigated in view of interfering substances, operational, and storage stability, calibration, electrochemical properties and dynamic behaviour.

#### Interferences

Due to the presence of the gas-permeable silicon rubber membrane, the effect of variations in the external medium was expected to be minimal or even neglectable. Indeed, variation of the pH value from 1 - 14 did not change the sensor output in a significant manner ( $<50$  nA) (data not shown). Also the addition of various sodium chloride concentrations up to 1 M remained without effect. The addition of ascorbic acid or any of the analytes investigated later in this study showed any change in sensor response. Furthermore the integrity of the silicon rubber membrane could be tested by the addition of  $\text{Na}_2\text{SO}_3$ . If any short cut through holes in the silicon rubber membrane to the external medium existed, this test led to a strong increase of the electrode output instead of a decrease due to oxygen depletion (Figure 3.5).

#### Operational stability

The thick film sensors were investigated for their signal stability in comparison to a commercial device (DO-14P Dissolved Oxygen Meter, TOA Electronics Ltd., Tokyo Japan). Figure 3.2 shows a typical result for a preconditioned electrode. It has to be stated, that the first run-in for both electrode types could be maximally longer by a factor 5.

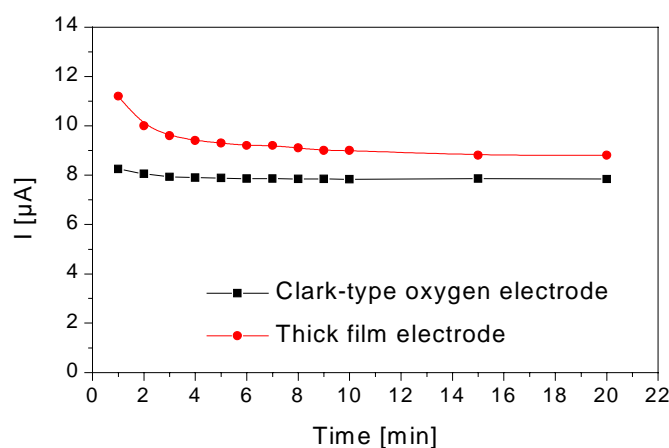


Figure 3.2: Signal stability and run-in behaviour of a screen printed and commercial oxygen electrode.

The operational stability of the screen printed sensors was one of the bigger problems in designing high quality transducers. In some cases, a reduced signal stability was detected. Here the current output for oxygen saturated solutions

decreased steadily from the usual initial value to approx. 20 - 50 nA within four hours of continuous polarisation. This can be explained either by electrode fouling or a shift of the internal electrolyte pH. Additionally visual investigations of the electrode condition after measurement using a binocular revealed a dissolving of the rhodium graphite working electrode. This could be avoided in further experiments by the additional fixation of the working electrode by cellulose acetate (0.5 % in acetone). Under optimised conditions, in 90 % of all investigated electrodes a continuous polarisation and oxygen measurement was possible for at least 6 - 8 hours.

### Storage stability

The storage stability of the screen printed oxygen electrodes was longer than one year at room temperature if air and humidity could be excluded. The storage limit under these conditions was not found within this study. Storage of hydrated electrodes in contact with solution led to a swelling of the tape mask/silicon interface after approx. one day. For storage the better way was to dry and rehydrate again previously hydrated electrodes.

### Calibration

The disposable oxygen sensor was calibrated using a commercial device for measuring dissolved oxygen (DO-14P). Different concentrations were adjusted by addition of variable amounts of  $\text{Na}_2\text{SO}_3$  to oxygen saturated water or buffer solution. The screen printed electrode displayed a linear relationship between current output and detected oxygen concentration by using the commercial probe (Figure 3.3).

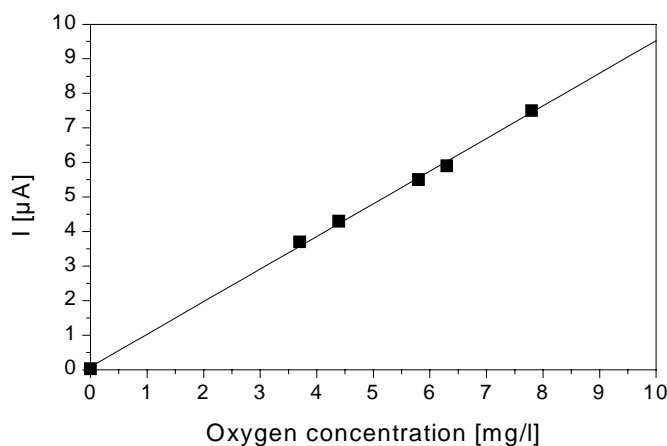


Figure 3.3: Calibration of a SPOE using a commercial dissolved oxygen probe.

### Electrochemical properties

A comparison of the electrochemical properties of SPOEs and the commercial probe is illustrated in Figure 3.4. The figure shows results of hydrodynamic voltamograms for both electrodes in the presence and absence of oxygen. The Clark-type

commercial oxygen probe (Figure 3.4 b) behaved in a desired way for amperometric electrodes. Over a wide potential range from 500 - 1100 mV the current was independent from the applied overpotential. As expected, no current was measured in the absence of oxygen.

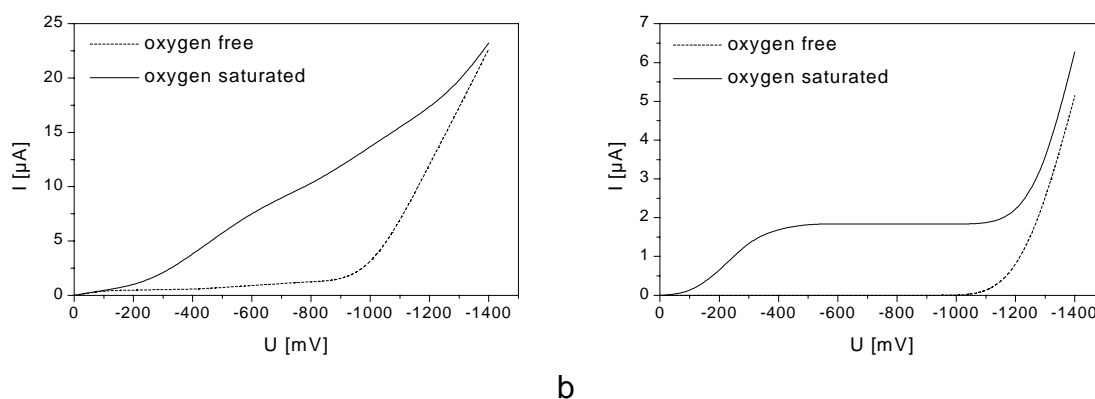


Figure 3.4: Hydrodynamic voltammograms of SPOE (a) and commercial Clark-type oxygen electrode (b) in oxygen free ( $\text{Na}_2\text{SO}_3$ ) and oxygen saturated (air) solutions.

In the case of the SPOE (Figure 3.4 a) the observations were different. Here, no clear plateau was found for the current depending on the overpotential and the current continuously increased with increasing negative potential. In the absence of oxygen no significant current was detected up to a polarisation potential of - 500 mV. For this reason, the working potential for the SPOE was set to  $U_{\text{pol}} = - 300$  mV in all further experiments (all results in this study were obtained using this potential, unless stated otherwise).

### Dynamic characteristics

The SPOEs were monitored in view of their kinetic properties. For this purpose, the sensors were exposed to oxygen saturated (air) and oxygen free ( $\text{Na}_2\text{SO}_3$ ) solutions. All SPOEs showed an immediate response to the changing medium but needed about 10 - 15 minutes to reach a steady state signal again. If smaller changes in oxygen concentration occurred, as they were applied in the calibration experiment, the sensor equilibrated more rapidly. Figure 3.5: Recorder output of sensor responses upon oxygen free ( $\text{Na}_2\text{SO}_3$ ) and oxygen saturated (air) solutions. shows the corresponding signals to the change of oxygen concentration. Additionally to the fast response the sensors displayed a remarkable signal stability.

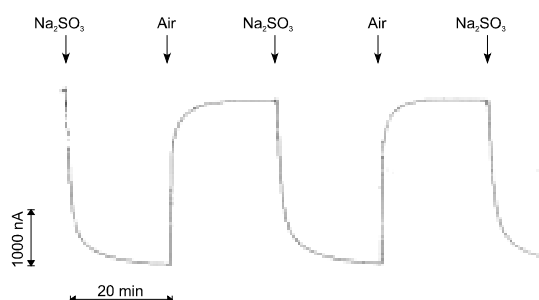


Figure 3.5: Recorder output of sensor responses upon oxygen free ( $\text{Na}_2\text{SO}_3$ ) and oxygen saturated (air) solutions.



### 3.2.2 Development of the microbial sensor

#### 3.2.2.1 Preparation of the biological receptor: Cultivation of *Ralstonia eutropha* JMP 134 on different carbon sources

In order to perform multianalyte detection, the microbial multisensor should be equipped with differently induced *R. eutropha* JMP 134 cells. Therefore, the growth of *R. eutropha* JMP 134 on various carbon sources was investigated. Figure 3.6 shows growth curves for four different substrates. Cells incubated with these substances were later used in the multisensor approach. The best growth was found with phenol and 2,4-D as sole carbon sources. Here already after 6 hours the stationary phase was reached. Consequently these cells were harvested at the latest after 6 hours. Cultures with 2-MPA as substrate displayed a slower increase in optical density than it was observed for 2,4-D and phenol. For practical reasons the cells were harvested after 9 hours. The substrate which led to the slowest growth was MCPA. Here the cells grew over a period of 48 hours to an optical density of 0.2. For immobilisation the cells were harvested after 24 hours cultivation.

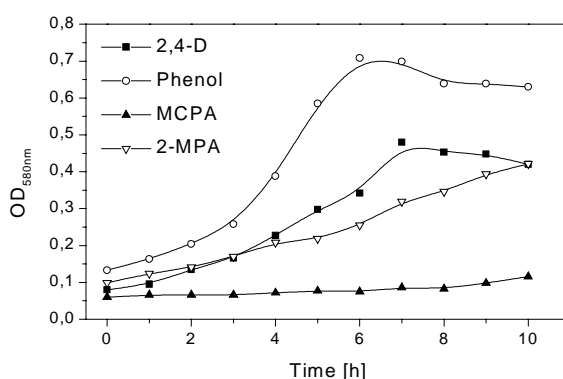


Figure 3.6: Growth of *Ralstonia eutropha* JMP 134 on different carbon sources (Cs = 2 mM)

#### 3.2.2.2 Determination of induction states

Cells harvested according to chapter 3.2.2.1 were investigated in order to clarify their induction state. Therefore the oxygen uptake rates upon 2,4-DCP, 4-CP and phenol addition were determined using a YSI Biological Oxygen Monitor. As can be clearly seen in Figure 3.7, cells from all four differently grown cultures displayed an individual response pattern upon analyte addition. 2,4-D grown cells reacted strongly to 2,4-DCP, moderately to 4-CP but not to phenol. Cells cultivated on MCPA showed a similar pattern but also responded to phenol addition. Equal reaction was found for 2-MPA upon addition of all three analytes. Fortunately, phenol grown cells exhibited an opposite behaviour as compared to 2,4-D grown cells, so the multisensor approach seemed to be feasible.

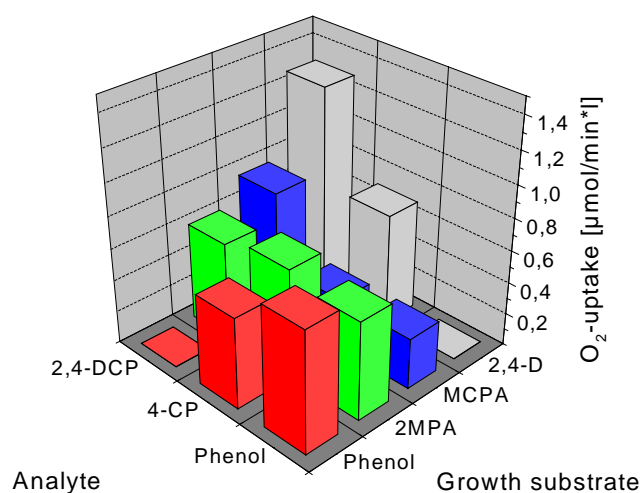


Figure 3.7: Determination of specific oxygen uptake rates of non-immobilised cells using a YSI Biological Oxygen Monitor.  $V = 3 \text{ ml}$ , oxygen saturated TBS,  $30^\circ\text{C}$ ) ( $100 \mu\text{l}$  Cell susp.  $\text{OD}_{580\text{nm}}=2$ ) ( $C_s = 16 \text{ mM}$ )

### 3.2.2.3 Immobilisation of the biological receptor

The immobilisation on the gas permeable silicon rubber membrane turned out to be the crucial step in the development of the microbial biosensor. As the electrode design was planar and silicon rubber is highly hydrophobic, the adhesion of any hydrophilic immobilisation matrix was extremely weak. On the other hand, the use of more hydrophobic immobilisation matrices turned out to have negative effects on the cell viability. Table 3.20 gives a summary of the protocols for immobilisation of microbial membranes on planar oxygen electrodes investigated within this study.

Table 3.20:

Investigated matrices and protocols for immobilisation of *R. eutropha* JMP 134 on planar oxygen electrodes. (A. = Adhesion, S. = Sensor response upon the addition of substrate)

Matrix	A.	S.	Remark
1) PU3 (1 - 20 %)	+	-	Rapid polymerisation, strong adhesion, weak signal.
2) PU6 (1 - 20 %)	+	-	Rapid polymerisation, strong adhesion, weak signal.
3) Al-Alginate	-	-	No signal, weak adhesion.
4) Ca-Alginate	-	-	No signal, weak adhesion.
5) ENT/ENTP	-	-	No signal, weak adhesion.
6) PVA-SbQ	-	-	Swelling, weak adhesion.
7) PVA-SbQ/10% APTS	+	+	Swelling, instable adhesion.
8) NC-Filter, glue fixation	+	-	Complicated construction, weak signal, long equilibration of basic current (> 1 h).
9) Ca-Alginate / NC-Filter	+	+	Weak adhesion, complicated construction, weak signal, long equilibration of basic current (> 1 h).
10) PU6 / NC-Filter	+	+	Strong adhesion, complicated construction, long equilibration of basic current (> 1 h), low sens.
11) Ca-Alginate/Nylon nets	-	-	Weak adhesion, complicated construction, weak signal, long equilibration of basic current (> 1 h).
12) Ca-Alginate/Shin Etsu Silicone	+	-	Material is probably toxic to cells.
13) Shin Etsu Silicone	+	-	Material is probably toxic to cells.
14) Dow Corning Silicone	+	-	Material is probably toxic to cells.
15) Ca-Alginate/Dow Corning Silicone	+	-	Material is probably toxic to cells.
16) Ca-Alginate/Nylon nets/Shin Etsu Silicone	+	-	Strong adhesion, complicated construction, long equilibration of basic current (> 1 h), low sensitivity.
17) NC/Shin Etsu Silicone	+	-	Strong adhesion, complicated construction, long equilibration of basic current (> 1 h), low sensitivity.

None of the above mentioned immobilisation techniques could provide a good adhesion like the polyurethane matrices as well as the ideal viability preservation properties known by alginate immobilisation. Therefore further experiments were directed towards the optimisation of the alginate adhesion on the hydrophobic silicon rubber membrane.

As it was known from preliminary experiments, the incubation of the oxygen electrode with an 10% aqueous solution of APTS for 30 min improved the adhesion of a 20 mg/ml PVA-SbQ matrix. However these results were fairly reliable due to the swelling properties of PVA-SbQ. Additionally these findings could not be transferred to calcium alginate immobilisation. For this reason an increased content of APTS of 98 % was investigated to improve the adhesion by intensive aminosilanisation. Although

this treatment significantly amended the attachment of the microorganism membrane, the results were irreproducible. Within a set of 10 multisensors at least 4 membranes were detached. As a further drawback, the operational stability was not satisfactory. For this reason an additional modification of the sensor surface was performed.

Figure 3.6 shows the stepwise creation of a highly hydrophilic sensor surface. The optimal conditions were 60 seconds incubation with 98% APTS. Shorter expositions were not sufficient for adhesion and longer expositions led to negative effects in electrode performance. Directly after this treatment and intensive washing, the dry electrodes were exposed to glutaraldehyde vapor for 20 min at room temperature. The electrode preparation was finished by incubating the active sensor surface with a 5 % BSA solution for 10 min. at room temperature. Lower concentrations and shorter expositions did not result in good adhesion properties of the sensor surface. The styles for the chemical reaction of RTV rubber curing [150] and silanisation using APTS are illustrated in Figure 3.8:

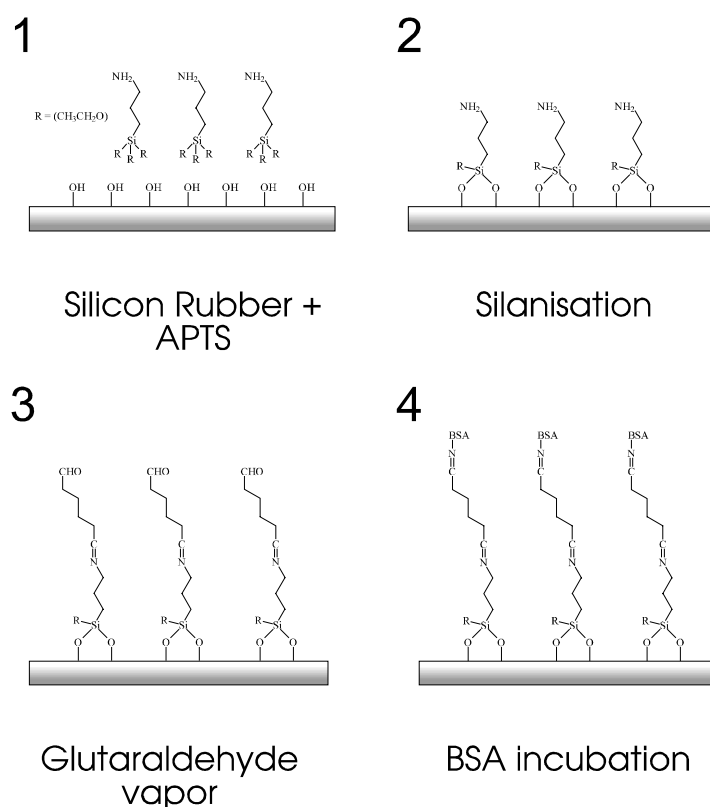


Figure 3.8: Surface modification of planar oxygen electrode silicon rubber membrane, simplified reaction scheme. 1: Silicon rubber membrane and APTS, 2: Aminosilanised silicon rubber membrane, 3: Modification with glutaraldehyde, 4: BSA coupling.

The activation level of the silicon rubber surface was monitored using the TNB-test (2,4,6-Trinitrobenzenesulfonate). The reaction of TNB with amino or aldehyde groups forms deeply orange coloured products and is oftenly used for activation monitoring in affinity chromatography [146]. In Figure 3.9 the results of the TNB test are shown

for each step of surface modification. No visible colour change of the sensor surface occurred if TNB was not applied. The use of APTS formed white crystal-like structures on the silicon rubber. In contrast the degree of activation could be clearly seen after APTS and glutaraldehyde reaction which result by theory in an increase of free aldehyde groups (Figure 3.8). After the incubation with BSA a thick white, sponge-like layer was formed in the TNB test. Thus, the disappearance of any orange colour revealed the complete reaction of all amino or aldehyde groups.

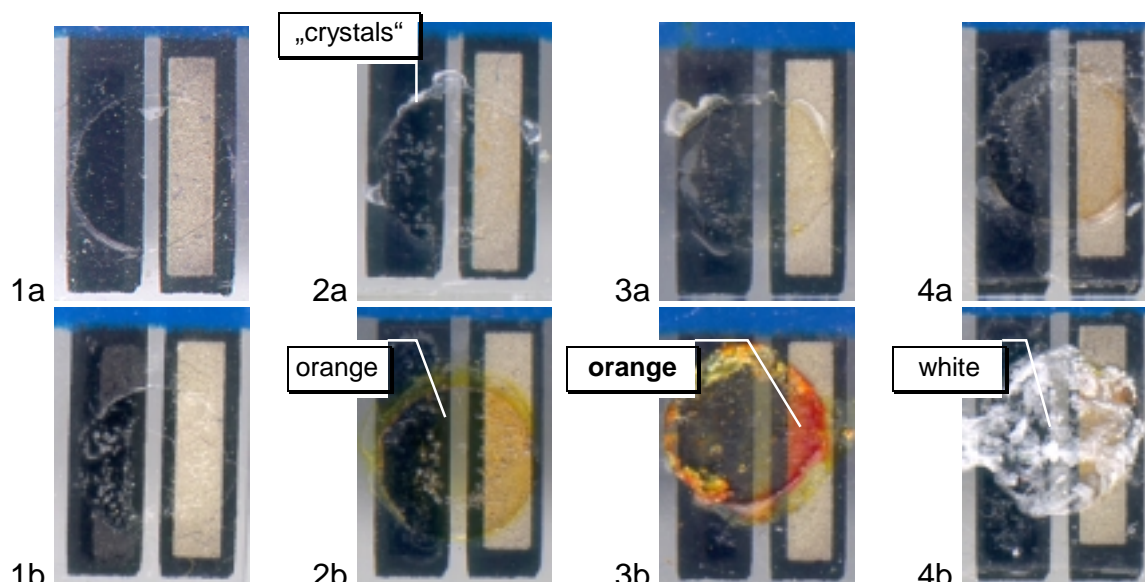


Figure 3.9: Monitoring of surface modification of planar oxygen electrode silicon rubber membrane by TNB-test. (a) blanc (b) TNB-test, 1: silicon rubber membrane and APTS, 2: aminosilanised silicon rubber membrane, 3: glutaraldehyde modified electrode, 4: after BSA coupling.

The hydrophilized sensor surface could be now used for a stable immobilisation of a microbial membrane formed by gelation of sodium alginate mixed with *R. eutropha* JMP 134 cells. The optimal alginate concentration was found to be 2 % with a cell concentration of 100 mg/ml.

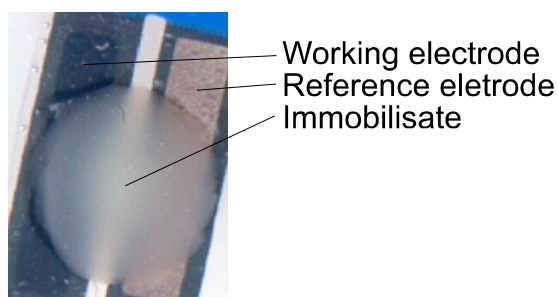


Figure 3.10: Magnification of active area of a microbial sensor. Immobilisate contained 10  $\mu$ l of alginate/*R. eutropha* JMP 134 suspension after gelation in 0.2 M calcium chloride.

### 3.2.2.4 Basic biosensor characterisation

Before multi-analyte detections were carried out with the microbial sensors, a set of comprehensive characterisations in view of dynamic characteristics, sensitivity, storage and operational stability and reproducibility was performed. All experiments in this section were conducted with the representative model system of 2,4-D as analyte and growth substrate.

#### Dynamic characteristics

To investigate the influence of the immobilisation matrix on the oxygen diffusion to the sensor surface, three types of sensors were exposed to changing oxygen concentrations. Oxygen saturation was provided by aeration of buffer and oxygen free medium by nitrogen stream. As sensors a blank sensor without immobilization, one with 10  $\mu$ l alginate, and one with the standard immobilized cells were tested. The results are shown in Figure 3.11. Surprisingly the highest impact on the dynamic properties of the sensor had the sensor itself. Only approx. 21 % of the time to reach 90 % of the full signal ( $t_{90\%}$ ) were contributed by the alginate and another 17 % by the cells.

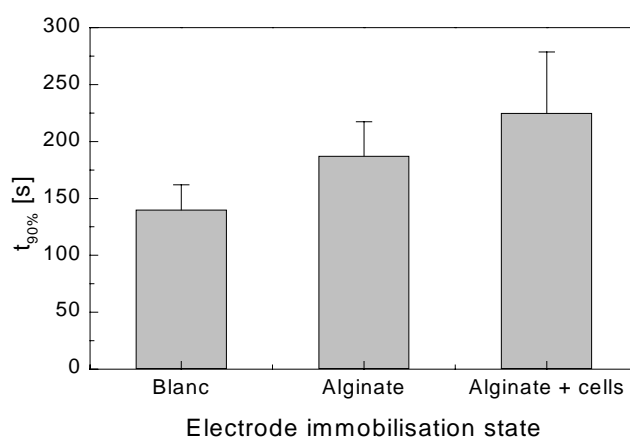


Figure 3.11: Investigation of the microbial biosensor's dynamic properties:  $t_{90\%}$  values of sensors with different immobilizations.

## Sensitivity

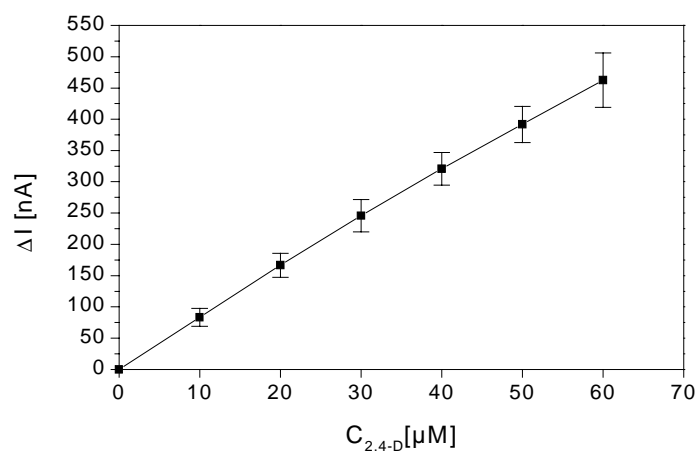


Figure 3.12: Standard curve for 2,4-D using 2,4-D grown cells. (n=3)

Figure 3.12 shows the results for sensor responses towards 2,4-D in concentrations of 0 to 60  $\mu M$ . The relation was linear over the whole range investigated with a sensitivity of 7.8 nA/ $\mu M$ . A mean standard deviation of  $\pm 10\%$  was determined over the complete detection range. The detection limit of 2,4-D was determined to 2  $\mu M$  with a signal to noise ratio of 5.5 (n=5). A representation of a real signal is shown in Figure 3.13.

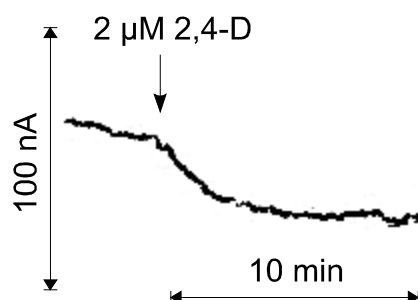


Figure 3.13: Sensor signal upon addition of 2,4-D at the detection limit.

## Operational stability

The microbial sensors properties should be stable during storage and operation in order to make the multianalyte detection approach possible. To prove operational stability, the sensors were used for repeated measurements of 20  $\mu M$  2,4-D. In between two measurements the sensors were thoroughly washed and polarisation was turned off. Therefore the variation of the basic signal possibly also arose from changes in the run-in behaviour. In all later experiments the sensors were permanently polarised in order to speed up the measurement frequency.

The sensors, which were equipped with 2,4-D grown cells displayed a stable signal over 6 repeated measurements. The mean sensor response to 20  $\mu\text{M}$  2,4-D was 194 nA with a standard variation of  $\pm 33$  nA (17%). The mean decrease per measurement was - 5,3 nA (2,7%) (slope of linear regression). The basic dissolved oxygen signal itself showed a variation of  $\pm 74$  nA (3,2 %) and an absolute mean value of 2330 nA.

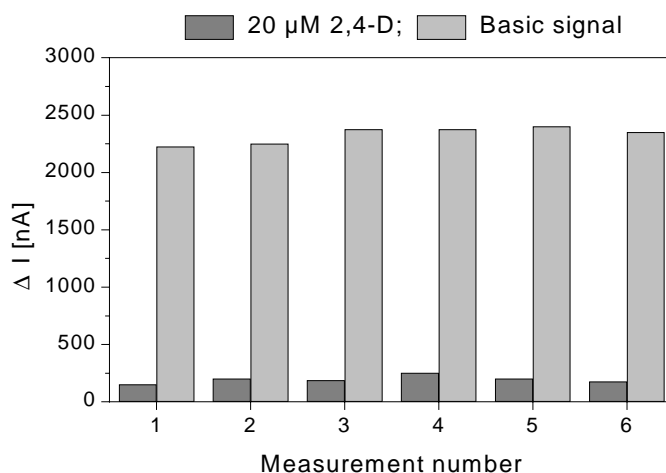


Figure 3.14: Investigation of operational sensor stability. Repeated measurements of 20  $\mu\text{M}$  2,4-D using a single sensor equipped with 2,4-D grown cells.



Figure 3.15: Overlay of Figure 3.14 signals. The signals are congruent in terms of equilibration time, noise, response time and signal height.

Although these experiments revealed a relatively high signal variation, the stability of the transducer and the immobilisation matrix was confirmed and repeated measurements could be reliably performed.

The operational stability of the biosensor signals was influenced by two major parameters, the adhesion of the microbial membrane to the silicon rubber and the stability of the alginate matrix itself. Whereas the adhesion of the membrane could be followed visually, the integrity of the alginate matrix was only detectable by a change of the signal height. A detachment of the microbial membrane could be noticed as an increase of the basic signal and a decrease of the response upon analyte addition.



Detailed investigations were performed for finding the optimal buffer system for the microbial sensor. As for the gelation of the Na-alginate matrix  $\text{Ca}^{2+}$  ions were used, phosphate buffer systems resulted in immediate dissolving of the membrane. Tris buffer systems were found to be more suitable. Best results with the bare transducer itself were found using a Tris buffer 10 mM Tris/HCl containing 10 mM NaCl. The absence of NaCl negatively affected the sensor equilibration and the noise intensity after sample application. Repeated measurements in this buffer were problematic, as the microbial membrane was usually dissolved at the latest after the fourth cycle. In one measurement cycle the sensor was exposed to a buffer volume of approx. 25 ml (5 ml for measurement, 20 ml for rinsing). A dissolving of  $\text{Ca}^{2+}$ -ions from the matrix was suspected to be responsible for this observation. Intermediate regenerations for 5 min in 0.2 M  $\text{CaCl}_2$  severely decreased the analyte signals. For this reason various concentrations of  $\text{CaCl}_2$  were added to the buffer and the analyte signal stability was monitored. Out of a concentration range of 0,1 to 1 mM  $\text{CaCl}_2$ , 0,5 mM resulted in best performance of the sensor. Lower concentrations led to an increase of the analyte signals in each cycle. Higher concentrations had the opposite effect (data not shown).

### Reproducibility

The envisaged application as a multisensor required a high reproducibility of the single sensor in terms of measurement repetition. As four electrodes were intended to be used in parallel, the corresponding sensors should also have equal signals. It is shown in Figure 3.15 for a complete multisensor equipped with the identical cells, grown on 2,4-D, that this task could be fulfilled. The mean signal after addition of 20  $\mu\text{M}$  2,4-D was 266 nA. The mean errors for single sensors were  $\pm 11.2\%$  and the sensor-to-sensor error was  $\pm 11.4\%$ . The mean standard deviation of the basic signals was 5 % for single sensors and 18 % for the sensor-to-sensor comparison. Interestingly the variation in basic currents, which can be explained with differences in electrode preparation, did not cause a proportional variation in the analyte signals. A standardisation calculated from relative signals was therefore dispensable.

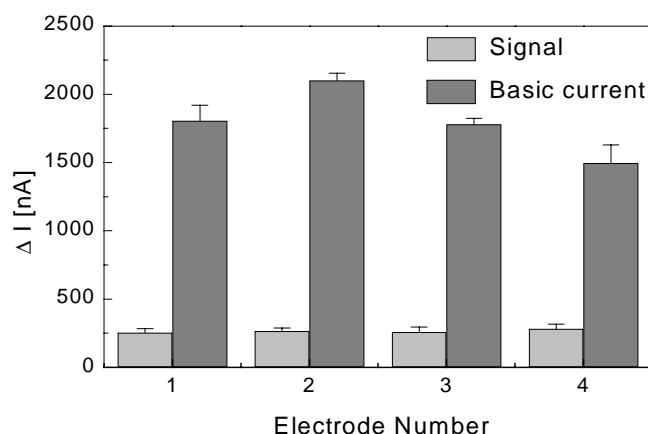


Figure 3.16: Repeated measurements of 20  $\mu\text{M}$  2,4-D with complete multisensor. Cells were grown on 2 mM 2,4-D. ( $n = 5$ )  
Selectivity

Furthermore the selectivity, reproducibility and stability of the analyte specific signal was monitored after exposure to different analytes. Figure 3.17 shows results obtained with a sensor equipped with 2,4-D grown cells. It is obvious, that the sensor fulfilled all desired properties. First the selectivity between two analytes was confirmed. Second the signals for each analyte were reproducible and third stable after overnight storage at 4°C.

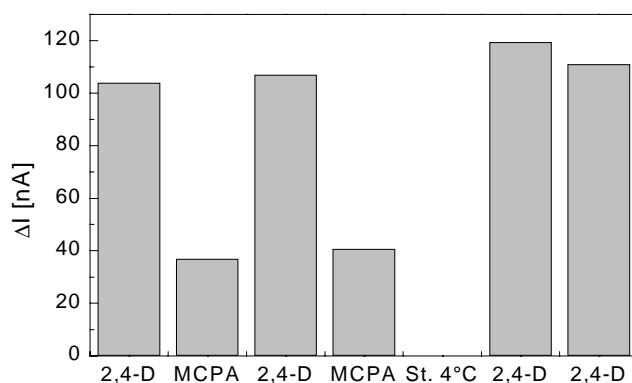


Figure 3.17: Repeated measurement of 20  $\mu\text{M}$  2,4-D and MCPA using a sensor equipped with 2,4-D grown cells. (St. 4°C = storage over night at 4°C)

In addition to 2,4-D grown cells, sensors with MCPA grown cells were subjected to repetitive measurements. As can be seen in Figure 3.18, the sensor responses were also reproducible. In measurement number three, the two analytes were added sequentially. The corresponding cumulative signal was additive.

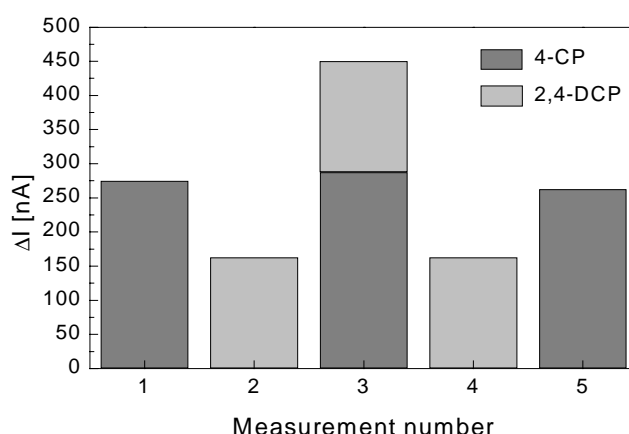


Figure 3.18: Repeated measurement of 4-chlorophenol and 2,4-dichlorophenol using a sensor equipped with MCPA grown cells. Comparison if individual and cumulative measurement. In measurement number 3 the analytes were added sequentially.

### Exposure time

In further experiments the effect of exposure time on the sensor specificity was monitored. Therefore, sensors with 2,4-D and phenol grown cells were firstly exposed to 2,4-DCP. In this case, strong responses to this analyte were found for sensors equipped with 2,4-D grown cells but rather small signals for the other. In case of phenol addition, the response was in the opposite ratio, with no signal for the 2,4-D grown cells. A prolonged exposure to phenol with continuous measurement of the sensor response revealed a developing signal for 2,4-D grown cells after 40 min exposure. After washing and reequilibration a new measurement was performed. Now the sensor which was equipped with 2,4-D grown cells displayed a strong response towards phenol, in the same height as it was found after the 40 min incubation. In view of these results, the exposure time to the analytes was kept at a minimum, i.e. not exceeding 20 min.

It can be concluded that the development of a new disposable microbial sensor was achieved. This biosensor displayed all desired criteria such as sensitivity, selectivity and stability. Specific attention, however, had to be paid to sensor / analyte exposure time. Based on this sensor prototype, the realization of the multisensor approach could be started.

### 3.2.3 Multi-analyte detection I: Phenol and 2,4-dichlorophenol

The multianalyte detection approach based on the use of a multisensor bearing four distinct biosensors and subsequent data processing by artificial neural networks. In the first round of experiments the simultaneous detection of phenol and 2,4-dichlorophenol was performed. To achieve this goal, microbial multi-sensors were prepared using the four electrode multisensors described in chapter 2.2.5.1 using cultures of *R. eutropha* JMP 134 grown on 2,4-D, MCPA, 2-MPA and phenol. This batch of multisensors is herein referred to as multisensor M1.

#### 3.2.3.1 Data generation

In the first stage of the experiment a data set of multisensor responses was generated by measuring binary mixtures of phenol and 2,4-dichlorophenol in concentration ranges of 0 - 40  $\mu\text{M}$ . As it was already found for the single sensors in chapter 3.2.2.4, the multisensors showed a rapid equilibration of the basic current within 10 to 15 min to a mean value of 1600 nA. All sensors responded within 10 seconds upon addition of the analyte. The time to reach 90 % of the signal was 3 min  $\pm$  1 min. Between each measurement the sensors was thoroughly rinsed with TBS until the initial base line was reached again. The results of the complete set of measurements obtained by the use of 5 electrodes is shown in Figure 3.19.

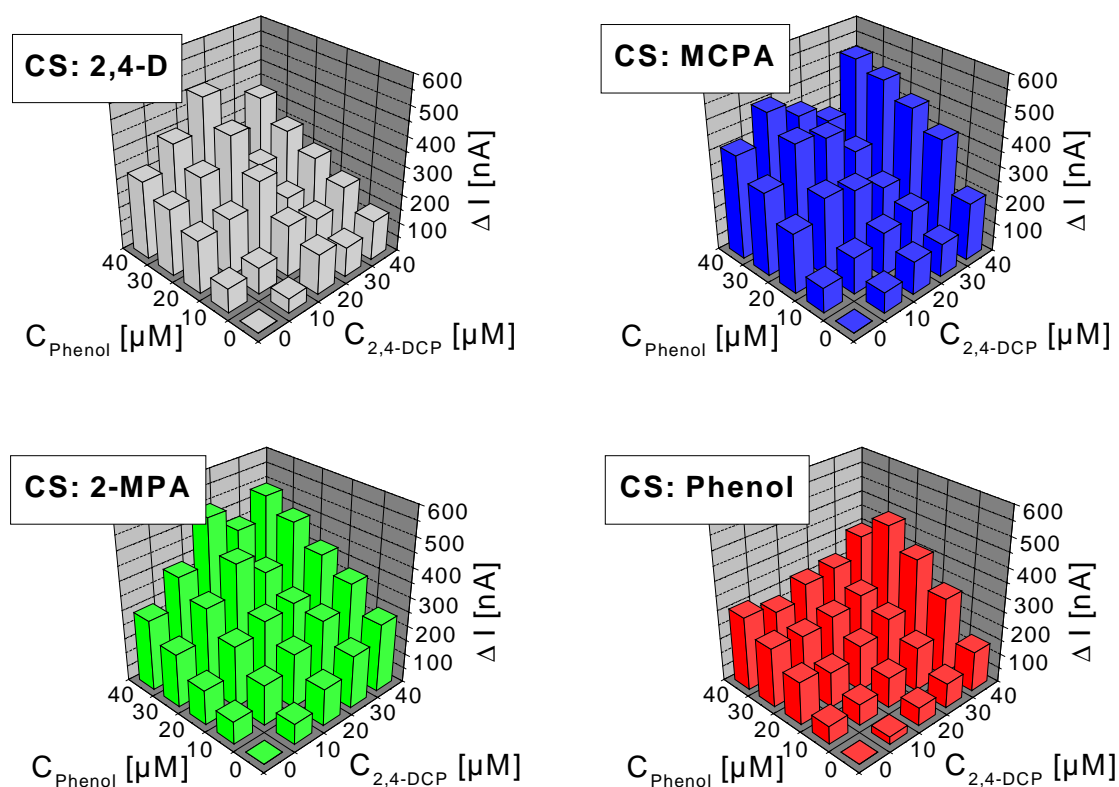


Figure 3.19: Signal patterns of microbial multisensor M1 for binary mixtures of 2,4-DCP and phenol. (CS: Carbon source (2mM) used for cultivation of microorganisms prior to immobilisation)

All sensors were used for a measuring time of 2 to 6 hours. During this time, the sensor was continuously polarised. The sensors were discarded if their analyte signal showed either an increase of noise or the initial base line could not be reached after a washing step. As it is visible in Figure 3.19, all four sensors showed an individual response pattern for the analyte mixture. Unlike observations made with the YSI biological oxygen meter for free cells, the immobilised microorganisms displayed different response patterns. For instance sensors equipped with 2,4-D grown cells responded to phenol addition. On the other hand, sensors with phenol growth cells showed reaction upon 2,4-DCP addition. In order to have standard sensors in every batch, experiments to investigate these findings were performed. 2,4-D grown cells in the free state displayed a clear response to 2,4-DCP but not to phenol, as determined with the YSI oxygen monitor (Figure 3.7). In contrast the cells from the same batch showed a response to phenol and 2,4-DCP right after immobilisation. The reason for this behaviour could not be identified. As the culturing conditions could be excluded as factor, the effect of immobilisation itself was investigated. Firstly freshly harvested cells were incubated for 20 min with 0.2 M  $\text{CaCl}_2$  according to the protocol of alginate immobilisation or resuspended in aqua dem to simulate electrode rehydration. After this treatment the cells still displayed an unchanged response pattern similar to Figure 3.7 for 2,4-D cells. The influence of alginate itself was also excluded. In this experiment cells were immobilized in alginate beads and their oxygen uptake rate was determined qualitatively in the YSI oxygen monitor as the exact cell concentration was impossible to determine. In each measurement 10 beads of approx. 10  $\mu\text{l}$  calcium alginate with a calculated  $\text{OD}_{580} = 4$  were used in 3 ml solution. Electrode cross talk was also excluded, as these findings were confirmed for single sensors as well as for multisensors. As these investigations did not lead to sufficient explanations, the influence of sensor age was investigated more specifically. In a typical time course of experiments the cells were harvested and used for sensor experiments at the same day. During an experimental time of 12 hours no change of induction state could be observed for sensors which were used continuously. For this reason sensors were stored for 24 hours after immobilisation. Surprisingly for sensors equipped with 2,4-D grown cells the induction state had changed again after this period towards the pattern found for free cells. Despite the fact that the signal patterns did not meet the theoretical expectations, they were used for neural network calculations as they were consistent for the complete sensor batch.

### 3.2.3.2 Data processing

The data sets were initially used to create artificial neural networks which displayed a satisfactory performance. Networks which had a number of hidden neurons greater than 5 showed significant overtraining effects. For this reason the network topologies were optimized using automated methods (pruning algorithms). For pruning of multisensor M1 data the methods MagPruning, Skeletonisation and Non-Contributing Units were used. Here Non-Contributing Units led to the best results giving networks for 2,4-DCP and phenol discrimination as shown in Figure 3.20.

---

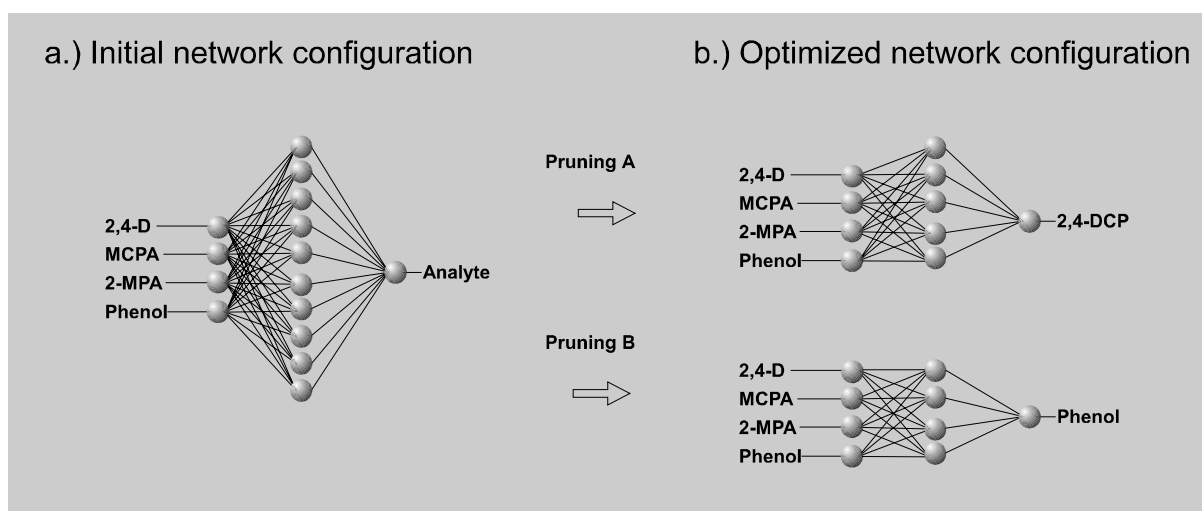


Figure 3.20: Results of network topology optimisation using pruning algorithms. The data sets used were generated with multisensor M1.

These optimized networks were used in further training runs for calibration and cross validation using data set M1. Figure 3.21 shows the development of the network error for both networks and analytes.

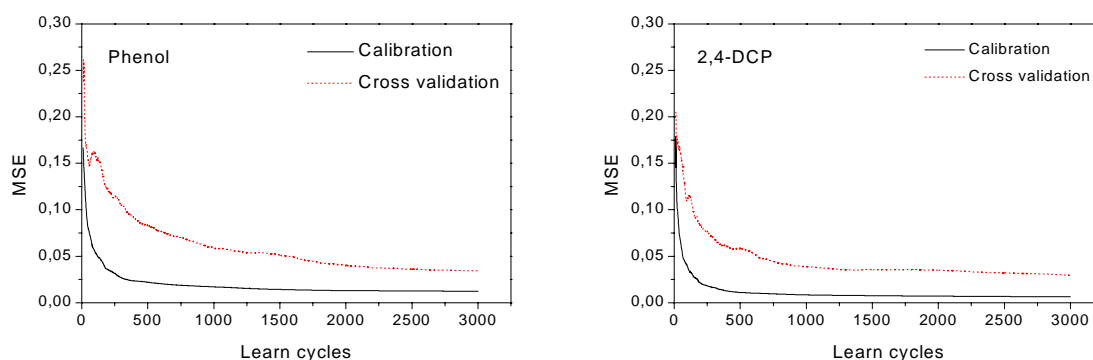


Figure 3.21: Development of network error (MSE) of neural networks shown in Figure 3.20 for Phenol and 2,4-DCP, while training with data set M1.

In both cases the network error converged rapidly towards zero. As it was expected from the relatively small amount of data, the cross validation error remained higher as compared to the calibration. It could be demonstrated that the network did not show any overtraining effects as it was found for networks with larger topologies before pruning. Extended training did not result in significantly improved network abilities and was therefore not performed, also in view of the prolonged training time.

### 3.2.3.3 Multianalyte detection results

The prediction ability of the microbial multisensor in combination with the ANN data processing is shown in Figure 3.22. As demonstrated, the prediction was clearly

possible for the whole detection range investigated. The data represent mean values of 10 training runs and of all possible combinations within the data set, which explains that the prediction ability for the zero values of both analytes showed the biggest error. Details of the network properties are summarised in Table 3.21. The microbial multisensor was capable for a simultaneous determination of 2,4-DCP and phenol with prediction errors of 4,21 and 3,95  $\mu\text{M}$  respectively. These results demonstrate the general feasibility of this approach but still let space for further development.

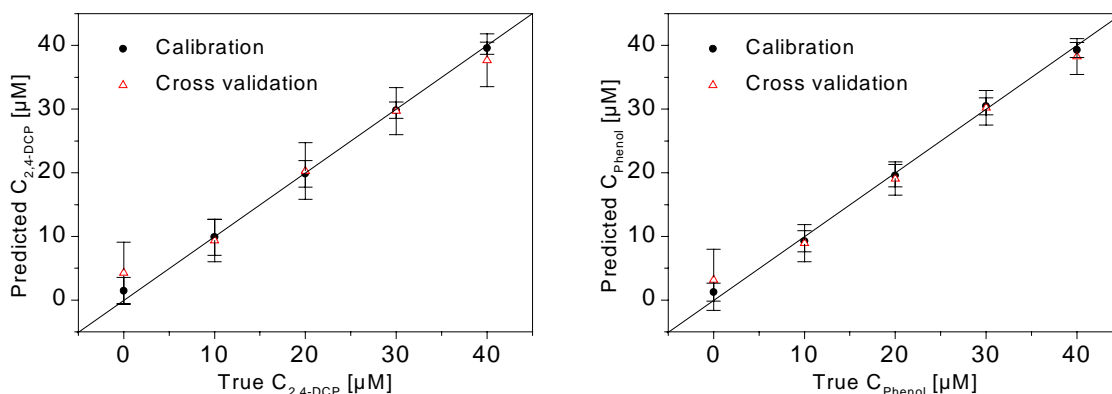


Figure 3.22: True vs. predicted plots for neural network calculations of microbial multisensor responses to binary analyte mixtures. The figures represent the mean results of ten network training runs.

The errors in predicting single compound concentrations presumably resulted from two major parameters. As a first reason, considering 50 measurements the data set generated with the microbial multisensor was relatively small. However, calculating a measuring time of minimal 20 min for one data point, this value could not be increased in a reasonable manner. Possible changes in microbial biosensor properties during this storage time would have an adverse effect on the network performance. As a second reason, the use of 5 different multisensors may increased the network error, although the sensor-to-sensor-error could be determined with 11.4 % in previous experiments.

#### 3.2.3.4 Improving the multianalyte detection resolution

A second round of experiments was conducted focussing on generating the complete data set with only one microbial multisensor, herein referred to as multisensor M2. During these experiments special focus was given on the sensor stability, which was provided mainly by extended rinsing steps in between two measurements. This prolonged the overall experimental time but had no adverse effects on the transducer stability itself. The complete response patterns of multisensor M2 are shown in Figure 3.23. In contrast to multisensor M1, the patterns shown here proved less variation for each single sensor.

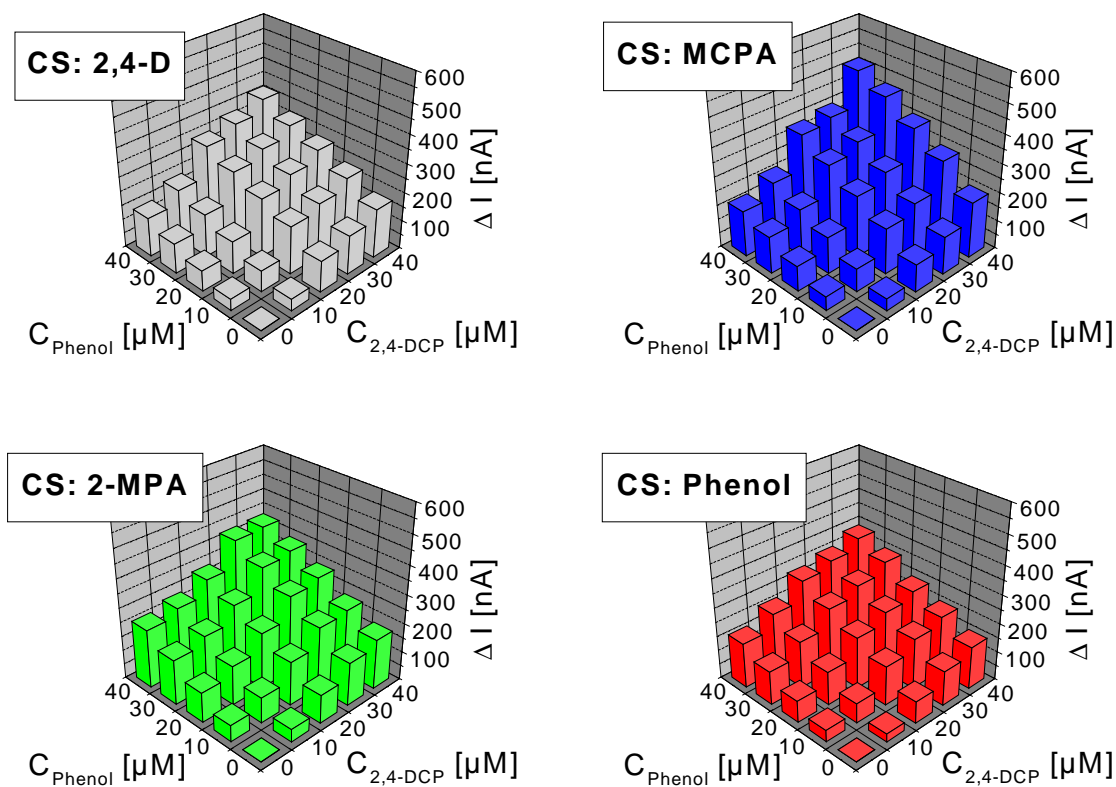


Figure 3.23: Signal patterns of microbial multi-sensor M2 for binary mixtures of 2,4-DCP and phenol. (CS: Carbon source (2mM) used for cultivation of microorganisms prior immobilisation)

In a similar manner as shown for M1, these sensor data were used for neural network calculations. The network optimisation performed for multisensor M2 resulted for both analytes in a 4:5:1 fully interconnected network as it was found for 2,4-DCP in the case of M1. Calibration and cross validation of the neural network using dataset M2 resulted in the data shown in Figure 3.25. The corresponding learn curves are displayed in Figure 3.24.

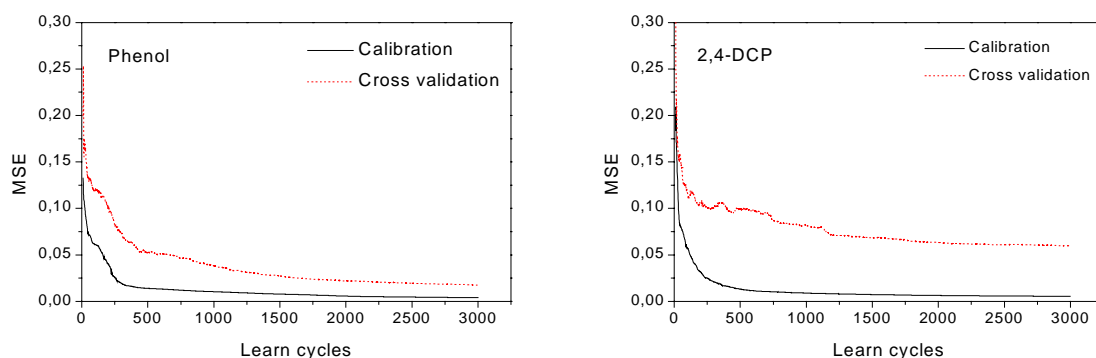


Figure 3.24: Development of network error (MSE) of neural networks generated for multisensor M2 for Phenol and 2,4-DCP during calibration and cross validation.



As shown in Table 3.21, the overall performance of the multisensor could be improved. In particular for the calibration runs, the network errors could be significantly reduced. In contrast, progress could be made for cross validation in the case of phenol but not for 2,4-DCP. Table 3.21 gives a summary of the results obtained for the discrimination of 2,4-dichlorophenol and phenol in binary mixtures.

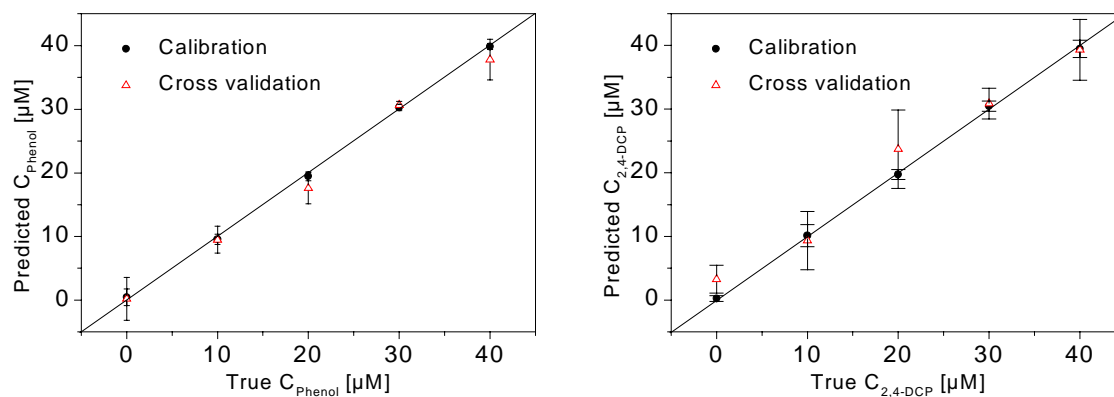


Figure 3.25: True vs. predicted plots for neural network calculations of microbial multisensor M2 responses to binary mixtures of 2,4-DCP and phenol.

Table 3.21:

Results of the neural network evaluation of binary mixture analyses using multisensors M1 and M2.

			Multisensor M1		Multisensor M2	
			2,4-DCP	Phenol	2,4-DCP	Phenol
Calibration	RMSE	[μM]	2.04	2.25	1.30	1.19
	AbsE	[μM]	1.60	1.74	0.94	0.87
	MaxE	[μM]	5.30	6.32	3.45	3.52
	RelE	[%]	9.12	10.66	5.69	4.44
Cross-Validation	RMSE	[μM]	5.56	5.36	7.32	4.87
	AbsE	[μM]	4.21	3.95	4.97	3.29
	MaxE	[μM]	17.60	18.29	24.98	17.52
	RelE	[%]	22.24	20.52	25.68	14.02

(RMSE, root mean square error; AbsE, mean absolute error; MaxE, maximal absolute error; RelE, mean relative error)

### 3.2.4 Multi-analyte detection II: 4-Chlorophenol and 2,4-dichlorophenol

The simultaneous detection of phenol and twice chlorinated phenol was realized in the preceding experiments. The target of the development of microbial biosensors was the detection and differentiation of a broad range of halogenated analytes. In this context the next step was the investigation of more closely related compounds, such as mono- and dichlorinated phenols. In this approach, 4-chlorophenol and 2,4-dichlorophenol were chosen as analytes as they displayed distinct response patterns in experiments for the determination of oxygen uptake rates as described in chapter 3.2.2.2.

#### 3.2.4.1 Data generation

In this experiments a microbial multisensor (M3) was equipped with cells as described before for M1 and M2. In total, 30 data sets were generated, derived from binary mixtures of 4-CP and 2,4-DCP in the concentration range of 0 - 40  $\mu\text{M}$  of each compound. Figure 3.26 gives the results for the sensors responses upon each analyte addition.

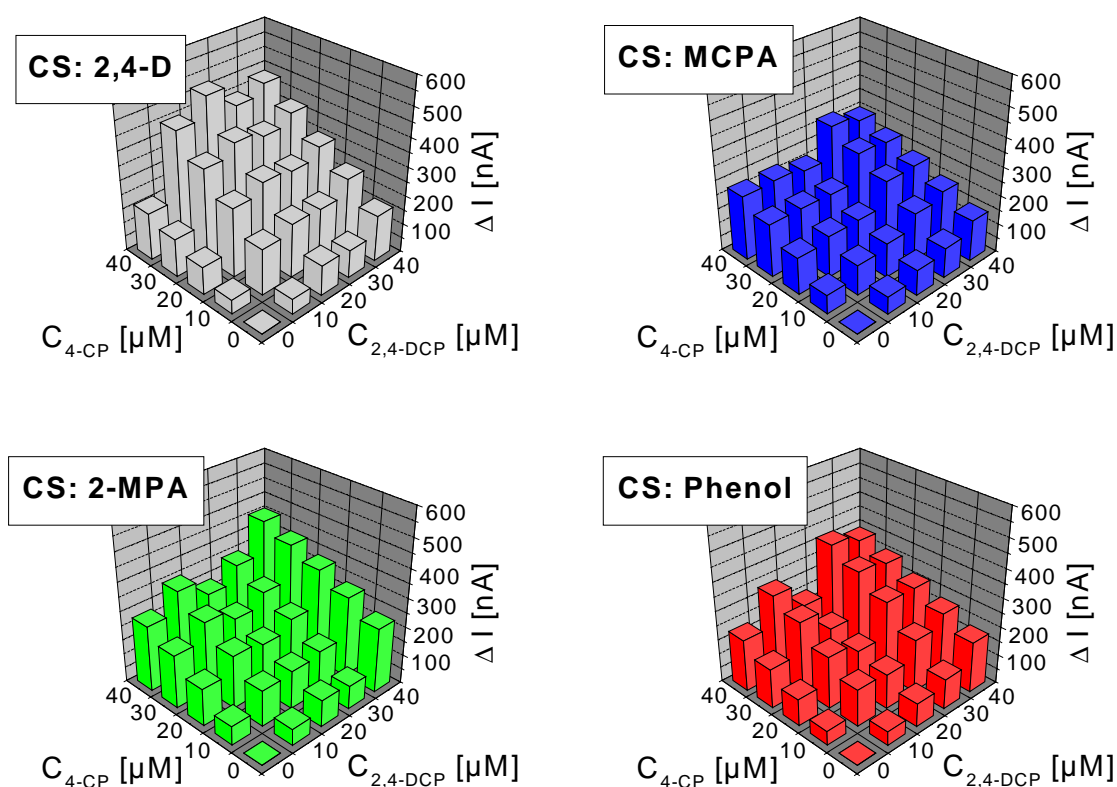


Figure 3.26: Signal patterns of microbial multi-sensor M3 for binary mixtures of 2,4-DCP and 4-chlorophenol. (CS: Carbon source (2mM) used for cultivation of microorganisms prior to immobilisation)

## 3.2.4.2 Data processing

In analogy to the data processing described for M1 and M2, the data sets generated with multisensor M3 were subjected to neural network processing. Again the network topology was optimized using pruning methods. Surprisingly the number of inputs was also reduced for networks used for the determination of 4-CP.

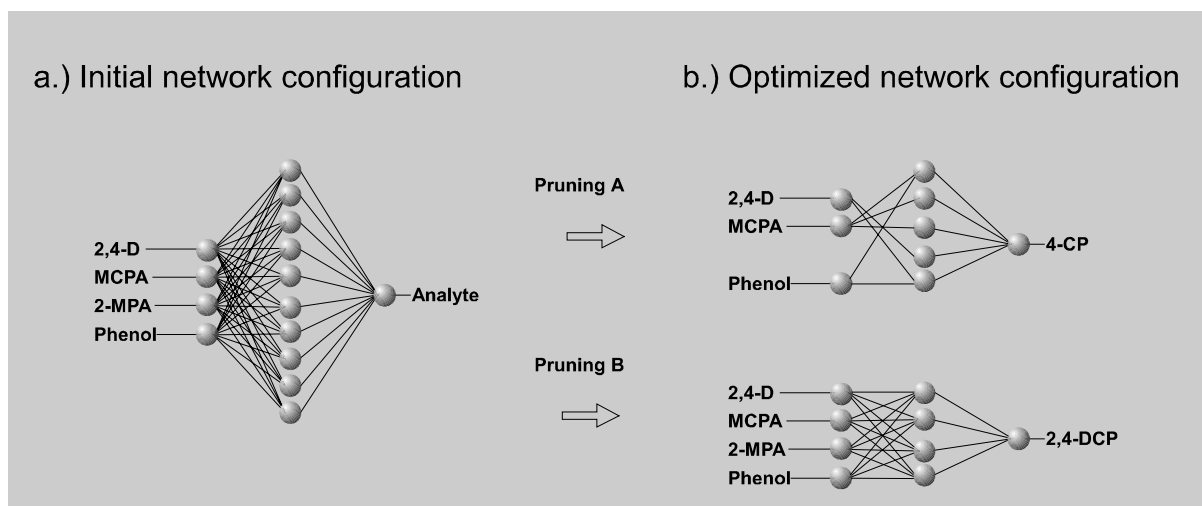


Figure 3.27: Neural network topology optimisation using pruning algorithms for M3 for 4-CP and 2,4-DCP.

The training of the neural networks shown in Figure 3.21, was followed by monitoring the neural network error. In case of 4-CP this error converged very rapidly and remained stable after 1000 training cycles. In contrast the network designed for the discrimination of 2,4-DCP could not be trained with a comparable result. Several attempts to use neural networks with advanced architectures (up to 3 hidden layers) or variations in learning algorithms did not led to any improvement. As a consequence the results of prediction were significantly better for 4-CP.

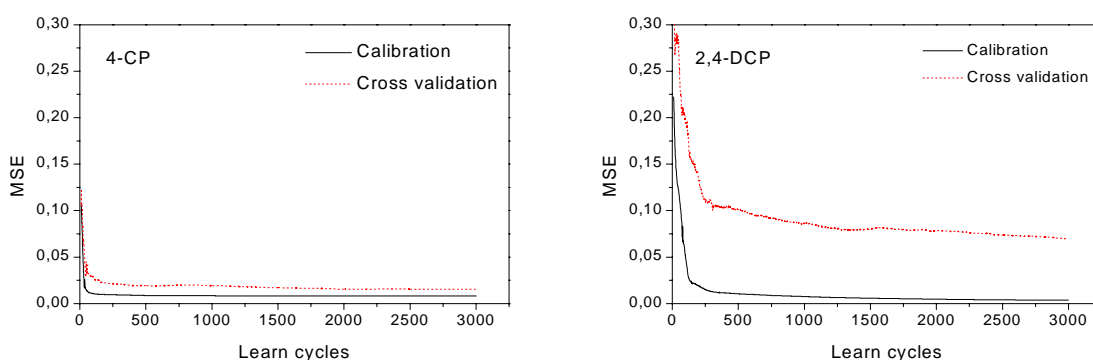


Figure 3.28: Development of network error (MSE) of neural networks generated for multisensor M3 for 4-CP and 2,4-DCP.

### 3.2.4.3 Multianalyte detection results

As it was expected from the observations during network training, the multisensor/ANN combination performed better for 4-CP than for 2,4-DCP. As can be seen in Figure 3.29, the prediction of 4-CP concentrations was rather reliable over the complete detection range. In case of 2,4-DCP determination, larger variations were also found for medium range concentrations.

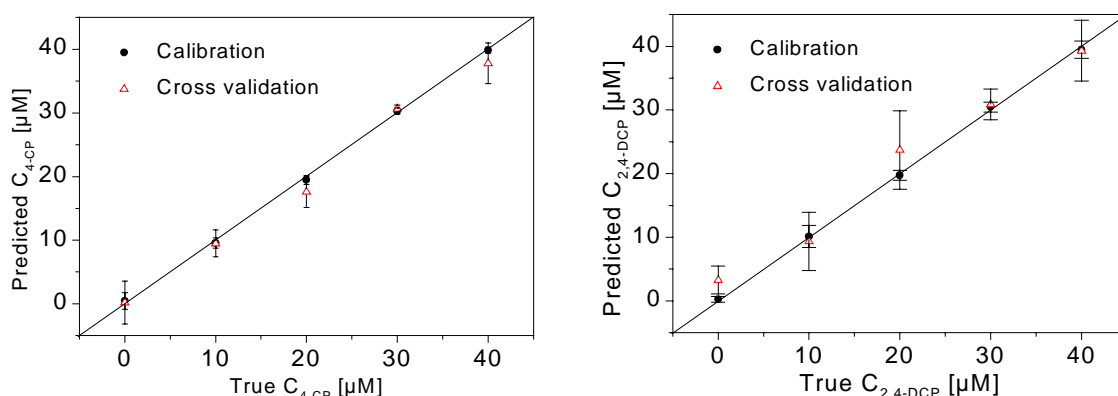


Figure 3.29: True vs. predicted plots for neural network calculations of microbial multisensor M3 responses to binary mixtures of 2,4-DCP and 4-CP.

Table 3.22 summarizes the results obtained for the multianalyte detection of 4-CP and 2,4-DCP. 4-CP was determined with a mean error of 2.74  $\mu\text{M}$  compared to 2,4-DCP with 6  $\mu\text{M}$ . Especially the maximum errors found for predictions experiments revealed this characteristic for 2,4-D.

### 3.2.4.4 Improving the multisensor resolution

as it has been already demonstrated for the phenol/2,4-DCP detection using M1 and M2, the multianalyte detection of 4-CP and 2,4-DCP mixtures should be improved. Following the previous experiments also here the effect of the use of onyl one single sensor on the discrimination performance was investigated. The data generation, network set-up, optimisation and training followed the same protocol as described for M3. The sensor used in this experiments is herein after called M4.

Figure 3.30 shows sensor responses upon analyte mixtures in standard solutions in the range of 0 - 40  $\mu\text{M}$ . Figure 3.31 displays the development of the network error obtained during training of 4:3:1 nets for 2,4-DCP and 3:4:1 (phenol out) nets for 4-CP. Finally in Figure 3.32, the discrimination ability of multisensor M4 is shown as true vs. predicted concentration plots. The details of these experiments are given in Table 3.22.

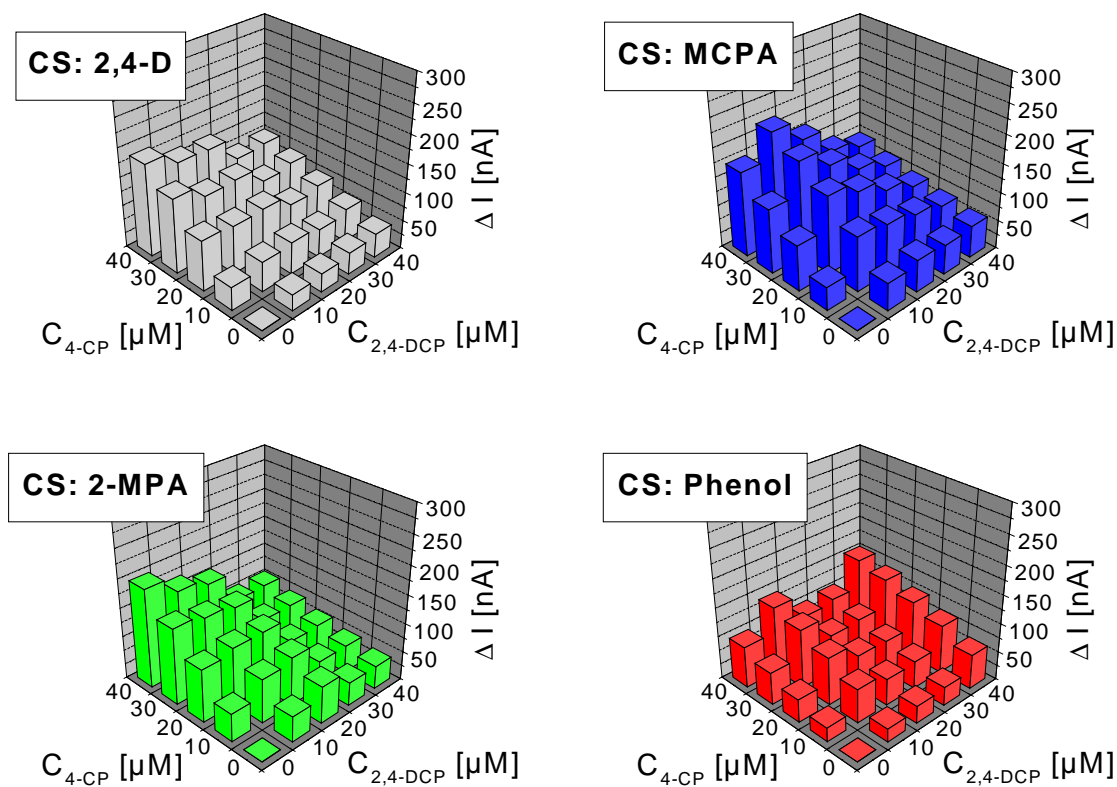


Figure 3.30: Signal patterns of microbial multi-sensor M4 for binary mixtures of 2,4-DCP and 4-chlorophenol. (CS: Carbon source (2mM) used for cultivation of microorganisms prior immobilisation.)

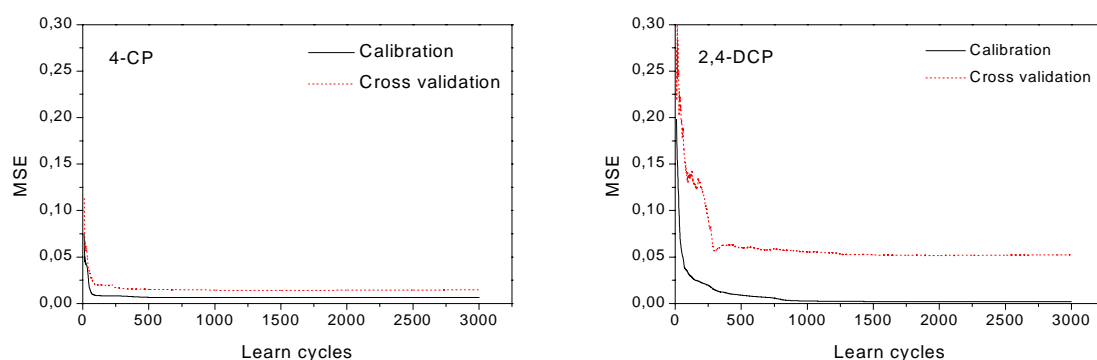


Figure 3.31: Development of network error (MSE) of neural networks generated for multisensor M4 for 4-CP and 2,4-DCP.

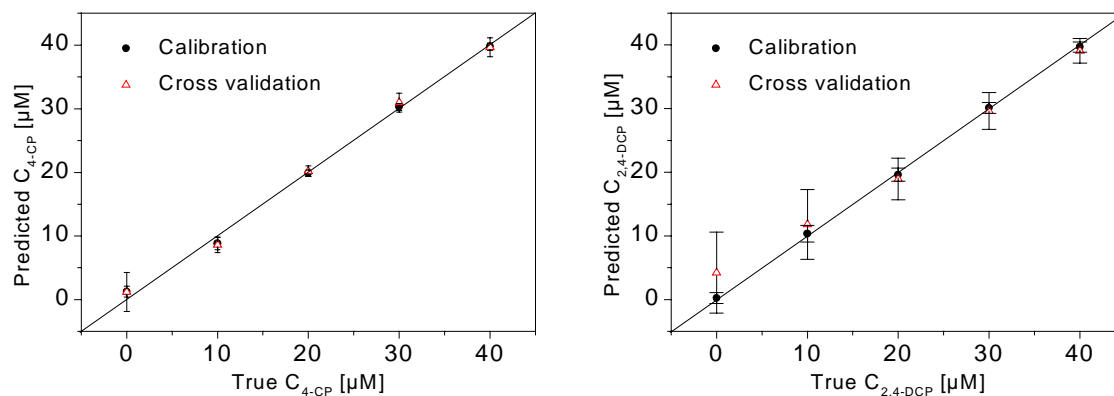


Figure 3.32: True vs. predicted plots for neural network calculations of microbial multisensor M3 responses to binary mixtures of 2,4-DCP and 4-CP.

Table 3.22:

Results of neural network evaluation of binary mixture analysis using multisensor M3 and M4.

			Multisensor M3		Multisensor M4	
			2,4-DCP	4-CP	2,4-DCP	4-CP
Calibration	RMSE	[ $\mu\text{M}$ ]	1.3	1.9	1.5	1.8
	AbsE	[ $\mu\text{M}$ ]	1.1	1.5	1.2	1.2
	MaxE	[ $\mu\text{M}$ ]	2.8	4.6	3.7	5.8
	RelE	[%]	5.9	7.8	6.4	7.2
Cross-Validation	RMSE	[ $\mu\text{M}$ ]	8.8	3.2	6.3	3.8
	AbsE	[ $\mu\text{M}$ ]	6.1	2.7	4.2	2.5
	MaxE	[ $\mu\text{M}$ ]	24.7	7.3	18	13.6
	RelE	[%]	37.3	14.2	20	13.5

(RMSE, root mean square error; AbsE, mean absolute error; MaxE, maximal absolute error; RelE, mean relative error.)

The results given in Table 3.22 demonstrate, that the performance multianalyte detection can be improved by using a single sensor. Interestingly this effect was mostly restricted to the validation results of the network. Here especially the mean absolute error was optimized. The training results of both networks remained in the same order.

## 4 Discussion

The aim of this work was to develop new biosensor formats for multianalyte detection. The basic idea of this new approach was the usage of biological receptors with different sensitivities towards the desired analytes. These different sensitivities were thought to enable pattern recognition using data processing of biosensor outputs by artificial neural networks. This task was successfully fulfilled by designing two new sensor systems. First, a novel insecticide biosensor was developed which used AChE as the sensitive element. Second, a microbial multisensor for chlorinated phenols was created. Both sensors used newly developed disposable multisensors as transducers. The characteristics of the two novel detection systems will be discussed in the following section. The major request on the new system was the ability to detect several signals in parallel and to be disposable. The motivation to produce this kind of sensors can be explained as follows:

- Stability: Biosensors and in particular microbial biosensors are usually fairly stable. As a general rule, the problem of storage stability can be solved much easier than it is the case for the operational stability, i.e. by cryoconservation or freeze drying [151]. As a concept, sensors for single use could therefore be specifically stabilized and would have to exhibit only a limited operational stability.
  - Costs: The manufacturing of disposable sensors has a great potential for mass production. Among several techniques which are only cost effective at higher quantities (i.e. semiconductor/ thin film technology), screen printing is an ideal method to produce medium quantities of sensors at reasonable costs.
  - Commercialization: The goal of the multisensor project was to arrive at a sensor prototype with a high potential for commercialization. Experiences with commercial blood glucose or BOD sensors showed, that there is a high demand for simple and cheap tests. It was concluded, that this could be best fulfilled by using sensors of a disposable type.
-

## 4.1 Multianalyte AChE sensors

Aspects of AChE multisensor development and the results obtained thereof are discussed in three parts:

- Basic sensor development
- AChE multisensor performance
- Real sample detection and rating

### 4.1.1 Development of the disposable sensor platform

#### 4.1.1.1 Manufacturing of the basic sensor

For the production of the basic sensor platform several technological approaches were available. In principle, there were two major aspects to solve for the development of a disposable AChE biosensor, the fabrication of the transducer itself and the immobilisation of the enzyme on the electrode. The production of disposable biosensors using screen printing is an established procedure so in this study benefit could be made from these experiences [15;152;14;29;153;23;92].

#### The transducer

The screen printing of disposable electrodes was performed on PVC sheets as it is described elsewhere [15;23;92]. The advantage of this material over a ceramic substrate [29] is, that there is no need for costly equipment to fire the electrodes after the process. Also these electrodes can be more easily processed after manufacturing and are less brittle. The electrode design was mainly taken from Kulys and D'Costa [15] but several modifications were investigated. As the electrodes should be manufactured in large batches, a uniform production technique was envisaged. For this reason all production steps should be feasible by this technique. Attempts to print working electrodes containing cobalt phthalocyanine [14;92], TCNQ [15;154], or ruthenium [13] as mediators mixed with graphite powders has been repeatedly described in the literature. The screen printing inks mainly contained HEC as binder for higher printing viscosity. Consequently this was investigated in this study finding rhodium graphite electrodes more instable and less sensitive than electrodes containing TCNQ. Besides the properties of the mediator itself, the influence of the graphite material was obvious. Whilst activated carbon was much more difficult to deposit by printing, the T15 graphite gave best results. The good performance of TCNQ mediated electrodes in this study can therefore be related to the mediator as well as the strong attachment of the graphite due to a very hydrophobic surface. This also led to a smaller loss of active material as compared to rhodium which was deposited on activated carbon.

---



### Exploring possibilities for enzyme immobilization

The deposition of enzyme layers on the electrodes was tried by adsorption, drop coating, screen printing together with the graphite paste and be separate printing. Adsorption as it was described by Cagnini *et al.* [13] for choline oxidase resulted in rather instable electrodes, presumably due to weak adsorption to the activated carbon. Nevertheless, these authors reported detection limits of 0.22 µg/l carbofuran using a soluble acetylcholinesterase. Drop coating is one of the mostly distributed immobilization methods found for AChE based biosensors [15;155]. The results obtained with these sensors in this study were satisfying but had certain drawbacks. First, the technique is a manual method and therefore highly error sensitive - as it was experimentally shown. Second, the procedure does not fit in the strategy of a uniform production process. Other methods to deposit enzyme layers on screen printed electrodes like ink jet printing or air- brush techniques may be more suitable [156]. The printing of enzyme together with rhodium graphite led to decreasing signals. Other reports used a similar method and found relatively sensitive electrodes with a detection limit of 2.7 µg/l paraoxon [92]. The decrease of activity found in this study was related to enzyme loss which should be prevented by means of an outer polyurethane membrane. Hart *et al.* [92] described a stabilization effect using this method, but found a decreased sensitivity as compared with the 0.1 µg/l in this study. A reduced sensitivity was also found in this work probably due to restricted diffusion behaviour of analytes and acetylthiocholine. Consequently this method was stopped and separate screen printing of working electrode and enzyme layer was started.

### Final enzyme immobilization method

Screen printing of TCNQ as mediator on graphite for thiocholine oxidation, similar as described by Kulys and D'Costa [15], essentially proved satisfactory for obtaining transducers on which eeAChE could be immobilised, but the following modifications were made for improvement: Whereas Kulys and D'Costa [15] immobilised butyrylcholinesterase by drop-coating, we found that the immobilisation step could be included in the screen printing process, thus simplifying the overall procedure significantly. Hart *et al.* [92] used a screen printing ink which contained glutaraldehyde for cross-linking of an AChE from electric eel on a screen printed sensor. In our study, the more gentle cross-linking by glutaraldehyde vapour was used, thereby reducing the loss of activity during the immobilisation process. Taking 3 µl as the estimated volume maximally printed per electrode, a 4.5 times lower loss of activity was found for immobilisation by screen printing and glutaraldehyde vapour as compared to pipetting using the method described by Kulys and D'Costa [15]. The use of glutaraldehyde vapor has been described for other biosensors containing urease [142] or glucose oxidase [157].

During the preparation of this report, a study on immobilization of ACHE by glutaraldehyde was published by a chinese group [154]. Li *et al.* investigated various concentrations for glutaraldehyde for immobilization of 0.1 µl drop coated enzyme solution. The performance of this sensor, however, was rather poor giving 50 µg/l paraoxon as detection limit and 0.26 mM as an apparent  $K_m$  (all determined at 7.5 mM acetylthiocholine). This high apparent  $K_m$  value indicates a strong diffusional

---

limitation which was not monitored for the sensor described in our study. Here with an apparent  $K_m$  value of 0.08 mM the diffusion limitation can be considered as rather small.

Sensors with the above described method were highly reproducible which was indicated by a 1.7% variation for acetylthiocholine measurements. This property was also displayed in inhibition experiments, however with a reduced reproducibility of approx. 90 %. To increase the sensor's performance even further, i.e. to increase the sensor speed, the immobilization matrix for AChE was changed. Suspected limiting factors were the BSA content and HEC. In contrast to BSA the use of HEC was regarded as problematic, as it is water soluble and presumably is dissolved during measurements. Other reports using glycerol as binder [157;142] were found not to be useful due to the same property of this compound. Better performance was expected from the use of a photocross linkable polymer, PVA-SbQ [143;158]. Indeed a reduced equilibration time was monitored due to the use of PVA-SbQ. A noteworthy advantage of this method was the possibility to print the electrodes and cure the immobilisate easily by illumination. Accordingly, a separated cross linking in glutaraldehyde vapour could be abolished. At the end, the new sensor design was fully manageable by screen printing and opened all possibilities for large scale manufacturing of multisensors for multi-analyte detection.

In Table 4.23, the sensors described in this study are compared to a selection of detection systems for cholinesterase inhibitors. It is important to notice that none of the mentioned biosensors was able to discriminate between analytes.

Table 4.23:  
Performance characteristics of selected biosensors for the detection of cholinesterase inhibitors.

Analyte	Detection limit	Biological recognition element	Transducer	Ref.
<u>Carbofuran</u>	<u><math>9.0 \times 10^{-10}</math> M</u>	<u>dmAChE and mutants</u>	<u>SPE</u>	<u>this work</u>
Carbofuran	$1.0 \times 10^{-9}$ M	eeAChE (sol.) ChO	SPE	[13]
Carbofuran	$1.0 \times 10^{-7}$ M	eeAChE	Optode	[159]
Carbofuran	$2.2 \times 10^{-9}$ M	beAChE	Mag.particles FIA	[90]
<u>Paraoxon</u>	<u><math>7.0 \times 10^{-10}</math> M</u>	<u>dmAChE</u>	<u>SPE</u>	<u>this work</u>
Paraoxon	$1.8 \times 10^{-7}$ M	eeAChE	SPE	[154]
Paraoxon	$3.0 \times 10^{-8}$ M	horse BuChE	Carbon	[155]
Paraoxon	$5.0 \times 10^{-8}$ M	AChE	SPE	[14]
Paraoxon	$1.0 \times 10^{-8}$ M	eeAChE	SPE	[92]
Paraoxon	$5.4 \times 10^{-9}$ M	eeAChE	Carbon paste	[86]
Paraoxon	$1.0 \times 10^{-9}$ M	eeAChE	Biocomposite	[160]
Paraoxon	$5.0 \times 10^{-8}$ M	eeACHE	QCM	[89]
Paraoxon	$1.8 \times 10^{-9}$ M	beAChE	Spectrometric	[44]
Diazinon	$1.5 \times 10^{-9}$ M	horse BuChE	Carbon paste / FIA	[158]
DIFP	$3.2 \times 10^{-7}$ M	BuChE	SPE	[15]
Trichlorfon	$2.0 \times 10^{-13}$ M	BuChE/ChO/HRP	pH Electrode	[84]

As can be seen from Table 4.23, the AChE sensor described in this report performed in the lower detection range for cholinesterase inhibitors. With the background of this good sensitivity the investigation of multi-analyte detection could be started.

## 4.1.2 The AChE multisensor approach

### 4.1.2.1 Wild-type AChE multisensor

#### Properties

The fabrication of the wild-type AChE multisensor was performed in a batch of 100 electrodes. The quality of this process was demonstrated in experiments analyzing the sensor response towards repeated substrate additions. Whilst the sensor error for one AChE variant was relatively small, the difference between these variants were significant. Inhibition experiments, however, revealed no influence of  $I_{\max}$  on the detection error. In fact an improvement towards lower variation was observed. Problematic was the sensor in position four which was filled by the eeAChE. For this position, the highest variation was found though out the project. Although the high activity of eeAChE compared to the other enzymes may have played a role, a technical problem during screen printing was suspected. This findings emphasize the importance of sound screen printing equipment. So did previous attempts for producing disposable biosensors using a less costly device to completely unacceptable results. Especially the printing of a highly active enzyme like the AChE will lead to drastic errors if only slight variations occur.

The amount of immobilized enzymatic activity can be calculated considering the definition of electric current and the 2<sup>nd</sup> Faraday law:

$$Q = I \cdot t = n \cdot z \cdot F$$

with ( $I$  = Electric current;  $Q$  = electric charge;  $n$  = molarity;  $z$  = number of transferred charges;  $F$  = Faraday constant (96486.7 [C/mol]))

For the wild-type AChE multisensor the immobilized enzymatic activities can therefore be calculated with: rbAChE 19  $\mu$ U, dmAChE 27  $\mu$ U, beAChE 29  $\mu$ U, and eeAChE 45  $\mu$ U.

#### Multi-analyte detection

In multi-analyte detection, the sensors achieved a resolution error of 0.9  $\mu$ g/l paraoxon and 1.4  $\mu$ g/l carbofuran in the investigated detection range of 0 - 20  $\mu$ g/l of each compound. Using these data, a detection limit for paraoxon and carbofuran in binary mixtures of 2.7 and 4.2  $\mu$ g/l respectively can be calculated. Considering comparable systems in the literature, these results are promising. The potentiometric biosensor described by Danzer *et al.* [96;97] was only investigated for 1 mg/l of each analyte, which is a value that ranges well above the permitted limit of 0.1  $\mu$ g/l for single pesticides, as laid down by the european [36] and german drinking water legislation [161]. With its discrimination capability and sensitivity, the multisensor described in our study achieved a value of 0.2  $\mu$ g/l, which is much closer to the permitted limit. The assay reported by Schäfer *et al.* [95] also showed a high

compound-specific detection potential using soluble AChE in the microtiter plate method. However, this elaborated assay procedure, which also involves extensive chemometric data analysis, seems to be restricted to laboratory use only. In contrast, the disposable multisensor-neural network combination a mixture analysis of samples can be performed within less than 60 minutes under field conditions. This is already less than the time required for sample preparation for GC analysis [162], without taking the time required for sample transportation into consideration, which could be avoided with our system. Although the multisensor displayed already good performance, the assay time required for the wild-type AChE-multisensor needed to be reduced even further in order to meet consumer demands. As a consequence, AChE variants with higher  $k_i$  values for the desired analytes were investigated as one possible approach for reducing the analysis time.

#### 4.1.2.2 Mutant AChE multisensors I and II

##### Selection of AChE variants for multisensor I

The selection of AChE mutants for the newly designed multisensor was made primarily in order to improve the discrimination resolution of the sensor. Accordingly, a set of cholinesterases with wide variation in their inhibition constants for paraoxon and carbofuran was selected for multisensor I. In the first AChE multisensor format, three out of four cholinesterases had a higher  $k_i$  value for carbofuran. Rat brain AChE, as the only cholinesterase with a stronger inhibition by paraoxon, proved hardly to be sensitive. Thus, in the novel approach, we focused on the use of *Drosophila*-derived AChE variants because the wild-type enzyme already displayed the highest inhibition values. A highly sensitive mutant, Y408F, was chosen as the best variant [104]. Using this mutant, the overall sensitivity of the sensor was thought to be greatly improved. An opposite ratio of  $k_i$  values as compared to Y408F and the wild-type enzyme was found for the mutants F369L and F368W [149]. Both were more sensitive for paraoxon than for carbofuran. In the case of F369L, the overall sensitivity was lower but its variation of  $k_i$  values compared to the other cholinesterases used in this multisensor recommended its inclusion nevertheless. The ratios of  $k_i$  values for paraoxon and carbofuran for the wild-type, Y408F, F368L and F368W were 0.29, 0.39, 3.1, and 3.64, respectively.

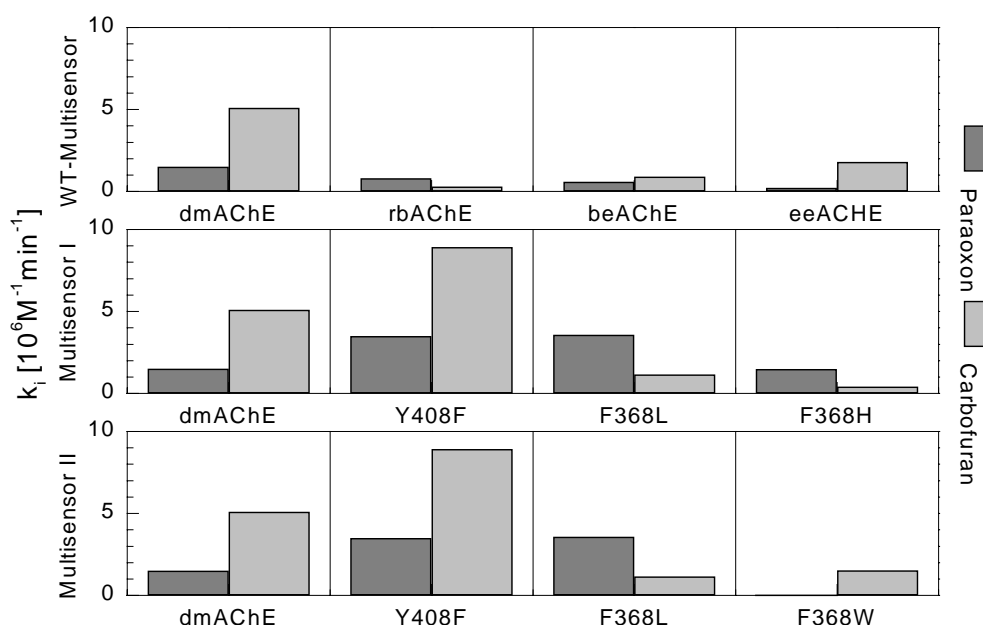


Figure 4.33: Comparison of inhibition constants for paraoxon and carbofuran of AChEs used for multisensors I and II [104;149] with the AChEs used for the wild-type AChE-multisensor (WT-multisensor) [94;163].

#### Selection of AChE variants for multisensor II

In the second round of experiments, the set of cholinesterases chosen for multisensor II was based on the results of multisensor I in order to reduce the network error, enhance sensitivity and minimise the number of total inputs required for discrimination. Whereas for the wild type AChE-sensor the network optimisation resulted in the use of three enzymes per analyte only, the new set-up required all four enzymes for discrimination. In the case of multisensor II, the cholinesterase mutant F368H, which contributed least in terms of sensitivity, was therefore replaced by F368W. This mutant had an extremely diminished sensitivity towards paraoxon, while the  $k_i$  value for carbofuran was still higher than for F368L. The ratio of  $k_i$  values of F368W for paraoxon and carbofuran was 0.01 [149].

#### Multi-analyte detection of paraoxon and carbofuran

The selection of *Drosophila melanogaster* AChE mutants and PVA-SbQ immobilisation successfully improved multianalyte detection with AChE-multisensors. The modified immobilisation protocol enabled a reduced assay duration of 40 min and a lower limit of detection of 0.5  $\mu\text{g/l}$  for each analyte in separate analysis. This result was achieved primarily by incorporating mutant Y408F, which was designed for sensitive insecticide detection by site-directed mutagenesis. Furthermore,

discrimination of binary mixtures of paraoxon and carbofuran could be improved as compared to the wild-type AChE-multisensor. Multisensor I was capable of simultaneously detecting and discriminating paraoxon and carbofuran with errors of prediction of 0.6 µg/l and 0.5 µg/l, respectively. Even better results were achieved with multisensor II, where a paraoxon-insensitive mutant was included. This sensor displayed a resolution error of 0.4 µg/l for paraoxon and 0.5 µg/l for carbofuran.

Rating these results in respect to the required limits of 0.5 µg/l for total and 0.1 µg/l for individual pesticide concentration in drinking water [36], the need for continued improvement of the multisensor approach becomes obvious. On one hand, a combination consisting of a suitable sample extraction and concentration steps could be used to enhance the system's sensitivity [87;44]. On the other, protein engineering methods could be used for targeted engineering towards mutants with an even higher sensitivity, as demonstrated for Y408F, leading to an accelerated and more sensitive assay [103;104].

#### Multi-analyte detection of paraoxon and malaoxon

The advantage of specially selected mutants has already been made clear in this report: the use of F368W reduced the number of enzymes necessary for the resolution of paraoxon and carbofuran to three and two, respectively. Consequently, multisensor II was examined in the light of a more demanding approach involving the simultaneous detection and discrimination of the two organophosphates, paraoxon and malaoxon. Again, multisensor II proved suitable for analyte discrimination with mean errors of prediction of 1.6 µg/l for paraoxon and 0.9 µg/l for malaoxon.

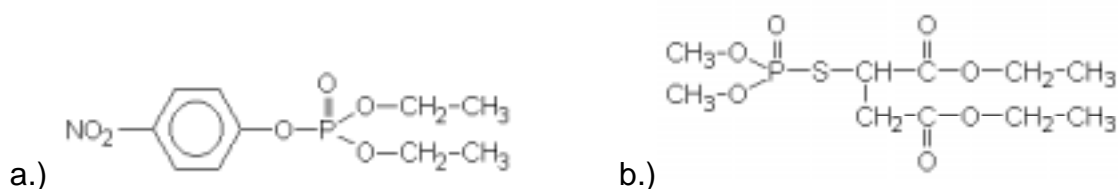


Figure 4.34: Structures of a.) paraoxon and malaoxon (b.) malathion), analyzed in binary mixtures using multisensor II

This results are especially important, as the discrimination of a carbamate from an organophosphate neurotoxin can be generally be performed by more simple methods which base on reactivation behaviour [95] [164] or usage of organophosphate hydrolase [165]. Tusarova *et al.* [165] used cholinesterase immobilized on textiles for optical assay formats. The discrimination was performed by monitoring spontaneous reactivation of carbamate inhibited cholinesterase versus reactivation by quarternary aldoximes. However, the detection limit was rather poor, e.g. 20 µg/l carbofuran or parathion methyl. Simonian *et al.* [165] used a FIA based system to treat binary mixtures of carbofuran and paraoxon with organophosphate hydrolase followed by inhibition detection of eeAChE. With this method a sample

discrimination in concentration ranges of  $10^{-7}$  M were performed. Whilst these assay formats are limited to the discrimination of organophosphates from carbamates, the AChE multisensor format described in this study based on a more promising principle which was confirmed by the discrimination of two closely related analytes from the same compound family.

#### 4.1.3 Artificial neural network performance

All data which were generated with multisensors used in this study were processed with NEMO 1.15.02. NEMO was used to generate feed forward networks which were trained with different backpropagation algorithms. The main property which made this program suitable for the multisensor approach was its cross validation feature. The variety of attempts which were undertaken in this study to arrive at a suitable strategy to generate optimal networks is not described in this report. The optimal strategy was found to use a set of automated pruning algorithms and train a set of networks with different topologies. This method had considerable advantages over building network topologies by hand and investigate their properties sequentially.

The key attributes of the multisensor data were their low number, high variation, and small range. Especially the low number of available data for training of the neural networks turned out as a major drawback. This effect was already described by other authors previously [57]. On the basis of an assay time of 40 min, the net time needed to generate 50 data sets was 33 hours. Compared to other applications of artificial neural networks the same procedure may take only few seconds [166] or minutes [51]. Especially chemosensors are more suitable in this respect [167]. Nevertheless, the usage of artificial neural networks proved to be successful for processing biosensor data. A prerequisite for the sensor component in this approach was a certain stability, in terms of operation and storage. Whilst this was the case for all AChE multisensors, difficulties arose when microbial multisensors were used (see chapter 4.2.4.2).

#### 4.1.4 Real sample analysis

The potential for discriminating binary mixtures in standard sample was successfully shown for all three AChE multisensor. The application on a real-world problem, however, was lacking. To demonstrate the ability of the system to carry out real sample analysis, waste water samples from the influent of a local sewage treatment plant and river water samples from the river Neckar, Stuttgart were investigated.

##### Waste water

The samples were analysed directly and after spiking with 5 µg/l of paraoxon or carbofuran, or with a mixture of both. The unspiked waste water revealed no

---



inhibitory effect. As in the case of the standard solutions, the concentrations of each analyte was determined using the AChE-multisensor in combination with the optimised neural networks. The networks were calibrated with the 50 data sets obtained by analysis of standard solutions. Using the inhibition data from waste water samples as independent test sets, discrimination was possible with mean errors of prediction calculated at 1.8 µg/l for each analyte. The recovery rates in spiked waste water samples were 67% for paraoxon and 118% for carbofuran. Although the performance of the sensor was obviously disturbed by the problematic sample matrix ( $\text{BOD}_5 > 100 \text{ mg/l}$  [148]), an identification of the analyte was still possible with the aid of neural network data processing.

#### River water

Another set of real sample determinations was performed using multisensor II for river surface water. Here, the problematic situation occurred, that the sample itself inhibited the sensor significantly. Nevertheless, the discrimination of spiked paraoxon and carbofuran concentrations could be managed with mean error of prediction of 1.1 µg/l paraoxon and 0.67 µg/l carbofuran.

These results demonstrate the high potential of the assay system for field detection. The problematic recovery rates are well known for samples with high matrix load. Usually for such samples solvent extraction is indispensable. Standard methods for the determination of organophosphates in water or foodstuffs use for example dichloromethane for extraction followed by gas-chromatographic detection [80]. To rate the quality of the AChE multisensor, it has to be kept in mind, that the detection limit of the classical method is 50 µg/kg [168]. In view of these conditions the discrimination potential and sensitivity of the multisensor has to be highlighted but these findings also indicate the need for further investigation of the sensor's performance in real samples. Nevertheless, it was demonstrated that the multisensor could be operated specifically in water samples and that discrimination was indeed possible. For a reliable analysis, however, the system should be combined with a suitable extraction method to avoid adverse matrix effects.

### 4.1.5 Conclusion

Our results demonstrate that binary mixtures of insecticides can be discriminated by a simple, disposable AChE-multisensor using suitable variants of AChE as biospecific ligands and by processing of sensor data by an artificial neural network algorithm. The simultaneous and selective determination of paraoxon and carbofuran in mixtures of 0 - 20 µg/l of each compound was possible with prediction errors of 0.9 µg/l and 1.4 µg/l, respectively. The cycle time required for calibration, inhibition and measurement was maximally 60 min, provided a neural network was calibrated previously. It can be further concluded that the use of recombinant acetylcholinesterase mutants in biosensors, as described here for the first time, in combination with the appropriate immobilisation method, enhances sensitivity and reduces the assay duration significantly. Discrimination of paraoxon and carbofuran

---

was now possible with prediction errors of 0.4  $\mu\text{g/l}$  and 0.5  $\mu\text{g/l}$ , respectively. The assay was even capable to detect simultaneously two organophosphates, paraoxon and carbofuran with a variation of 1.6  $\mu\text{g/l}$  and 1.0  $\mu\text{g/l}$ . Consequently, this biosensor has a good potential for bypassing the preconcentration steps in environmental analysis and for developing rapid, on-site detection systems.

The results of this work can increase the possibilities of cholinesterase-based biosensors dramatically; prior to this investigation, these were limited mainly to sum parameter detection. Based on this approach, it is now possible to make a tool available for cheap, rapid and compound-specific on-site analysis which could be used by the standard consumer in food analysis, for example. The system can be further improved by a) reducing the network error by an increase in training data numbers in combination with higher sensor accuracy b) employing AChE mutants with higher  $k_i$  for the desired analytes; and c) using sets of AChE mutants with high variation in  $k_i$  values for the envisaged analyte spectrum. Investigations into these topics, and into multisensor application in food samples in particular, are now underway.

## 4.2 Multianalyte microbial sensors

The development of the multisensor for chlorinated aromatics can be discussed separately in four parts:

- the screen printed Oxygen electrode (SPOE),
- the integration of the biological receptor (*R.eutropha* JMP 134),
- the basic biosensor development, and
- the set-up and performance of the multianalyte biosensor.

### 4.2.1 Screen printed oxygen electrodes

As no commercial oxygen multielectrode was available, the development of a suitable oxygen electrode was a precondition for the envisaged sensor project.

#### 4.2.1.1 Manufacturing of SPOE

The oxygen electrodes described in this study were produced by a combination of three techniques: screen printing, drop and spin coating. Finally, a lamination step was performed manually. Initially the sensor production was intended to be completely realized by screen printing. In the course of sensor development it turned out, that the electrolyte and silicon rubber deposition could not be performed by this method. Nevertheless, it would be an important task for commercialization to either solve the problem of screen printing or automate the drop and spin coating process.

In fact this has been done for the production of the commercialized micro oxygen electrode MOE by FDK Cooperation, Tokyo, Japan (Figure 4.35). This electrode has been developed by Suzuki and coworkers and was described in various publications [132;4;133;137]. Suzuki *et al.* described the deposition of the electrolyte layer by screen printing. Similar to SPOE fabrication, a mixture of KCl and binder was used (alginate, PVP). Nevertheless the authors reported considerable problems in deposition of the electrolyte on the electrodes. The gas-permeable silicon rubber membrane was deposited by a combination of screen printing and lift-off techniques. However the described electrodes by FDK were much smaller as compared to the SPOEs. Whilst an active surface of approx. 4 mm<sup>2</sup> can be estimated in the case of the micro oxygen electrodes, the SPOEs active surface measured 64 mm<sup>2</sup>. Additionally the use of a V-shaped groove for the internal electrolyte, formed by anisotropic etching probably eased the whole process as compared to the planar structure of the SPOE.

---

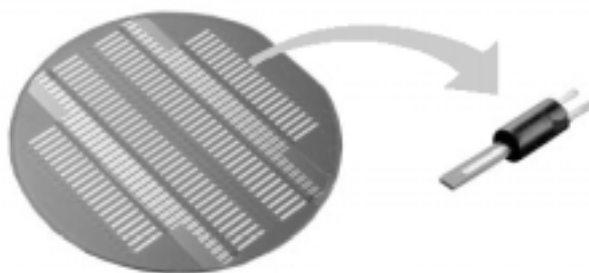


Figure 4.35: Miniature oxygen sensor, FDK Corporation, Tokyo, Japan

Yang *et al.* [136] reported an interesting approach of production of a paper based oxygen electrode by sputtering techniques. Here the electrolyte was applied to the electrode by soaking the basic filter paper in electrolyte after manufacturing the electrode. The advantage of SPOEs and other comparable systems was the possibility to accomplish the electrode and store it in a dry state. Under this conditions no detectable change of sensor properties occurred during one year of observation. With respect to these points, an application of the liquid electrolyte at the end of the SPOE production seemed rather improper.

Similar considerations can be drawn concerning the deposition of the final sensor mask. In the first phase of SPOE development, various attempts with negative results were undertaken. Although cells, immobilised on the silicon surface were most likely viable, no signal was obtained. The high diffusion coefficient of silicon rubber was a suspected reason for this observation. The construction of the SPOE as a multisensor with continuous silicon rubber membrane on the sensor surface, created leaks for oxygen diffusion. As the cells were immobilised in a circular area defined by the immobilisate volume and surface tension, gaps of non-covered silicon remained. Experiments of sealing the electrode surface by adhesive tape revealed that oxygen diffusion occurred through these parts. For this reason several methods of covering the silicon were investigated, all in consideration of mass producibility. As none of the screen printing paints adhered to the silicon surface, lamination was favored. Other publications of microbial sensors detecting cell respiration used miniaturized planar structured oxygen electrodes [138;139]. Here no masking was needed because of the size ratios of cell immobilisate versus active sensor surface.

It can be concluded, that the production of larger quantities of SPOEs was possible with a reasonable work effort. The last three steps in sensor production need to be simplified and, however, should be adapted to the demands of mass production. Nevertheless, numbers of several hundred electrodes could be produced in only 2-3 days.

#### 4.2.1.2 Characteristics of SPOE

The novel oxygen electrode exhibited several properties which made it suitable for the incorporation in multielectrode biosensors. High stability and kinetic behaviour were the main characteristics which were obtained after several modifications of the electrode design.

### Stability against interferences by use of a gas-permeable membrane

Initial approaches using bare electrodes of the same design as the SPOE but without gas permeable membrane created several problems due to the absence of electrolyte and membrane. These electrodes displayed a severe dependency on salt concentrations. Moreover a strong influence of interfering substances was found.

Although other problems arised by the use of additional membranes as far as diffusion limitation, membrane attachment and cell immobilisation was concerned, this way was chosen in further studies. Utilizing SPOEs equipped with the gas permeable membrane the influence of the external medium could be nearly excluded. Except on extreme conditions like heating, the sensor was not influenced by pH shifts or commonly used compounds for checking interferences like ascorbic acid, potassium ferricyanide or sodium sulfite. This can be easily explained by the high hydrophobicity typical to silicon rubber which excludes any diffusion of compounds dissolved in water. The only impact was found due to changes in electrolyte concentration evoked by the external ionic strength. The use of silicon rubber as gas permeable membrane for planar oxygen electrodes was firstly described by Koudelka *et al.* [131]. Although other possibilities for gas-permeable membranes were described such as negative photoresist [132;4;134], cellulose acetate [169], this material was chosen because of its exceptional properties. Besides its strong adhesion to surfaces other important aspects for the choice of silicon rubber were its high permeability for oxygen ( $3-4 \text{ mol O}_2 \text{ m}^{-1} \text{ s}^{-1} \text{ Pa}^{-1}$  [170]) and its mechanical strength ( $11 \text{ Kg/cm}^2$ ) (Product information Shin Etsu).

### Signal stability

SPOEs displayed stable signals over a operation period of 2 - 8 hours. As most of the electrodes showed a steady-state current, in some cases a continuous decrease of current output was detectable. The theoretic explanation can be related to several parameters. As a first rule, the current output of an amperometric electrode in case of diffusion limited conditions can be calculated according to Equation 4.3:

Equation 4.3:

$$I = n * A * F * D * C / \delta$$

(I: current, n: number of exchanged charge carriers, A: electrode area, F: Faraday constant; D: diffusion coefficient, C: concentration of analyte,  $\delta$ : diffusion layer thickness)

As the parameters A, D, n, and  $\delta$  can be considered as constant in homogeneous solutions, the current is proportional to the electrode surface area and the concentration of the electroactive substance. The experiments were performed in continuously stirred solutions, so the concentration of oxygen was regarded as constant. Investigations of the electrode condition by use of a binocular after rehydration and operation revealed a partial dissolution of the rhodium graphite working electrode. It can be inferred, that this process reduces the electrode surface considerably. To find a remedy, the electrodes were additionally fixated by means of cellulose acetate. Obviously, this minimized the material loss, as the current output

---

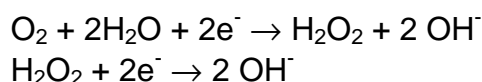
was significantly stabilized by this process. Nevertheless it can be suspected, that the success of this method was not complete, as still a slight current decrease occurred for some electrodes.

Other reasons for instable currents may be found in the condition and properties of electrolyte and reference electrode. As in Clark type oxygen electrodes the cathode is separated from the measurement solution by a gas permeable membrane, the use of an internal electrolyte is indispensable. If Ag/AgCl reference electrodes are used for planar oxygen electrodes, commonly the application of a polyelectrolyte containing KCl and a polymer is described [131;4;138]. As a polymer PVP was chosen for its excellent deposition behaviour. Furthermore PVP is highly hygroscopic and eases the rehydration after the sensor completion. Other materials like pHEMA (poly(2-hydroxyethyl methacrylate) [131], gelatin [169], alginate, agarose or polyacrylamide [133] which were also used in oxygen sensor production do not exhibit the same properties.

#### SPOE lifetime

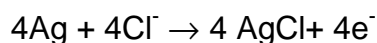
The lifetime of Ag/AgCl reference electrodes in two-electrode systems is determined by two main factors: current load and AgCl solubility. Firstly because the Ag/AgCl reference electrode works as counter electrode in two-electrode systems, it is subjected to a non neglectible current load. This reaction leads to a decrease of the basic silver material thickness and increases the Ag/AgCl layer on the electrode surface. The electrochemical reaction for the oxygen detection can be described with a two step, four electron transfer for the reduction of oxygen at the cathode:

#### Equation 4.4



Accordingly, the counterpart reaction at the Ag/AgCl reference electrode functioning as an anode can be formulated as:

#### Equation 4.5



The preformation of a stable Ag/AgCl layer and electrolyte solution is therefore recommended for reproducible oxygen detection. Secondly, as the solubility of AgCl increases with higher  $\text{Cl}^-$  concentrations, the content of chloride ions should, preferably be kept below 1 M. For miniaturized oxygen sensors the use of KCl solutions with defined concentrations (i.e. 0.1 - 0.3 M) rather than saturated KCl solutions as in macro reference electrodes can reduce this problem [131;137]. To keep SPOE manufacturing simple and reproducible, the Ag/AgCl reference electrode was preformed by screen printing of a commercial Ag/AgCl printing paste (Acheson).

A dissolving of the silver track or the Ag/AgCl excess can therefore be excluded as explanation for decreasing currents.

On the other hand it is important to mention, that the reduction of oxygen leads to formation of hydroxide ions which influences the internal electrolyte pH, as it can be seen in Equation 4.4. Thus, to avoid a shift in equilibrium, the electrolyte should be well buffered [135]. With reduction of oxygen considered as a two step mechanism with hydrogen peroxide as intermediate, the effect of an alkaline medium is obvious. Hydrogen peroxide can accumulate. It has been especially described for micro oxygen electrodes that an excess of hydrogen peroxide can cause a considerable chemical cross talk of the electrodes [133]. While other authors solved this problem by greater distances between working and reference electrode [135], in case of SPOE the uniform potential distribution over the working electrode was preferred. The possibility of electrochemical cross-talk could, however, not be excluded.

#### Dynamic characteristics of the SPOE

The kinetic properties of the SPOE were comparable to commercial electrodes or to other planar oxygen electrodes. Considering the run-in for the first use and polarization of the SPOE, it took a relatively long equilibration time of up to 20 to 30 minutes. This property has been described repeatedly for dissolved oxygen electrodes in the literature [170;133;134]. There are various attempts to explain this behaviour, but besides non-Faradayic currents, the most agreeable theory is the reduction of surface impurities with the first polarization. If compared to other thick film dissolved oxygen sensors [169], the SPOE was still relatively fast.

The SPOE responded immediately upon changes of oxygen concentration but it took up to 10 min until the next steady state current was reached again. The time to reach 90% of the signal value was 130 s. Other dissolved oxygen electrodes exhibited faster responses of 30 - 120 s [4;133], 12 s [136] and a  $t_{95\%}$  of 10 s was reported by Jobst *et al* [134]. The response characteristics of an oxygen electrode which is amperometrically operated, are mainly determined by the diffusion conditions on the electrode interface. If convective mass transport in the surrounding solution is provided, the rate limiting step becomes the diffusion through the gas-permeable membrane and the electrolyte layer. If the electrolyte layer is considered as a cylinder, its height can be calculated to 0.6 mm, plus 0.1 mm silicon rubber a total diffusion distance of 0.7 mm results. In fact, the surface of the silicon layer was convex, so the diffusion distance was site depended. Nevertheless, if compared to the micro oxygen electrode design described by Suzuki *et al*, [133] the drawbacks of this sensor design for the kinetic characteristics of the SPOE are obvious.

It can be concluded, that the novel oxygen sensor displayed operation characteristics which make it competitive to those probes described in the literature or which are commercially available. Further efforts to commercialize this sensor system would be presumably profitable.

## 4.2.2 The biological receptor

Investigations towards the use of *R.eutropha* JMP 134 as biological sensing element focused initially on the growth characteristics of this bacterial strain on various substrates. *R.eutropha* JMP 134 was chosen because of its unique enzyme set involved in the degradation of chlorinated phenoxyacetic acids and phenols and because of the specific induction pattern upon growth with different carbon sources [127;124;125]. During cultivation on 2,4-D, MCPA, 2-MPA and phenol *R.eutropha* JMP 134 showed growth at it has been described the literature [124;125]. 2,4-D, MCPA, 2-MPA and phenol were chosen as substrates, as their degradation was suspected to induce enzymatic activities which should lead to the desired response pattern needed for multianalyte detection of 2,4-DCP, 4-CP and phenol.

In oxygen uptake rate experiments Pieper *et al.* [124;125] reported O<sub>2</sub>-consumption rates upon different substituted phenols by 2,4-D, MCPA and 2-MPA grown cells which showed significant differences. 2,4-D and MCPA grown cells revealed high activity against 2,4-DCP but only minor activity was found against phenol. Cells from the early stationary phase showed same activity against 2,4-DCP but not against phenol. In the case of 2,4-D grown cells, 4-chlorophenol caused 40 % of the oxygen uptake rate as compared to 2,4-DCP. 2-MPA grown cells showed a higher activity against phenol as 2,4-DCP. In phenol grown cells, Pieper *et al.* [125] reported high activities of catechol 1,2-dioxygenase I which exhibited only low activities against chlorocatechols. In these cells no activity was found of the enzymes belonging to the chloroaromatic pathway.

These results were mainly confirmed with oxygen uptake rates reported in chapter 3.2.2.2. 2,4-D grown cells showed high activity against 2,4-DCP, about 50 % against 4-CP and no increase of oxygen uptake rate upon phenol addition. Similar results were found for MCPA grown cells. Only phenol resulted in a 30% oxygen uptake signal. 2-MPA as a growth substrate caused equal responses to all three tested substrates. In Phenol grown cells the opposite behaviour as for 2,4-D grown cells was found. Here 2,4-DCP led to no response and 4-CP to a 70 % signal related to the phenol value. It has to be mentioned, that the aim of this study was not the further investigation of degradation pathways in *R.eutropha* JMP 134 but the use of this organism for biosensors. The discussion of the response patterns and their physiological background is therefore based on literature data and further confirmative experiments were omitted.

The response of *R.eutropha* JMP 134 cells which were cultivated on the different substrates was tested in oxygen uptake assays against the target analytes 2,4-DCP, 4-CP and phenol. The response patterns, described in chapter 3.2.2.2, can be explained by the induction of catabolic enzymes shown in Figure 1.12 [124;125]. Derived from this pathway, the oxygen uptake can be explained. Figure 4.36 shows the initial steps of the proposed degradation pathways for the target analytes, causing oxygen consumption in the assay.

---



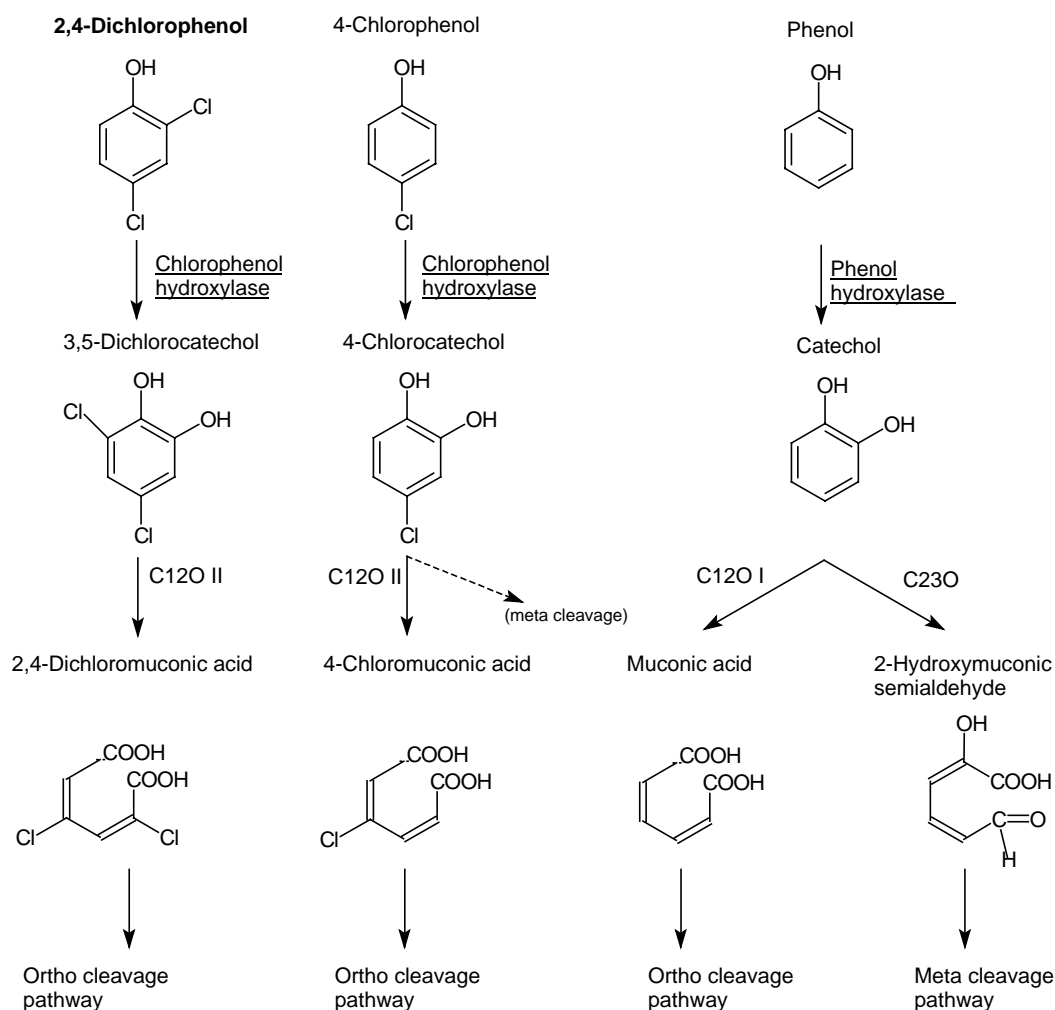


Figure 4.36: Proposed degradation steps of analytes investigated in oxygen uptake experiments.

Generally the oxygen uptake responses of *R.eutropha* JMP 134 cells may be related to the induction of the enzymes acting initially upon the analytes, the phenol hydroxylases. Pieper *et al.* reported several induction patterns depending on the compound which was used for induction experiments [127;124;125]. Figure 4.37 shows these literature data which can be used for understanding the different responses of *R.eutropha* JMP 134 cells in this report.

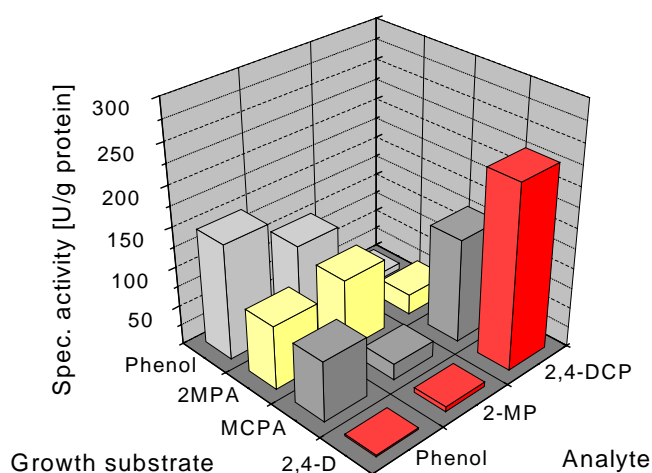
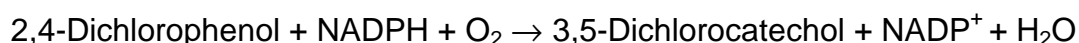


Figure 4.37: Specific phenol hydroxylating activities of *R.eutropha* JMP 134 after growth on different substrates [127].

#### Growth substrate 2,4-D

The behaviour monitored for 2,4-D grown cells can be explained most definitely. In particular the response to 2,4-DCP can be clearly understood. This compound is hydroxylated by 2,4-dichlorophenol hydroxylase to 3,5-dichlorocatechol and subsequently degraded by 3,5-dichlorocatechol 1,2-dioxygenase to chloromuconate. All enzymes involved in this reactions are fully induced by growth on 2,4-D forming the inducing agent chloromuconate. The responses of 2,4-D grown cells can obviously be related to 2,4-dichlorophenol hydroxylase (EC 1.14.13.20). The 2,4-dichlorophenol hydroxylase of *R.eutropha* JMP 134 is a homotetramer with native molecular mass of approximately 245 kDa [171] and catalyzes the reaction:



Liu and Chapman [172] purified and characterized this enzyme from *R.eutropha* JMP 134. They reported a 30 % hydroxylating activity of 2,4-dichlorophenol hydroxylase towards 4-CP. According to this report, phenol was no substrate for the 2,4-dichlorophenol hydroxylase, proving the findings in oxygen uptake measurements [172]. A comparison of these data with this report and data published by Pieper *et al.* [127;124;125] is shown in Figure 4.38.

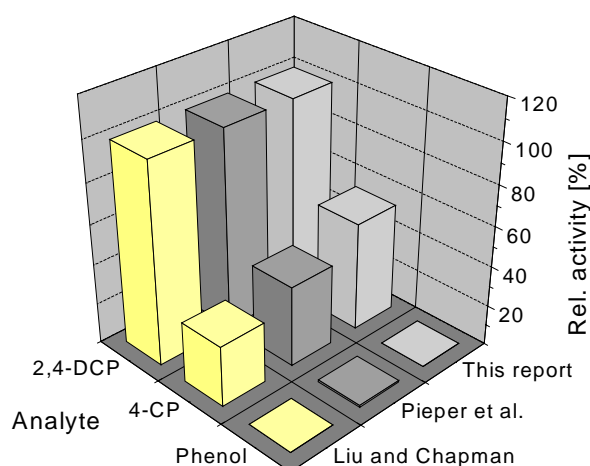


Figure 4.38: Relative activities of purified 2,4-dichlorophenol hydroxylase [172], and 2,4-D grown cells of *R.eutropha* JMP 134 ([124] and this report).

Responses to phenol by 2,4-D grown cells as they were frequently found for cells from the mid exponential phase must therefore base on the action of a second enzyme, namely phenol hydroxylase. The complete induction of the phenol degradation pathway can be excluded as Pieper *et al.* reported no activity of C23O, the enzyme initiating the meta pathway.

#### Growth substrate MCPA

As described previously, MCPA is degraded via the same pathway resulting in a similar induction pattern with high activities of 2,4-dichlorophenol hydroxylase and C12O. 2,4-dichlorophenol hydroxylase exhibits a 90 % activity towards 2-methyl-4-chlorophenol [172]. Besides the chlorophenol hydroxylating activity, an additional phenol and methylphenol hydroxylating activity was found by Pieper *et al.* Figure 4.35. The general level of induction was lower as compared to 2,4-D grown cells which explains the slower growth and the overall lower responses found in oxygen uptake assays. The response pattern of MCPA cultivated cells in oxygen uptake assays was therefore rather similar to cells derived from 2,4-D cultures with a difference in phenol response. Relatively high responses to phenol were also reported previously [125] and have to be explained by an induction of phenol hydroxylase (Figure 4.37).

#### Growth substrate 2-MPA

A more complex background can be suggested upon growth on 2-MPA. This compound is degraded by methylphenol hydroxylase towards methyl catechol which can be degraded via ortho or meta cleavage. The response towards phenol and 4-chlorophenol is supported by findings indicating high phenol hydroxylating activities

towards these two compounds in 2-MPA grown cells but reduced activity against 2,4-DCP (Figure 4.37). In oxygen uptake assays, however, equal activity was found for 2,4-DCP in this study or similarly in previous work [125] indicating, that the initial hydroxylation is not rate limiting in this case. In contrast quite high activities of C23O and C12O were found upon catechol addition but not for 3-chlorocatechol.

#### Growth substrate phenol

The reaction upon phenol addition can be understood in view of the degradation pathway and assumed induction mechanism. Pieper *et al.* [127] reported strong activities of phenol hydroxylase in phenol grown cells for phenol and methylphenol but not for 2,4-DCP (Figure 4.37). As the opposite behaviour could be found for 2,4-D and MCPA grown cells it can be presumed that no induction of the 2,4-dichlorophenol hydroxylase was caused by phenol or muconate.

It can be concluded, that *R.eutropha* JMP 134 cells showed the expected response upon target analytes depending on the cultivation substrate. Consequently the differences of their response patterns should enable a selective multianalyte detection.

### 4.2.3 Microbial sensor manufacturing

The microbial sensor described in this report marks a new milestone in biosensor development. The key features of the new sensor where its disposable transducer, the simple immobilisation and the multisensor approach.

#### 4.2.3.1 Immobilisation

The general protocol for microbial sensors uses conventional Clark-type dissolved oxygen probes. Consequently the immobilisation follows this scale and usually immobilization on a filter membrane, alginate or PVA is used. The microbial membrane is then fixed by means of a permeable membrane, i.e. dialysis tubing, and a rubber o-ring. This construction has considerable drawbacks especially its sensor life time and maintenance is concerned. Commercial microbial biosensors try to overcome this obstacle by use of a disposable sensor cap, bearing the microorganism membrane. The exchange of the electrolyte is, however, dependent on the abilities of an unskilled user.

The sensor described in this report was designed in order to exclude problems connected with operational stability and exchange of sensor parts by creating a fully disposable biosensor. Therefore the immobilisation had to follow the planar design and display adhesive properties. For the development of the novel sensor, the immobilisation turned out to be the most crucial step. For the immobilisation of microorganisms on planar electrodes several matrices are known and described in the literature, such as PCS [139], ENTP-3400 [138;135] and calcium-alginate [32].

---

Although PCS proved to be a suitable immobilisation polymer in other publications [35], the manufacturing of microbial sensors using this matrix turned out to be far too laborious and irreproducible for an automated manufacturing. This was mainly related to the adjustment of pH in the  $\mu\text{l}$  scale and the difficult drop coating. ENTP [173] was also tested but revealed problems with swelling and irreproducible diffusion behaviour. Further tests were performed with polyurethane prepolymers [174]. The disadvantage of the polyurethanes is their rapid polymerisation and negative effect on the cell viability due to the isocyanate end groups of the prepolymer. Accordingly no satisfying results were found with this matrix. A problem was either the deposition of the matrix or the swelling after polymerisation.

### PVA-SbQ

As next matrix, a derivatised polyvinylalcohol was tested [175]. PVA-SbQ is polyvinylalcohol bearing styrylpyridinium residues as photosensitive group and was successfully used for immobilizing AChE in this work [176]. Other authors used the non derivatised PVA for biosensors [129]. In this cases an additional membrane was needed to retain the micro-organisms during measurement as PVA is water soluble. The advantage of PVA-SbQ was the water insolubility and the possibility to use it within the screen printing process. The success of this approach, however, was fairly reproducible due to the high hydrophobicity of the silicon rubber membrane. Attempts to use drop coating instead could improve this method by means of using of APTS to obtain higher hydrophility. The first series of microbial multisensors were therefore constructed using this method. Similar to ENTP and polyurethane, the immobilized microbial membrane tended to show irreproducible swelling characteristics. Moreover a detachment of the membrane and problems with the uniform polymerisation were repeatedly observed.

### Silicone rubber

Several approaches to use silicone rubber as immobilisation matrix as well as for oxygen permeable membranes were undertaken. Based on reports by Kawakami *et al.* [177;178] and Oriel [179] an immobilisation of *R.eutropha* JMP 134 cells in silicone/alginate mixtures was investigated. Presumably due to the retarded diffusion of aqueous compartment no signal were obtained with this method. Another impairing effect may be assigned to organic solvent contents in the silicone preparation.

### Immobilisation on filter membranes

A common method to immobilize microorganisms for biosensor applications is the use of a filter membrane [180]. In this study several variations of this method were investigated. Especially combinations of the above mentioned matrices with filter membranes were tested, either with the filter membrane as an supporting material on the silicone or as a covering lid for additional stabilization of the weak hydrogel matrix. In fact, quite promising results were obtained with combinations of nitrocellulose and alginate, PVA-SbQ or PU6. Nevertheless, this method was stopped because of its complex construction, which led to high variations of the

---

sensor signals. As major drawback a prolonged equilibration up to 60 min was monitored, presumably due to the reduce oxygen diffusion through the filter paper. To avoid diffusion barriers the use of nylon nets instead of filter membranes was investigated. The construction of these arrangements, however, became far too complicated and was also discarded.

### Calcium alginate

The most reliable and best performing immobilisation method was drop coating of sodium alginate with subsequent calcium chloride gellation. The method was changed as compared to previous reports [32] due to the high hydrophobicity of silicon rubber. The disadvantage of this immobilisation matrix is obvious. As sodium alginate forms gels upon exchange of monovalent ions towards bivalent, a dissolution of a gel can be easily happen. A common problem of calcium alginate immobilisation is the sensitivity against phosphate ions, which lead to an immediate disruption of the membrane due to the lower solubility of calcium phosphate. For this reason, the use of phosphate buffered systems must be avoided and a low concentration of calcium chloride must be added to the measuring medium. Too high concentrations of the salt lead to an inactivation of the immobilized microorganisms because of the calcium interaction with the cell wall. If the concentration of calcium chloride is too low, a leaching of ions will occur and the membrane will be dissolved during washing steps. Additional investigations of using other counter ions for gelation focused aluminum ions. This method, however, inactivated the cells probably due to the low pH of 4 during the procedure. For an application in real samples this aspect has to be specifically considered.

#### 4.2.3.2 Properties of the basic microbial sensor

Prior multisensor experiments the sensor was characterized in detail. The measuring range of the sensor, which was equipped with 2,4-D grown cells, ranged from 2 - 60  $\mu\text{M}$  2,4-D. Expressed as weight per volume the range was 0.4 - 13.2 mg/l. It is obvious, that such a sensor would be not practicable for 2,4-D detection, as the detection limit is far from the 0.1  $\mu\text{g/l}$  limit for single pesticides in drinking water [36]. If the Maximum Residue Levels for 2,4-D in Germany are considered [181], the sensor is within the range of the demanded 2 mg/kg for citrus fruit but already not anymore in the 0.1 mg/kg range demanded for other foods of plant origin and citrus juices. In general the detection of 2,4-D can be performed with various immunosensing methods [182] [183] [184] including disposable test strips [185]. The task of this sensor was the detection of chlorinated hydrocarbons preferably in waste water. Here two aspects have to be considered. First, the concentrations of halogenated hydrocarbons determined as AOX may exceed 10 mg/l in industrial waste water. AOX concentrations in soil can even have values of several hundred mg/kg TS [109]. Second, the sensor was intended to be a prototype system to cover all relevant components of the AOX and be able to discriminate these compounds. A sensitive detection in the  $\mu\text{g/l}$  range was therefore not the primary goal, but the achieving of a high resolution. The detection range was independent from the induction substrate. In all cases, a linear relation was found up to 40  $\mu\text{M}$  and a lower detection limit was determined for 4-chlorophenol and 2,4-D grown cells with 2  $\mu\text{M}$ . A

---

comparison to data available from the literature, the microbial biosensor was in the range of reported data [121] or even slightly better [120].

### Stability

In characterizing experiments the sensor showed sufficient properties, to be used in a multisensor approach. Specific attention was paid on the stability of the selective sensor response. In enzymatic or immunological biosensors or assays the specificities remain the same over the whole test and are usually not affected by storage or exposition to an analyte, either substrate or hapten. In case microorganisms are used as biological component in biosensors this specificity is not guaranteed. As described for the cultivation of *R.eutropha* JMP 134 the pattern of enzymes expressed in the organism is dependent on the presence of an inducer.

Whilst this behaviour was a wanted effect during cultivation, the immobilized microorganisms should be stable in terms of their enzymatic pattern. For this reason repeated measurements with changing analytes were performed and the response of the same sensors was investigated after storage. Here, stable responses were found and no effect of the analyte in terms of induction was monitored. This confirmed either the suitability of the measurement protocol of approx. 10 min response monitoring and also the possibility to re-use the microbial sensors after storage. No delayed expression of new enzymatic activities was found using the microbial sensor. The situation changed with prolonged exposure time, when after 40 min an induction of phenol hydroxylating activities were found for sensors equipped with 2,4-D grown cells. It is a well known fact, that bacterial cells can be induced after immobilisation, either in biosensor applications [128;119;120] or in systems using reporter genes [186] especially for alginate immobilization [187]. For this reason, specific attention was paid to minimizing the exposure time towards the analytes ensuring a stable induction profile.

---

## 4.2.4 The microbial multisensor approach

### 4.2.4.1 Multisensor properties

The final task of this biosensor project was to arrive at an analysis system which is able to detect individual compounds out of the sum parameter AOX. Special focus was laid on compounds which display a rather high toxicity and which occur in waste water. Therefore chlorophenols were chosen out of a wide range of possible analytes because of their toxicological relevance and model character. In a first round of experiments the principle of the sensor system had to be proven by a discrimination of phenol and 2,4-dichlorophenol. The following step should be then the application of the sensor prototype on a more sophisticated problem, the simultaneous detection of 4-chlorophenol and 2,4-dichlorophenol.

In all experiments during the mixture analysis the microbial multisensor proved the properties which were monitored for the sensor prototype. A transfer from a single sensor to a multielectrode biosensor was successfully performed. The analyte specific response patterns displayed by the sensors, however, did not completely match with the values obtained with freely suspended cells from the same batch. As all possible factors like electrode cross talk, calcium chloride, alginate or osmotic stress could be excluded, the final explanation is still lacking. It is noteworthy that this deviation of the response pattern by free cells can not be related to cultivation conditions as these have always been constant. The most probable reason for this behaviour was the induction on the sensor [120;121;187], although experiments investigating this fact revealed that the exposition time had to exceed 30 - 40 min until an induction on the sensor was detectable. Nevertheless, the measurements revealed individual response patterns which were consistent for a sensor batch and measuring period and they were consequently used for neural network calculations.

The artificial neural network performance used for the microbial multisensor approach followed the experiences made in this study with the AChE multisensor data. Also here the use of higher numbers of neurons or connections was useless or had adverse effects. As it was estimated for the small number of data, the variation of single network runs was relatively high. The discrimination ability, however, could be demonstrated. The aspects of generating the optimal networks for the multisensor approaches is discussed in the AChE multisensor section.

### 4.2.4.2 Judging the multisensor performance

The quality of the novel microbial multisensor can be estimated with respect to two different viewpoints: the potential use for real-world applications and the comparison to similar sensing systems. As mentioned above, the purpose of this project was to demonstrate the potential of microbial multisensors for selective halogenated compound detection. This system was coupled with the information processing

---



capabilities of neural networks. The value of this system over other analytical methods can be derived from the following criteria:

- Selectivity
- Sensitivity
- Assay speed
- Stability
- Robustness

As it was outlined before, the sensor showed a certain selectivity depending on the cultivation and immobilization procedure. The major aspect of this question was the use of one single microbial strain. With this strain, *R.eutropha* JMP 134, the selectivity could be achieved by induction of several degradative pathways - which turned out to be not exclusive. A comparison to other detection systems is just possible in the case of chromatographic methods. Phenolic compounds and organochlorine pesticides are for example detected according to EPA Methods 604 and TO-10A in concentration ranges of 1 to 50 mg/l by GC/ECD or 0.2 to 10 mg/l HPLC. Note that these detection methods require careful sample pretreatment steps, i.e. methylene chloride extraction steps. All other test systems which can be used for field tests, including biosensors, are not capable for mixture analysis. Calculated from the mean relative error of prediction, the microbial multisensors displayed the following selectivities:

Table 4.24:

Selectivities of microbial multisensors in %, calculated from relative errors of prediction

Sensor	2,4-DCP	4-CP	Phenol
M1	77	-	74
M2	79	-	86
M3	63	83	-
M4	80	86	-

The detection limit for single analytes could be determined with 2  $\mu$ M (0.44 mg/l 2,4-D, 0.32 mg/l 2,4-DCP). For multianalyte detection, the sensitivity of the microbial multisensor was slightly lower. In 2,4-DCP/phenol mixtures the resolution limit using 3 times the mean absolute error, was calculated as 2.05 mg/l 2,4-DCP and 0.93 mg/l phenol. In 2,4-DCP/4-CP mixtures the limits were 2.05 and 0.96 mg/l respectively. Considering these sensitivities, the microbial sensor can compete with standard operation methods. In view of the analyte spectrum, however, the biosensor has certain drawbacks as compared to liquid chromatography methods.

If other detection methods than microbial test systems are considered, the sensitivity could not compete for the detection of comparable analytes. For example simple immunotest strips for 2,4-D reach detection limits of 0.5  $\mu$ g/l [185] or 0.1  $\mu$ g/l in the case of amperometric immunosensors [11]. Nevertheless, as mentioned before, the

microbial sensor described in this work was as sensitive as other microbial sensors for chlorinated phenols [120;121;32]. These systems, however, used only one sensor and were therefore not capable for a discrimination between analytes at all. An alternative method to leave the univariate readout of microbial sensors was described by Slama *et al.* [72]. In this study, the time dependent response concerning different analytes was used for multicomponent analysis of binary gluconate and acetate mixtures. Although this sensor showed a surprising performance in the mg/l range, this approach seems rather limited to only few analytes, whereas the multisensor approach can be easily expanded by adding additional sensors/receptors.

The sensitivity of a microbial detection system may be improved by factors of immobilisation and matrix optimization. The use of genetically optimized strains, i.e. membrane mutants for facilitated analyte uptake [188], offer a further chance to enhance the sensors properties. It has been furthermore demonstrated previously, that the use of organic solvents, i.e. *n*-hexane, improves a microbial sensors detection limit significantly [32].

Directly connected to the sensors sensitivity, the overall assay time has to be considered. In case of the microbial multisensor, the assay time for repeated measurements was clearly depending on the analyte concentration and exposure time in the previous test. This parameters mainly influenced the time needed for washing of the multisensor and regenerating the sensors baseline. Calculating a medium washing phase of 10 min, a complete assay time of 30 min could be given. Here the advantage of the use of artificial neural networks has to be pointed out. Whilst in conventional chemometric methods, each analysis has to be calculated separately in time efficient procedures which can easily exceed the intrinsic measurement time, artificial neural networks operate faster. Their advantage over other chemometric systems is that the main computational effort can be done prior the actual test. Using this technology, a single measurement can be calculated within seconds and is therefore not the bottle neck in analysis. Consequently, the main parameter effecting sensor speed in this work was the equilibration time which was mostly dependend on the transducer itself and not on the immobilized hydrogel.

The last two criteria, stability and robustness, can be closely related to each other. The biosensors stability is a major obstacle in biosensor commercialisation. The microbial multisensor used in this study displayed a stability and robustness which was sufficient for laboratory use but fairly suitable for real world demands. Considering the application protocol for such a system, an extended storage stability is an absolute precondition. As the systems requires batch calibration and training of the neural networks, only sensors from the same batch fit to the trained algorithm. Sensor drifts or loss of single multisensor components would lead to a failure of the detection system. In this study, however, it was found that microbial sensors can fairly be stored with a high constancy of their properties. For future developments a dedicated treatment of microbial stability, i.e. by cryoconservation [151], would be indispensable. The microbial sensors robustness was also defined by the biological component and the immobilization matrix. Whilst the basic transducer was

---

remarkable stable against chemical and physical treatment, the assembled biosensor had to be treated more carefully. Besides required storage at 4 °C in humid atmosphere, the biosensor was sensitive towards calcium binding components in the measuring solution and mechanical forces. These drawbacks have been noticed and were subjected in preliminary experiments. As the multisensor showed promising results, these approaches will be followed in future studies.

A last aspect of robustness is related to the basic detection of cell respiration. The amperometric method used in this study as well as in nearly all previous microbial sensor reports, suffers from the need of stirred solutions. This is a direct effect of the oxygen consumption during the measurement. As a general rule, dissolved oxygen electrodes are therefore flow dependent. A possible solution of this problem might be a chronoamperometric oxygen measurement as it was performed by Yang *et al.* [135]. This attempt, however, replaced the obstacle of mechanical instrumentation by a more sophisticated electrochemical system.

#### Concluding remark

It can be stated that the microbial multisensor, which is the first biosensor of this kind presently known in the literature, displayed a remarkable sensitivity and sufficient stability. The multi-analyte detection approach was fulfilled and the resolution reached by this sensor would be sufficient for the desired application. The specific multisensor design and the properties demonstrated in this report open now the possibility to develop next generation biosensors exploring the manifold specificities provided by the entire microbial world.

---

## 5 References

- [1] Clark Jr., L.C., Lyons, C., 1962. Electrode systems for continuous monitoring in cardiovascular surgery. *Ann. N. Y. Acad. Sci.* 102, 29 - 32.
  - [2] IUPAC, 1996. A definition of biosensors. *Biosens. Bioelectron.* 11, i.
  - [3] Eijkel, J.C.T., Olthuis, W., Bergveld, P., 1997. An ISFET-based dipstick device for protein detection using the ion-step method. *Biosens. Bioelectron.* 12, 991-1001.
  - [4] Suzuki, H., Sugama, A., Kojima, N., Takei, F., K, I., 1991. A miniature Clark-type oxygen electrode using a polyelectrolyte and its application as a glucose sensor. *Biosens. Bioelectron.* 6, 395-400.
  - [5] Disley, D.M., Cullen, D.C., You, H.-X., Lowe, C.R., 1998. Covalent coupling of immunoglobulin G to self-assembled monolayers as a method for immobilizing the interfacial-recognition layer of a surface plasmon resonance immunosensor. *Biosens. Bioelectron.* 13, 1213-1225.
  - [6] Watson, L.D., Maynard, P., Cullen, D.C., Sethi, R.S., J, B., R, L.C., 1987. A microelectronic conductimetric biosensor. *Biosensors* 3, 101-115.
  - [7] Wessa, T., Rapp, M., Ache, H.J., 1999. New immobilization method for SAW-biosensors: covalent attachment of antibodies via CNBr. *Biosens. Bioelectron.* 14, 93-98.
  - [8] Thavarungkul, P., Suppakitnam, P., Kanatharana, P., Mattiasson, B., 1999. Batch injection analysis for the determination of sucrose in sugar cane juice using immobilized invertase and thermometric detection. *Biosens. Bioelectron.* 14, 19-25.
  - [9] White, S.F., Turner, A.P.F. (1997) *in* Handbook of biosensors and electronic noses (Kress-Rogers, E., Ed.), CRC Press, Boca Raton.
  - [10] Prudenziati, M., 1994. Thick film sensors, Elsevier, Amsterdam.
  - [11] Skladal, P., Kalab, P., 1995. A disposable amperometric immunosensor for 2,4-dichlorophenoxyacetic acid. *Anal. Chim. Acta* 304, 361-368.
  - [12] Kroger, S., Setford, S.J., Turner, A.P., 1998. Immunosensor for 2,4-dichlorophenoxyacetic acid in aqueous/organic solvent soil extracts. *Anal. Chem.* 70, 5047-5053.
  - [13] Cagnini, A., Palchetti, I., Lioni, I., Mascini, M., Turner, A.P.F., 1995. Disposable ruthenized screen-printed biosensors for pesticides monitoring. *Sens. Act. B* 24-25, 85-89.
  - [14] Hartley, I.C., Hart, J.P., 1994. Amperometric measurement of organophosphate pesticides using a screen printed disposable sensor and biosensor based on cobalt phthalocyanine. *Anal. Proc.* 31, 333-336.
-

- 
- [15] Kulys, J., D'Costa, E.J., 1991. Printed amperometric sensor based on TCNQ and cholinesterase. *Biosens. Bioelectron.* 6, 109-115.
- [16] Pemberton, R.M., Hart, J.P., Foulkes, J.A., 1998. Development of a sensitive, selective electrochemical immunoassay for progesterone in cow's milk based on a disposable screen - printed amperometric biosensor. *Electrochim. Acta* 43, 3567-3574.
- [17] Keay, R.W., McNeil, C.J., 1998. Separation-free electrochemical immunosensor for rapid determination of atrazine. *Biosens. Bioelectron.* 13, 963-970.
- [18] Skladal, P., Nunes, G.S., Yamanaka, H., Ribeiro, M.L., 1997. Detection of carbamate pesticides in vegetable samples using cholinesterase-based biosensors. *Electroanal.* 9, 1083-1087.
- [19] Marrazza, G., Chianella, I., Mascini, M., 1999. Disposable DNA electrochemical sensor for hybridization detection. *Biosens. Bioelectron.* 14, 43-51.
- [20] Wang, J., Rivas, G., Cai, X., Parrado, C., Chicharro, M., Grant, D., Ozsoz, M., 1997. DNA electrochemical biosensors. *Proc. - Electrochem. Soc.* 97-19, 727-740.
- [21] Wang, J., Rivas, G., Ozsoz, M., Grant, D.H., Cai, X., Parrado, C., 1997. Microfabricated Electrochemical Sensor for the Detection of Radiation-Induced DNA Damage. *Anal. Chem.* 69, 1457-1460.
- [22] Bilitewski, U., Rüger, P., Drewes, W., Bechtold, F., Schmid, R.D., 1991. Thick Film Biosensors for Ethanol and Urea. *GBF Monographs* 17,
- [23] Yee, H., Park, J., Kim, S., 1996. Disposable thick film amperometric biosensor with multiple working electrodes fabricated on a single substrate. *Sens. Act. B* 34, 490-492.
- [24] Schreiber, A., Feldbrugge, R., Key, G., Glatz, J.F.C., Spener, F., 1997. An immunosensor based on disposable electrodes for rapid estimation of fatty acid-binding protein, an early marker of myocardial infarction. *Biosens. Bioelectron.* 12, 1131-1137.
- [25] Dennison, M.J., Hall, J.M., Turner, A.P.F., 1996. Direct monitoring of formaldehyde vapor and detection of ethanol vapor using dehydrogenase-based biosensors. *Analyst* 121(12), 1769-1773.
- [26] Wang, J., Chen, Q., 1994. Screen printed glucose strip based on palladium dispersed carbon ink. *Analyst* 119, 1849-1851.
- [27] Compagnone, D., Bugli, M., Imperiali, P., Varallo, G., Palleschi, G., 1997. Determination of heavy metals using electrochemical biosensors based on enzyme inhibition. *NATO ASI Ser., Ser. 2* 38, 220-226.
-

- 
- [28] Loechel, C., Chemnitz, G.-C., Borchardt, M., Cammann, K., 1998. Amperometric bi-enzyme based biosensor for the determination of lactose with an extended linear range. *Z. Lebensm.-Unters. Forsch. A* 207, 381-385.
- [29] Jäger, A., Bilitewski, U., 1994. Screen-printed electrode for the determination of lactose. *Analyst* 119, 1251-1255.
- [30] Ge, F., Zhang, X.E., Zhang, Z.P., Zhang, X.M., 1998. Simultaneous determination of maltose and glucose using a screen-printed electrode system. *Biosens. Bioelectron.* 13, 333-339.
- [31] Schmidt, J.C., 1998. Enzyme-based electrodes for environmental monitoring applications. *Field Anal. Chem. Technol.* 2, 351-361.
- [32] Bachmann, T.T., Bilitewski, U., Schmid, R.D., 1998. Determination of chlorinated xenobiotic compounds by microbial biosensors: an improved biosensor for the selective detection of monochlorinated aromatics in water and organic solvent based on *Pseudomonas putida* DSM 548. *Anal. Lett.* 31, 2361-2373.
- [33] Hart, J.P., Pemberton, R.M., Luxton, R., Wedge, R., 1997. Studies towards a disposable screen-printed amperometric biosensor for progesterone. *Biosens. Bioelectron.* 12, 1113-1121.
- [34] Bäumner, A., Schmid, R.D., 1998. Development of a new immunosensor for pesticide detection: a disposable system with liposome-enhancement and amperometric detection. *Biosens. Bioelectron.* 13, 519-524.
- [35] Eggenstein, C., Borchardt, M., Diekmann, C., Grundig, B., Dumschat, C., Cammann, K., Knoll, M., Spener, F., 1999. A disposable biosensor for urea determination in blood based on an ammonium-sensitive transducer. *Biosens. Bioelectron.* 14, 33-41.
- [36] EC Council Directive, 30.08.1980. EU Directive on Drinking Water Quality. 80/778/EEC L 229, 11-19.
- [37] Jaskulké, E., Patta, L., Bruchnet, A. (1998) in *Pesticide Chemistry and Bioscience, The Food-Environment Challenge* (Brooks, G. T., and Roberts, T. R., Eds.), p. 368-385, Royal Society of Chemistry, London.
- [38] EU, Commission of the European Community-Standards, Measurements and Testing programme, Project STM4-CT96-2142.
- [39] DIN 38409-14, 1985. German standard methods for the examination of water, waste water and sludge. General measures of effects and substances (group H); determination of adsorbable organic halogen (AOX) (H 14).
- [40] Kulys, J., Schmid, R.D., 1990. A sensitive enzyme electrode for phenol monitoring. *Anal. Lett.* 23,
-

- 
- [41] Satoh, I., Kasahara, T., Goi, N., 1990. Amperometric biosensing of copper(II) ions with an immobilized apoenzyme reactor. *Sens. Act. B1*, 499-503.
- [42] Nakamura, K., Amano, Y., Nakayama, O., 1989. Determination of free sulphite in wine using a microbial sensor. *Appl. Microbiol. Biotechnol.* 31, 351-354.
- [43] Hikuma, M., Matsuoka, H., Takeda, M., Tonooka, Y., 1993. Microbial electrode for nitrate based on *pseudomonas aeruginosa*. *Biotech. Techn.* 7, 14-18.
- [44] DIN 38415-1, 1995. German standard methods for the examination of water, waste water and sludge.
- [45] Richman, S.J., Karthikeyan, S., Bennett, D.A., Chung, A.C., Lee, S.M., 1996. Low Level Immunoassay Screen for 2,4-Dichlorophenoxyacetic Acid in Apples, Grapes, Potatoes, and Oranges, Circumventing Matrix Effects. *J. Agric. Food Chem.* 44, 2924-2929.
- [46] Wortberg, M., Goodrow, M.H., Gee, S.J., Hammock, B.D., 1996. Immunoassay for Simazine and Atrazine with Low Cross-Reactivity for Propazine. *J. Agric. Food Chem.* 44, 2210-2219.
- [47] Wittmann, C., Hock, B., 1993. Analysis of Atrazine Residues in Food by an Enzyme Immunoassay. *J. Agric. Food Chem.* 41,
- [48] Kress-Rogers, E., 1997. Handbook of Biosensors and Electronic noses. Medicine, Food and the Environment, CRC Press, Frankfurt.
- [49] Göpel, W., Ziegler, C., Breer, H., Schild, D., Apfelbach, R., Joerges, J., Malaka, R., 1998. Bioelectronic noses: a status report. Part I. *Biosens. Bioelectron.* 13, 479-493.
- [50] Jonsson, A., Winqvist, F., Schnurer, J., Sundgren, H., Lundstrom, I., 1997. Electronic nose for microbial quality classification of grains. *Int. J. Food Microbiol.* 35, 187-193.
- [51] Seemann, J., Rapp, F.-R., Zell, A., Gauglitz, G., 1997. Classical and modern algorithms for the evaluation of data from sensor arrays. *Fres. J. Anal. Chem.* 359, 100-106.
- [52] Walt, D.R., Dickinson, T., White, J., Kauer, J., Johnson, S., Engelhardt, H., Sutter, J., Jurs, P., 1998. Optical sensor arrays for odor recognition. *Biosens. Bioelectron.* 13, 697-699.
- [53] Carey, W.P., Beebe, K.R., Kowalski, B.R., 1987. Multicomponent analysis using an array of piezoelectric crystal sensors. *Anal. Chem.* 59, 1529-1534.
- [54] Ferguson, J.A., Boles, T.C., Adams, C.P., Walt, D.R., 1996. A fiber-optic DNA biosensor microarray for the analysis of gene expression. *Nat. Biotechnol.* 14, 1681-1684.
-

- 
- [55] Cheung, V.G., Morle, M., Aguilar, F., Massimi, A., Kucherlapati, R., Childs, G., 1999. Making and reading microarrays. *Nature Genetics* 21, 15 - 19.
- [56] MG Weller, R.N., 1997. Affinity patterns of enzyme tracers for triazine immunoassays. *SPIE Proc.* 3105, 341-352.
- [57] Wittmann, C., Löffler, S., Zell, A., Schmid, R.D. (1997) *in* *Immunochemical Technology for Environmental Applications*, p. 343-352, Am. Chem. Soc.
- [58] Brecht, A., Klotz, A., Barzen, C., Gauglitz, G., Harris, R.D., Quigley, Q.R., Wilkinson, J.S., Sztajn bok, P., Abuknesha, R., Gascon, J., Oubina, A., Barcelo, D., 1998. Optical immunoprobe development for multiresidue monitoring in water. *Anal. Chim. Acta* 362, 69-79.
- [59] Mallat, E., Barzen, C., Klotz, A., Brecht, A., Gauglitz, G., Barcelo, D., 1999. River Analyzer for Chlorotriazines with a Direct Optical Immunosensor. *Environ. Sci. Technol.* 33, 965 - 971.
- [60] Winkel mair, M., Schuetz, A.J., Weller, M.G., Niessner, R., 1999. Immunochemical array for the identification of cross-reacting analytes. *Fres. J. Anal. Chem.* 363, 731-737.
- [61] Jiang, J.H., Shen, G.L., Yu, R.Q., Chu, X., 1996. Simultaneous immunoassay using piezoelectric immunosensor array and robust method. *Anal. Chim. Acta* 336, 185-193.
- [62] Spohn, U., van der Pol, J., Eberhardt, R., Jocksch, B., Wandrey, C., 1994. An automated system for mutli-channel flow injection analysis. *Anal. Chim. Acta* 292, 281-287.
- [63] Hitzmann, B., Kullick, T., 1994. Evaluation of pH field effect transistor measurement signals by neural networks. *Anal. Chim. Acta* 294, 243-249.
- [64] Hitzmann, B., Ritzka, A., Ulber, R., Scheper, T., Schügerl, K., 1997. Computaional neural networks for the evaluation of biosensor FIA mesurements. *Anal. Chim. Acta* 348, 135-141.
- [65] Starodub, N.F., Kanjuk, N.I., Kukla, A.L., Shirshov, Y.M., 1999. Multi-enzymatic electrochemical sensor: field measurements and their optimisation. *Anal. Chim. Acta* 385, 461-466.
- [66] Skladal, P., Kalab, T., 1995. A multichannel immunochemical sensor for determiantion of 2,4-dichlorophenoxyacetic acid. *Anal. Chim. Acta* 316, 73-78.
- [67] Goldberg, H.D., Brown, R.B., Liu, D.P., Meyerhoff, M.E., 1994. Screen printing: a technology for the batch fabrication of integrated chemical sensor arrays. *Sens. Act. B* 21, 171-183.
-



- 
- [68] Seddon, B.J., Shao, Y., Girault, H.H., 1994. Printed microelectrode array and amperometric sensor for environmental monitoring. *Electrochim. Acta* 39, 2377-2396.
- [69] Kermani, B.G., Schiffman, S.S., Nagle, H.T., 1999. Using neural networks and genetic algorithms to enhance performance in an electronic nose. *IEEE Trans. Biomed. Eng.* 46, 429-439.
- [70] Shaffer, R.E., Rose-Pehrsson, S.L., McGill, R.A., 1999. A comparison study of chemical sensor array pattern recognition algorithms. *Anal. Chim. Acta* 384, 305-317.
- [71] Carey, W.P., Beebe, K.R., Sanchez, E., Gerald, P., Kowalski, B.R., 1986. Chemometric analysis of multisensor arrays. *Sens. Act.* 9, 223-234.
- [72] Slama, M., Zaborosch, C., Wienke, D., Spener, F., 1996. Simultaneous Mixture Analysis using a Dynamic Microbial Sensor Combined with Chemometrics. *Anal. Chem.* 68, 3845-3850.
- [73] Zupan, J., Gasteiger, J., 1991. Neural Networks: A new method for solving chemical problems or just a passing phase? *Anal. Chim. Acta* 248, 1-30.
- [74] Zell, A., 1994. *Simulation neuronaler Netze*, Addison-Wesley, Bonn.
- [75] Rapp, F., Gauglitz, G., Zell, A., NEMO 1.15.02 (1997) University of Tübingen, Germany
- [76] Jury, A.W., Winer, A.M., Spencer, W.F., Focht, D.D., 1987. *Env. Contam. Toxicol.* 99, 119-123.
- [77] Yess, N.J., Gunderson, E.L., Roy, R.R., 1993. U.S. Food and Drug Administration monitoring of pesticide residues in infant foods and adult foods eaten by infants/children. *J. AOAC. Int.* 76, 492-507.
- [78] Wiles, R., Davies, K., Campbell, C., 1998. *Overexposed: Organophosphate insecticides in children's food.*, Environmental Working Group, Washington D.C.
- [79] FQPA, 1996. The Food Quality Protection Act, US Pub. L. 104-170.
- [80] EPA Method 8141A, Organophosphorus compounds by gas chromatography: capillary column technique, US Environmental Protection Agency.
- [81] Lacorte, S., Barcelo, D., 1995. Determination of organophosphorus pesticides and their transformation products in river waters by automated on-line solid-phase extraction followed by thermospray liquid chromatography-mass spectrometry. *J. Chrom. A* 5 712, 103-112.
- [82] Saul, A.J., Zomer, E., Puopolo, D., Charm, S.E., 1995. Use of new rapid bioluminescence method for screening organophosphate and n-
-

- methylcarbamate insecticides in processed baby foods. *J. Food Proc.* 59, 306-311.
- [83] Evtugyn, G.A., Budnikov, H.C., Nikolskaya, E.B., 1996. Influence of surface-active compounds on the response and sensitivity of cholinesterase biosensors for inhibitor determination. *Analyst* 121, 1911-1915.
- [84] Ghindilis, A.L., Morzunova, T.G., Barmin, A.V., Kurochkin, I.N., 1996. Potentiometric biosensors for cholinesterase inhibitor analysis based on mediatorless bioelectrocatalysis. *Biosens. Bioelectron.* 11, 837-880.
- [85] Palleschi, G., Bernabei, M., Cremisini, C., Mascini, M., 1992. Determination of organophosphorus insecticides with a choline electrochemical biosensor. *Sens. Act. B* B7, 513-517.
- [86] Skladal, P., Mascini, M., 1992. Sensitive detection of pesticides using amperometric sensors based on cobalt phthalocyanin-modified composite electrodes and immobilized cholinesterases. *Biosens. Bioelectron.* 7, 335-343.
- [87] Mionetto, N., Marty, J.-L., Karube, I., 1994. Acetylcholinesterase in organic solvents for the detection of pesticides: Biosensor application. *Biosens. Bioelectron.* 9, 463-470.
- [88] Guilbault, G.G., Ngeh-Ngwainbi (1988) *in* Analytical uses of immobilized biological compounds for detection, medical and industrial uses. (Guilbault, G. G., and Mascini, M., Eds.), p. 187, Reidel, The Netherlands, Dordrecht.
- [89] Abad, J.M., Pariente, F., Hernández, L., Abruña, H.D., Lorenzo, E., 1998. Determination of Organophosphorus and Carbamate Pesticides Using a Piezoelectric Biosensor. *Anal. Chem.* 70, 2848-2855.
- [90] Kindervater, R., Künnecke, W., Schmid, R.D., 1990. Exchangeable immobilized enzyme reactor for enzyme inhibition tests in flow-injection analysis using a magnetic device. Determination of pesticides in drinking water. *Anal. Chim. Acta* 234, 223-226.
- [91] Morelis, R.M., Coulet, P.R., 1990. A sensitive biosensor for choline and acetylcholine involving fast immobilisation of a bienzyme system on a disposable membrane. *Anal. Chim. Acta* 231, 27-32.
- [92] Hart, A.L., Collier, W.A., Janssen, D., 1997. The response of screen printed enzyme electrodes containing cholinesterase to organophosphates in solution and from commercial formulations. *Biosens. Bioelectron.* 12, 645-654.
- [93] Palchetti, I., Cagnini, A., DelCarlo, M., Coppi, C., Mascini, M., Turner, A.P.F., 1997. Determination of anticholinesterase pesticides in real samples using a disposable biosensor. *Anal. Chim. Acta* 337, 315-321.
- [94] Herzsprung, P., Weil, L., Quentin, K.E., 1989. Determination of organophosphorus compounds and carbamates by their inhibition of
-

- cholinesterase. Part 1: Inhibition values on immobilized cholinesterase. *Z. Wass. Abwass. Forsch.* 22, 67-72.
- [95] Schäfer, O., Weil, L., Niessner, R., 1994. Bestimmung von Phosphorpestiziden und insektiziden Carbamaten mittels Cholinesterasehemmung 4. Mitt.: Qualitative und quantitative Bestimmung eines Mehrkomponenten-Pestizidgemisches in Wasser unter Verwendung bioanalytischer und chemometrischer Methoden. *Vom Wasser* 82, 233-246.
- [96] Danzer, T., Schwedt, G., 1996 a. Multivariate evaluation of inhibition studies on an enzyme electrodes system with pesticides and mixtures of mercury and pesticides, Part 1 Development of an Enzyme electrodes system for pesticide and heavy metal screening using selected chemometric methods. *Anal. Chim. Acta* 318, 275-286.
- [97] Danzer, T., Schwedt, G., 1996 b. Multivariate evaluation of inhibition studies on an enzyme electrodes system with pesticides and mixtures of mercury and pesticides. *Anal. Chim. Acta* 325, 1-10.
- [98] Sum, S.T., Despagne, F., Lavine, B.K., Brown, S.B., 1996. Chemometrics. *Anal. Chem.* 68, 21R-61R.
- [99] Vellom, D., Radic, Z., Li, Y., Pickering, N., Camp, S., Taylor, P., 1993. Amino acid residues controlling acetylcholinesterase and butyrylcholinesterase specificity. *Biochemistry* 32, 12-17.
- [100] Ashani, Y., Radic, Z., Tsigelny, I., Vellom, D.C., Pickering, N.A., Quinn, D.M., Doctor, B.P., Taylor, P., 1995. Amino acid residues controlling reactivation of organophosphonyl conjugates of acetylcholinesterase by mono- and bisquaternary oximes. *J. Biol. Chem.* 270, 6370-6380.
- [101] Faerman, C., Ripoll, D., Bon, S., Le Feuvre, Y., Morel, N., Massoulie, J., Sussman, J., Silman, I., 1996. Site-directed mutants designed to test back-door hypotheses of acetylcholinesterase function. *FEBS Lett.* 386, 65-71.
- [102] Masson, P., Froment, M., Bartels, C., Lockridge, O., 1996. Asp70 in the peripheral anionic site of human butyrylcholinesterase. *Eur. J. Biochem.* 235, 36-48.
- [103] Pleiss, J., Mionetto, N., Schmid, R.D., 1997. Protein engineering of rat brain acetylcholinesterase: a point mutation enhances sensitivity to pesticides. *Prot. Eng.* 10, 66-70.
- [104] Villatte, F., Marcel, V., Estrada-Mondaca, S., Fournier, D., 1998 a. Engineering sensitive acetylcholinesterase for detection of organophosphate and carbamate insecticides. *Biosens. Bioelectron.* 13, 157-162.
- [105] Pleiss, J., Mionetto, N., Schmid, R.D., 1999. Probing the acyl binding site of acetylcholinesterase by protein engineering. *J. Mol. Cat. B* in print.
-

- 
- [106] Mionetto, N., Morel, N., Massoulié, J., Schmid, R.D., 1997. Biochemical determination of insecticides via cholinesterases. 1. Acetylcholinesterase from rat brain: functional expression using a baculovirus system, and biochemical characterization. *Biotechnol. Techn.* 11, 805-812.
- [107] Estrada-Mondaca, S., Fournier, D., 1998. Stabilization of recombinant *Drosophila* acetylcholinesterase. *Prot. Exp. Purif.* 12, 166-172.
- [108] Heim, J., Schmidt-Dannert, C., Atomi, H., Schmid, R.D., 1998. Functional expression of a mammalian acetylcholinesterase in *Pichia pastoris*: comparison to acetylcholinesterase, expressed and reconstituted from *Escherichia coli*. *Biochim. Biophys. Acta* 1396, 306-319.
- [109] DECHEMA e.V., 1995. Industrial Waste Water: The Problem of AOX. DECHEMA Fachgespräche Umweltschutz 1-20.
- [110] Streit, B., 1994. Lexikon Ökotoxikologie, VCH, Weinheim.
- [111] Ballschmitter, K., Haltrich, W., Kühn, W., Niemitz, W., 1987. HOV essay of the Working Party Water Chemistry, GDCh.
- [112] Belouscheck, P., Brand, H., Lönz, P., 1992. Determination of chlorinated hydrocarbons by combined headspace and gas chromatography/mass spectrometry techniques. *Vom Wasser* 79, 1-8.
- [113] Kontsas, H., Rosenberg, C., Pfaffli, P., Jappinen, P., 1995. Gas chromatographic-mass spectrometric determination of chlorophenols in the urine of sawmill workers with past use of chlorophenol- containing anti-stain agents. *Analyst* 120, 1745-1749.
- [114] Kulys, J., Schmid, R.D., 1990. A sensitive enzyme electrode for phenol monitoring. *Anal. Lett.* 23,
- [115] Schubert, F., Saini, S., Turner, A.P.F., Scheller, F., 1992. Organic Phase Enzyme Electrodes for the Determination of Hydrogen Peroxide and Phenol. *Sens. Act. B* 7, 408-413.
- [116] Commandeur, L.C.M., Parsons, J.R., 1990. Degradation of halogenated aromatic compounds. *Biodegradation* 1, 207-220.
- [117] Straube, G., 1987. Phenol hydroxylase from *Rhodococcus* s. P1. *J. Basic Microbiol.* 27, 229-234.
- [118] Riedel, K., Hensel, J., Ebert, K., 1991. Biosensors for the determination of phenol and benzoate on the basis of *Rhodococcus* cells and enzyme extracts. *Zentralbl. Mikrobiol.* 146, 425-434.
- [119] Riedel, K., Naumov, A., Boronin, A., Golovleva, L., Stein, H., Scheller, F., 1991. Microbial sensors for determination of aromatics and their chloroderivatives: I. Determination of 3-chlorobenzoate using a *Pseudomans*-containing biosensor. *Appl. Microbiol. Biotechnol.* 35, 559-562.
-

- 
- [120] Riedel, K., Hensel, J., Rothe, S., Neumann, B., Scheller, F., 1993. Microbial sensors for determination of aromatics and their chloroderivatives: II. Determination of chlorinated phenols using a *Rhodococcus*-containing biosensor. Appl. Microbiol. Biotechnol. 38, 556-559.
- [121] Riedel, K., Beyersdorf-Radeck, B., Neumann, B., Scheller, F., 1995. Microbial sensors for determination of aromatics and their chloroderivatives: III. Determination of chlorinated penols using a biosensor containing *Trichosporon beigelii (cutaneum)*. Appl. Microbiol. Biotechnol. 43, 7-12.
- [122] Beyersdorf-Radeck, B., Riedel, K., Karlson, U., Bachmann, T.T., Schmid, R.D., 1998. Screening of xenobiotic compounds degrading microorganisms using biosensor techniques. Microb. Res. 153, 239-245.
- [123] Streber, W.R., Timmis, K.N., Zenk, M.H., 1987. Analysis, Cloning, and High-Level Expression of 2,4-Dichlorophenoxyacetate Monooxygenase Gene *tdfA* of *Alcaligenes eutrophus* JMP 134. J. Bacteriol. 169, 2950 - 2955.
- [124] Pieper, D.H., Reinike, W., Engesser, K.-H., Knackmuss, H.-J., 1988. Metabolism of 2,4-dichlorophenoxyacetic acid, 4-chloro-2-methylphenoxyacetic acid and 2-methylphenoxyacetic acid by *Alcaligenes eutrophus* JMP 134. Arch. Microbiol. 150, 95 - 102.
- [125] Pieper, D.H., Engesser, K.-H., Knackmuss, H.-J., 1989. Regulation of catabolic pathways of phenoxyacetic acids and phenols in *Alcaligenes eutrophus* JMP 134. Arch. Microbiol. 151, 365 - 371.
- [126] Filer, K., Harker, A.R., 1997. Identification of the Inducing Agent of the 2,4-Dichlorophenoxyacetic acid pathway encoded by plasmid pJP4. Appl. Microbiol. Biotechnol. 63, 317 - 320.
- [127] Pieper, D. (1986) Dissertation, Fachbereich Naturwissenschaften II, Bergische Universität - Gesamthochschule Wuppertal, Wuppertal.
- [128] Riedel, K., Renneberg, R., Scheller, F., 1990. Adaptable Microbial Sensors. Anal. Lett. 23, 757-770.
- [129] Riedel, K., Lehmann, M., Adler, K., Kunze, G., 1997. Physiological characterization of a microbial sensor containing the yeast *Arxula adenivorans* LS3. Antonie Van Leeuwenhoek 71, 345-351.
- [130] Clark, L.C., 1956. Monitor and control of blood and tissue oxygen tensions. Trans. Am. Soc. Artif. Int. Organs 2, 41-46.
- [131] Koudelka, M., 1986. Performance characteristics of a planar "Clark-type" oxygen sensor. Sens. Act. B 9, 249-258.
- [132] Suzuki, H., Tamiya, E., Karube, I., 1988. Fabrication of an Oxygen Electrode Using Semiconductor Technology. Anal. Chem. 60, 1080-1082.
-

- 
- [133] Suzuki, H., Sugama, A., Kojima, N., 1992. Micromachined Clark Oxygen Electrodes and Biosensors. *Fujitsu Sci. Tech. J.* 28, 393-401.
- [134] Jobst, G., Urban, G., Jachimowitz, A., Kohl, F., Tilando, O., 1993. Thin-film Clark-type oxygen sensor based on novel polymer membrane systems for in vivo and biosensor applications. *Biosens. Bioelectron.* 8, 123-128.
- [135] Yang, Z., Sasaki, S., Karube, I., Suzuki, H., 1997. Fabrication of oxygen electrode arrays and their incorporation into sensors for measuring the biological oxygen demand. *Anal. Chim. Acta* 357, 41-49.
- [136] Yang, Z., Suzuki, H., Sasaki, S., Karube, I., 1997. Design and Validation of a low-cost paper-based oxygen electrode. *Anal. Lett.* 30, 1797-1807.
- [137] Suzuki, H., Hiratsuka, A., Sasaki, S., Karube, I., 1998. Problems associated with the thin-film Ag/AgCl reference electrode and a novel structure with improved durability. *Sens. Act. B* 46, 104-113.
- [138] Yang, Z., Suzuki, H., Sasaki, S., Karube, I., 1996. Disposable sensor for biochemical oxygen demand. *Appl. Microbiol. Biotechnol.* 46, 10-14.
- [139] König, A., Bachmann, T., Metzger, J., RD, S., 1999. Disposable sensor for measuring the biochemical oxygen demand for nitrification and inhibition of nitrification in wastewater. *Appl. Microbiol. Biotechnol.* 51, 112-117.
- [140] Chaabihi, H., Fournier, D., Fedon, Y., Bossy, J.P., Ravallec, M., Devauchelle, G., Cerutti, M., 1994. Biochemical Characterisation of *Drosophila melanogaster* acetylcholinesterase expressed by recombinant baculovirus. *Biochem. Biophys. Res. Comm.* 203, 734-742.
- [141] Ellmann, G.L., Courtney, K.D., Andres, V., Featherstone, R.M., 1961. A new and rapid determination of acetylcholinesterase activity. *Biochem. Pharmacol.* 7, 88-92.
- [142] Jdanova, A.S., Poyard, S., Soldatkin, A.P., Jaffrezic-Renault, N., Martelet, C., 1996. Conductometric urea sensor. Use of additional membranes for the improvement of its analytical characteristics. *Anal. Chim. Acta* 321, 35-40.
- [143] Marty, J.-L., Sode, K., Karube, I., 1989. Amperometric determination of choline and acetylcholine with enzymes immobilized in a photocross-linkable polymer. *Anal. Chim. Acta* 228, 49-53.
- [144] Riemiller, M., Braun, H., Ruspini, H. (1993) in *IEEE International Conference on Neural Networks (ICNN)* 586-591, San Francisco.
- [145] Smolensky, P., Mozer, M. (1989) in *Advances in neural information processing systems (NIPS)* 1 (Touretzky, D. S., Ed.), p. 107-115, Morgan Kaufmann Publishers Inc., San Mateo.
- [146] Cutracheas, P., 1970. Protein purification by affinity chromatography. *J. Biol. Chem.* 245, 3059-3065.
-

- 
- [147] Dow, R., Sietsma, J., 1991. Creating Artificial Neural Networks that Generalize. *Neural Networks* 4, 67-79.
- [148] Personal Communication, Sewage treatment plant Stuttgart University, Stuttgart-Büsnau (1998)
- [149] Villatte, F., Ziliani, P., Marcel, V., Menozzi, P., Didier, Fournier, 1998 b. A high number of mutations in insect acetylcholinesterase may provide insecticide resistance. *Ins. Biochem. Mol. Biol.* submitted.
- [150] Macosko, C.W., 1985. *in* *Rubber Chem. Technol.* 58, 436-440.
- [151] Malik, K.A., Beyersdorf-Radeck, B., Schmid, R.D., 1993. Preservation of immobilized bacterial cell-matrix by drying for direct use in microbial sensors. *World J. Microbiol. Biotechnol.* 9, 243-247.
- [152] Cardosi, M.F., Birch, S.W., 1993. Screen printed glucose electrodes based on platinised carbon particles and glucose oxidase. *Anal. Chim. Acta* 276, 69-74.
- [153] Hart, A., Turner, A., Hopcroft, D., 1996. On the use of screen- and ink-jet printing to produce amperometric enzyme electrodes for lactate. *Biosens. Bioelectron.* 11, 263-270.
- [154] Li, Y., Zhou, Y., Feng, J., Jiang, Z., Ma, L., 1999. Immobilization of enzyme on screen printed electrode by exposure to glutaraldehyde vapour for the construction of amperometric acetylcholinesterase electrodes. *Anal. Chim. Acta* 382, 277-282.
- [155] Skladal, P., 1992. Detection of organophosphate and carbamate pesticides using disposable biosensors based on chemicals modified electrodes and immobilized cholinesterase. *Anal. Chim. Acta* 269, 281-287.
- [156] Newman, J.D., Turner, A.P.F., 1992. Ink-jet printing for the fabrication of amperometric glucose biosensors. *Anal. Chim. Acta* 262,
- [157] Soldatkin, A., El'skaya, A., Shul'ga, A., Jdanova, A., Dzyadevich, S., Jaffrezic-Renault, N., Martelet, C., Clechet, P., 1994. Glucose sensitive conductometric biosensor with additional Nafion membrane: reduction of influence on buffer capacity on the sensor response and extension of its dynamic range. *Anal. Chim. Acta* 288, 197-203.
- [158] Evtugyn, G., Ivanov, A., Gogol, E., Marty, J., Budnikov, H., 1999. Amperometric flow-through biosensor for the determination of cholinesterase inhibitors. *Anal. Chim. Acta* 385, 13-21.
- [159] Höbel, W., Polster, J., 1992. Fiber optic biosensor for pesticides based on acetylcholine esterase. *Fres. J. Anal. Chem.* 343, 101-102.
- [160] Martorell, D., Céspedes, F., Martínez-Fàbregas, E., Alegret, S., 1997. Determination of organophosphorus and carbamate pesticides using a
-

- biosensor based on a polishable, 7,7,8,8-tetracyanoquinodimethane-modified, graphite-epoxy biocomposite. *Anal. Chim. Acta* 337, 305-313.
- [161] TrinkwV, 1986. Verordnung über Trinkwasser und über Wasser für Lebensmittelbetriebe. BGBl I, 760-773.
- [162] Pylypiw, H.M.J., 1993. Rapid gas chromatographic method for the multiresidue screening of fruits and vegetables for organochlorine and organophosphate pesticides. *J. AOAC. Int.* 76, 1369-1373.
- [163] Bachmann, T.T., Schmid, R.D., 1999. A disposable, multielectrode biosensor for rapid simultaneous detection of the insecticides paraoxon and carbofuran at high resolution. *Anal. Chim. Acta* submitted,
- [164] Tusarova, I., Halamek, E., WO 94/05808, Biosensor for detection of and distinguishing between cholinesterases inhibitors, 17.03.94.
- [165] Simonian, A.L., Rainina, E.i., Wild, J.R., 1997. A new approach for discriminative detection of organophosphate neurotoxins in the presence of other cholinesterase inhibitors. *Anal. Lett.* 30, 2453-2468.
- [166] Popova, S., Mitev, V., 1997. Application of artificial neural networks for yeast cells classification. *Bioproc. Engin.* 17, 111-113.
- [167] Gardner, J.W., Hines, E.L., Tang, H.C., 1992. Detection of vapors and odors from a multisensor array using pattern recognition techniques. Part 2 Artificial neural networks. *Sens. Act. B* 9, 9-15.
- [168] DFG (1987) *in* Manual of Pesticide Residue Analysis Volume I (Thier, H. P., and Zeumer, H., Eds.), p. 335-345, VCH, Weinheim.
- [169] Glasspool, W., Atkinson, J., 1998. A screen-printed amperometric dissolved oxygen sensor utilising an immobilised electrolyte gel and membrane. *Sens. Act. B* 48, 308-317.
- [170] Linek, V., Vacek, V., Sinkule, J., Benes, P., 1988. Measurement of oxygen by membrane covered probes, Ellis Worwood Ltd, Chichester, Great Britain.
- [171] Farhana, L., New, P., 1997. The 2,4-dichlorophenol hydroxylase of *Alcaligenes eutrophus* JMP134 is a homotetramer. *Can. J. Microbiol.* 43, 202-205.
- [172] Liu, T., Chapman, P.J., 1984. Purification and properties of a plasmid-encoded 2,4-dichlorophenol hydroxylase. *FEBS* 173, 314 - 318.
- [173] Tanaka, A., Yasuhara, S., Osumi, M., Fukui, S., 1977. Immobilization of yeast microbodies by inclusion with photo-crosslinkable resins. *Eur. J. Biochem.* 80, 193-197.
-



- 
- [174] Sonomoto, K., Nomura, K., Tanaka, A., Fukui, S., 1982. 11 $\alpha$ -Hydroxylation of progesterone by gel-entrapped living *Rhizopus stolonifer* mycelia. Eur. J. Appl. Microbiol. Biotechnol. 16, 57-62.
- [175] Ichimmua, K., 1987. Photocrosslinking behaviour of poly(vinyl alcohol)s with pendent styrylpyridinium or styrylquinolynium groups. Makromol.Chem. 188, 2973-2982.
- [176] Bachmann, T.T., Schmid, R.D., Leca, B., Marty, J.-L., Vilatte, F., Fournier, D., 1999. Improved Discrimination of Organophosphate and Carbamate Insecticides using Recombinant Mutants of *Drosophila* Acetylcholinesterase and a Disposable Multielectrode Biosensor. Biosens. Bioelectron. submitted,
- [177] Kawakami, K., Abe, T., Yoshida, T., 1992. Silicone-immobilized biocatalysts effective for biocentrations in nonaqueous media. Enzy. Microb. Technol. 14,
- [178] Kawakami, K., Nakahara, T., 1993. Importance of Solute Partitioning in Biphasic Oxidation of Benzyl Alcohol by Free and Immobilized Whole Cells of *Pichia pastoris*. Biotech. Bioeng. 43, 918-924.
- [179] Oriel, P., 1988. Immobilization of recombinant *Escherichia coli* in silicone polymer beads. Enzy. Microb. Technol. 10,
- [180] Karube, I., Suzuki, M., 1990. Microbial biosensors, Oxford University Press, Oxyfrod.
- [181] RHMV, 1994. Rückstands-Höchstmengenverordnung, 3. Verordnung zur Änderung der RHMV (BGBL1. 1997 I 2366). I 2299,
- [182] Gerdes, M., Meusel, M., Spener, F., 1999. Influence of antibody valency in a displacement immunoassay for the quantitation of 2,4-dichlorophenoxyacetic acid. J. Immunol. Meth. 223, 217-226.
- [183] Razak, C.N., Salam, F., Ampon, K., Basri, M., Salleh, A.B., 1998. Development of an ELISA for detection of parathion, carbofuran, and 2,4-dichlorophenoxyacetic acid in water, soil, vegetables, and fruits. Ann. N. Y. Acad.Sci. 864, 479-484.
- [184] Skladal, P., Minunni, M., Mascini, M., Kolar, V., Franek, M., 1994. Characterization of monoclonal antibodies to 2,4-dichlorophenoxyacetic acid using a piezoelectric quartz crystal microbalance in solution. J. Immunol. Meth. 176, 117-125.
- [185] Cuong, N.V., Bachmann, T.T., Schmid, R.D., 1999. Development of an immuno dipstick assay for quantitative determination of 2,4-dichlorophenoxyacetic acid in real water, fruit and urine samples. Fres. J. Anal. Chem. in print,
- [186] Ikariyama, Y., Nishiguchi, S., Koyama, T., Kobatake, E., Aizawa, M., 1997. Fiber-optic-based biomonitoring of benzene derivatives by recombinant *E. coli*
-

- bearing luciferase gene-fused TOL-plasmid immobilized on the fiber-optic end. Anal. Chem. 69, 2600-2605.
- [187] Matrubutham, U., Thonnard, J.E., Sayler, G.S., 1997. Bioluminescence induction response and survival of the bioreporter bacterium *Pseudomonas fluorescens* HK44 in nutrient-deprived conditions. Appl. Microbiol. Biotechnol. 47, 604-609.
- [188] Lee, S., Suzuki, M., Tamiya, E., Karube, I., 1992. Sensitive bioluminescent detection of pesticides utilizing membrane mutant of *Escherichia coli* and recombinant DNA technology. Anal. Chim. Acta 257, 183-188.
-

# Lebenslauf

Name	Jochen Till Tobias Bachmann
Geburtsdatum	27.06.1968
Geburtsort	Berlin
Staatsangehörigkeit	deutsch
Familienstand	ledig
Schulausbildung	1974-1987: Schulbesuch in Heilbronn. Abschluß: Abitur
Wehrdienst	1987-1988 in Bad Mergentheim als Sanitäter.
Studium	<p>1988-1994: Studium der Technischen Biologie an der Universität Stuttgart.</p> <p>Hauptfach: Bioverfahrenstechnik Nebenfächer: Industrielle Genetik Mikrobiologie Biochemie</p> <p>WS 1992/93: Studienarbeit bei Prof.Dr. M. Reuss am Institut für Bioverfahrenstechnik, Universität Stuttgart.</p> <p>SS 1994: Diplomarbeit bei PD Dr. U. Bilitewski und Prof.Dr. R.D. Schmid an der Gesellschaft für biotechnologische Forschung (GBF), Braunschweig und Institut für Technische Biochemie, Universität Stuttgart (ITB).</p> <p>Juni 1995: Aufnahme der experimentellen Arbeiten zur vorliegenden Dissertation am Institut für Technische Biochemie, Universität Stuttgart.</p> <p>Juni - August 1997: Forschungsaufenthalt bei Prof.Dr. I. Karube am Research Center for Advanced Science and Technology, Universität Tokyo, Japan.</p> <p>September 1997: Beginn der Tätigkeit als Arbeitsgruppenleiter der Abteilung Analytische Biotechnologie / Biosensoren am Institut für Technische Biochemie, Universität Stuttgart.</p>
Veröffentlichungen	<p><u>Till T. Bachmann</u>, U. Bilitewski, R. D. Schmid, „Determination of chlorinated xenobiotic compounds by microbial biosensors: an improved biosensor for the selective detection of monochlorinated aromatics in water and organic solvent based on Pseudomonas</p>

putida DSM 548“,Analytical Letters, 31 (14), 2361-2373 (1998).

B. Beyersdorf-Radeck, K. Riedel, U. Karlson, T. T. Bachmann, R. D. Schmid, "Screening of xenobiotic compounds degrading microorganisms using biosensor techniques", Microbial Research, 153 (3), 239-245, (1998).

A. König, T. T. Bachmann, J. W. Metzger, R. D. Schmid „Disposable biosensor for the detection of nitrification inhibitors in waste water and the determination of N-BOD“ Applied Microbiology Biotechnolog, 51, 112-117 (1999).

N. V. Cuong, T. T. Bachmann, R. D. Schmid „Development of an immuno dipstick assay for quantitative determination of 2,4-dichlorophenoxyacetic acid in real water, fruit and urine samples“, Fresenius J. Anal. Chem. in print.

K. Riedel, T. T. Bachmann, R. D. Schmid, „Microbial sensors for determination of artomatics and their halogenated derivatives", Biosensors for environmental monitoring, Harwood Academic Publishers, in print.

Till T. Bachmann, Rolf D. Schmid, „A Disposable Multielectrode Biosensor for the Discrimination of Organophosphate and Carbamate Insecticides in the Submicromolar Range using Native and Recombinant Variants of Acetylcholinesterase“, Analytica Chimica Acta, in print.

Till T. Bachmann, Rolf D. Schmid, Béatrice Leca, Jean-Louis Marty, Francois Vilatte, Didier Fournier, „Improved Discrimination of Organophosphate and Carbamate Insecticides using Recombinant Mutants of *Drosophila* Acetylcholinesterase and a Disposable Multielectrode Biosensor“, Biosensors Bioelectronics, submitted.